AD NUMBER: AD0489923

LIMITATION CHANGES

TO:

Approved for public release; distribution is unlimited.

FROM:

Distribution authorized to U.S. Gov't. agencies and their contractors; Administrative/Operational Use; 15 Jun 1966. Other requests shall be referred to the Army Missile Command, Redstone Arsenal, AL 35309.

AUTHORITY

OASD, DOD, 29 MAY 1969

REPORT NO. 3509
COPY NO. 45

DEVELOPMENT OF AN ALL-FLUID PNEUMATIC PRESSURE REGULATOR

Technical Documentary Report

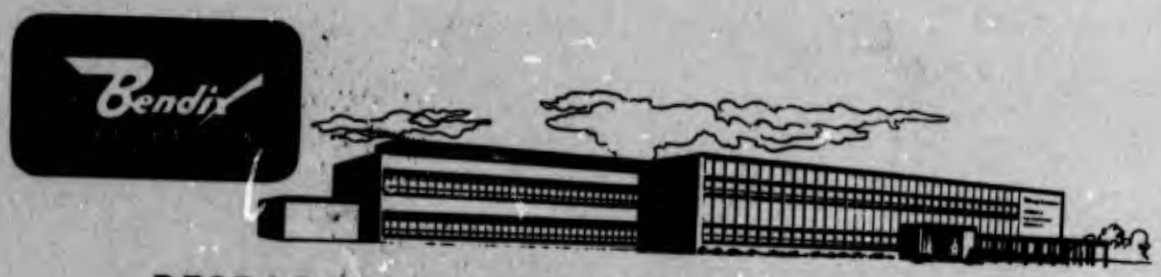

RESEARCH LABORATORIES DIVISION
SOUTHFIELD, MICHIGAN

Report No. 3509

(6) DEVELOPMENT OF AN ALL-FLUID PNEUMATIC PRESSURE REGULATOR.

(9) Technical ~~Documentary Report~~. Feb 65 - Jun 66.

(11) 15 June 1966

(12) 124P. (14) RLD-3509

(15) DA-01-021-AMC-11805(Z)

Submitted to

Army Inertial Guidance and Control Laboratory
U. S. Army Missile Command
Redstone Arsenal, Alabama 35309

By

The Bendix Corporation
Research Laboratories Division
Southfield, Michigan 48076

(304 180)

ABSTRACT

The requirements of an all-fluid pneumatic pressure regulator (having no moving parts) have been investigated and several regulation concepts have been studied and designed. The three major pressure regulator subsystem functions are: (1) throttling, (2) feedback signal transfer, and (3) reference, or error detection. The throttling function is adequately performed by a vortex fluid state device. The feedback signal transfer is adequately performed by a confined-jet fluid state amplifier, and the reference or error detection is a built-in phenomenon of the confined-jet amplifier. These confined-jet amplifiers combine high supply pressure recovery with low control-to-supply pressure ratio.

An alternate hybrid regulator that avoids the limitations imposed by the vortex throttle element and uses a mechanical variable area is investigated. This device is extremely practical, having a minimum of moving parts while retaining the high reliability and other desirable characteristics of a completely all-fluid system.

FOREWORD

This report was prepared by the Research Laboratories Division of The Bendix Corporation under U.S. Army Contract DA 01-021-AMC-11805 (Z).

This work was sponsored by the Army Inertial Guidance and Control Laboratory, U.S. Army Missile Command, Redstone Arsenal, Alabama, and was conducted under the direction of Mr. B. J. Clayton, the Army Project Engineer.

Bendix personnel who managed the program, and added significantly to its technical accomplishment are as follows:

G. I. Boyadjieff
R. B. Hollstien
E. A. Mayer
J. G. Rivard
L. B. Taplin
J. H. Tarter
K. W. Verge

Work described in this report was conducted during the period February 1965 through June 1966, inclusive.

The manuscript was submitted for publication as a Technical Documentary Report on June 15, 1966.

TABLE OF CONTENTS

LIST OF ILLUSTRATIONS

SECTION 1

INTRODUCTION

This final report summarizes the work accomplished under Contract DA 01-021-AMC-11805 (Z) to investigate methods for all-fluid pressure regulation.

Section 2 of this report reviews the pressure regulator requirements and describes the subsystem functions required to satisfy these requirements. Each of the subsystem requirements is then examined in detail and methods of performing the functions are explored experimentally.

Section 3 summarizes various regulator approaches using the elements described in Section 2. Each concept is analyzed and breadboarded together when feasible to check operation. Two different concepts, one an all-fluid blowdown regulator and the other a hybrid fluid state-mechanical element combination, were built as deliverable items under the project and are also described and analyzed in this Section.

Section 4 summarizes the results of the project, exhibits the principal conclusions, and lists the advantages and disadvantages of each regulator studied in Section 3.

Appendix A gives the notation used in the main body of the report. Appendix B presents a somewhat more detailed analysis and description of the vortex valve. Appendix C presents a dynamic stability analysis of the hybrid regulator. Finally, Appendix D describes the pneumatic flow characteristics of a series of n identical orifices.

BLANK PAGE

SECTION 2

INVESTIGATION OF COMPONENTS FOR ALL-FLUID PRESSURE REGULATION

2.1 REQUIREMENT, CONCEPT, AND SUBSYSTEM FUNCTIONS

2.1.1 AMC Technical Requirement No. 715 -- Summary

The regulator concept being investigated is based upon the use of vortex-type fluid elements to deliver a constant output pressure from a variable supply pressure. The objective of the investigation is to determine the feasibility of regulating the pressure of gas supplied to an all-fluid missile control system from a pressurized gas storage bottle without the use of conventional mechanical regulators. The gas (air or nitrogen) is to be stored at 1000 psig. The function of the regulator is to deliver a constant pressure of 15 psig to a fixed load orifice of 0.02 in^2, while the supply pressure decreases from 1000 to 100 psig. A variation of plus or minus 1.5 psi is allowed, and the flow through the load orifice is sonic for all allowable output pressures.

2.1.2 Concept and Subsystem Functions

The three subsystem functions required to provide closed-loop regulation are: (1) throttling the flow of gas from the storage bottle, (2) reference or comparison of the output pressure with the desired output pressure, and (3) the transfer of feedback signals to exercise control of the throttling elements as a function of the deviation of the output pressure from the desired pressure. Although the term "regulator" implies the use of feedback, it is not necessary (at least in principle) to use feedback to satisfy the requirements of the regulator. An alternative approach is to program the effective area of the throttling element as a function of the storage bottle pressure. This concept uses the fact that, because the load orifice is sonic and the area is fixed, the regulator would ideally deliver a constant flow to the load. The effective area of the throttling element must, therefore, vary in inverse proportion to the bottle absolute pressure, and this variation could be programmed without feedback. This investigation is centered on the application of

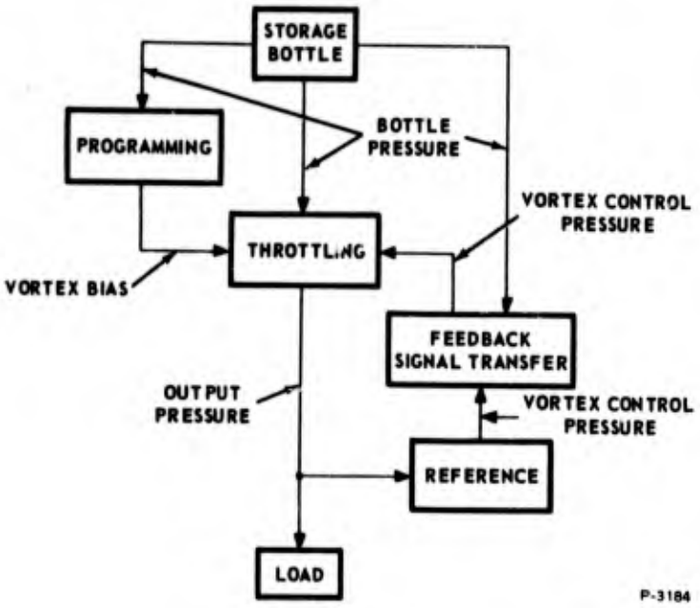

Figure 2-1 - Regulator Concept and Subsystem Functions

closed-loop control in anticipation of future AMC regulator requirements with variable load conditions, but a combination of open-loop programming with feedback control is thought to offer the potential advantages of both approaches. The interconnection of subsystem functions in the regulator is represented in Figure 2-1.

2.1.3 Throttling

The required nominal load flow at 15 psig output pressure is

$$w_L = (C_D C_2 / T^{1/2}) A_L P_R$$

$$= ((1)(0.532)/(530)^{1/2})(0.02)(29.7) \qquad (2\text{-}1)$$

$$= 0.0138 \text{ lb/sec}$$

where the coefficient of discharge for the load orifice is assumed to be one. The effective area of the throttling element must increase to 8.0 times its initial value, as the bottle pressure decreases from 1015 to

115 psia and the regulated pressure from 31.2 to 28.2 psia, to satisfy the equation

$$\begin{aligned} w_T &= (C_D C_2 / T^{1/2}) A_T P_S \\ &= w_L^* \\ &= (C_D C_2 / T^{1/2}) A_L P_R \end{aligned} \qquad (2\text{-}2)$$

The extreme effective areas of the throttling element must be

$$A_T \Big|_{P_B = 1015} = \frac{A_L P_{R\max}}{P_{B\max}} = 0.000615 \text{ in}^2$$

and

$$A_T \Big|_{P_B = 115} = \frac{A_L P_{R\min}}{P_{B\min}} = 0.0049 \text{ in}^2$$

Taking a discharge coefficient of 0.8 for the effective throttling orifice gives an effective diameter range of 0.031 to 0.088 inch.

2.1.4 Feedback

The pressure signal output from the reference element must be capable of changing the impedance (or effective area) of the throttling element. Vortex valves require control pressures greater than the supply pressure, so feedback signal transfer devices must operate at bias ratios (output/input) near 1000/20 - 50/1 when the bottle pressure is a maximum and the output of the pressure reference is 20 psia. This does not imply that the perturbation signal amplification must be 50; the amplification required for the feedback signal transfer will depend on the loop gain required for the regulator and the distribution of this gain between the reference, feedback, and throttling elements.

The output bias of the feedback amplifier must track the required throttling element control pressure to within its perturbation signal range. By feedback "amplifier" we mean all of the elements required to perform the function of feedback signal transfer from the reference element output pressure to the throttling element control pressure.

2.1.5 Pressure Reference

The deviation of the output pressure from the desired value must be sensed to provide an input to the feedback amplifier. The pressure reference may require separate devices for this function alone, or the reference function may be an intrinsic part of the characteristics of the first (low pressure) stage of the feedback amplifier. In either case, it is necessary to provide a means of manually adjusting the regulated pressure. The output pressure is a "gage" pressure so the reference function is relative to the regulator ambient pressure.

2.2 THROTTLING METHODS

2.2.1 General Description of Vortex Valves

Vortex valves are all fluid devices that exhibit a variable and controlled impedance. The performance of vortex valves will, therefore, govern the feasibility of the throttling function required for the regulator.

The impedance of vortex valves is produced by a combination of the pressure-flow characteristics of orifices and the radial pressure distribution in a vortex flow; the variable impedance is induced by control of the tangential velocity of the vortex field. A detailed analysis of the valve operation is given in Appendix B. In this Section, only the salient characteristics that determine the effectiveness of vortex valves in the regulator throttling application are described from the viewpoint of input-output characteristics. The geometry and nomenclature of Bendix vortex valves will be introduced as these characteristics are described.

The elementary vortex valve configuration is shown in Figure 2-2. The supply flow enters the valve inlet port and is routed to the vortex chamber through the annular space around the valve "button." In the absence of control flow, the flow is radial from the outer wall of the chamber toward the outlet orifice; then, because the pressure drop is small through the relatively large passages between the valve inlet and the outlet orifice, the flow through the valve is determined by the supply pressure, exit pressure, and the area of the outlet orifice in the equation

$$w_o = (C_D C_2 / T^{1/2}) A_e P_S f_1 (P_e / P_S) \qquad (2\text{-}3)$$

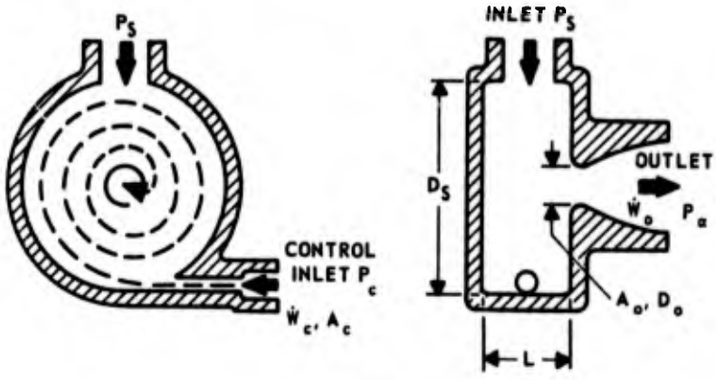

VALVE
SCHEMATIC

Figure 2-2 - Elementary Vortex Valve Configuration and Nomenclature

When the control port pressure is higher than the pressure at the outer wall of the vortex chamber, a control flow enters the chamber tangentially and produces a vortex flow. The vorticity of the combined supply and control flows is determined by their relative momenta and the geometrical effectiveness of the valve design. The radial pressure distribution in the vortex chamber (and hence the pressure at the radius of the outlet orifice) is determined by the centrifugal forces on the individual elements of fluid in the vortex chamber. The flow through the valve is a function of the pressure at the radius of the outlet orifice. Therefore, the flow for a given supply pressure is determined by the control pressure through its influence on the vortex field.

The static performance characteristics of vortex valves are conveniently represented by a family of curves of flow versus supply pressure with fixed control pressure (Figure 2-3). The upper envelope of the curves of constant control pressure is the orifice flow characteristic for the outlet orifice; when $P_C < P_S$, there is no control flow or pressure drop from the outer wall of the vortex chamber to the radius of the outlet orifice. The lower bound on the curves of constant control pressure are points at which the supply flow is shut off completely and the flow through the outlet orifice of the valve is equal to the control flow. The "turndown ratio" of the vortex valve is defined as

$$\text{Turndown Ratio} = \left. \frac{\dot{W}_o \; P_C \leq P_S}{\dot{W}_o \; P_C \geq P_{CSC}} \right|_{P_S = \text{constant}} \qquad (2\text{-}4)$$

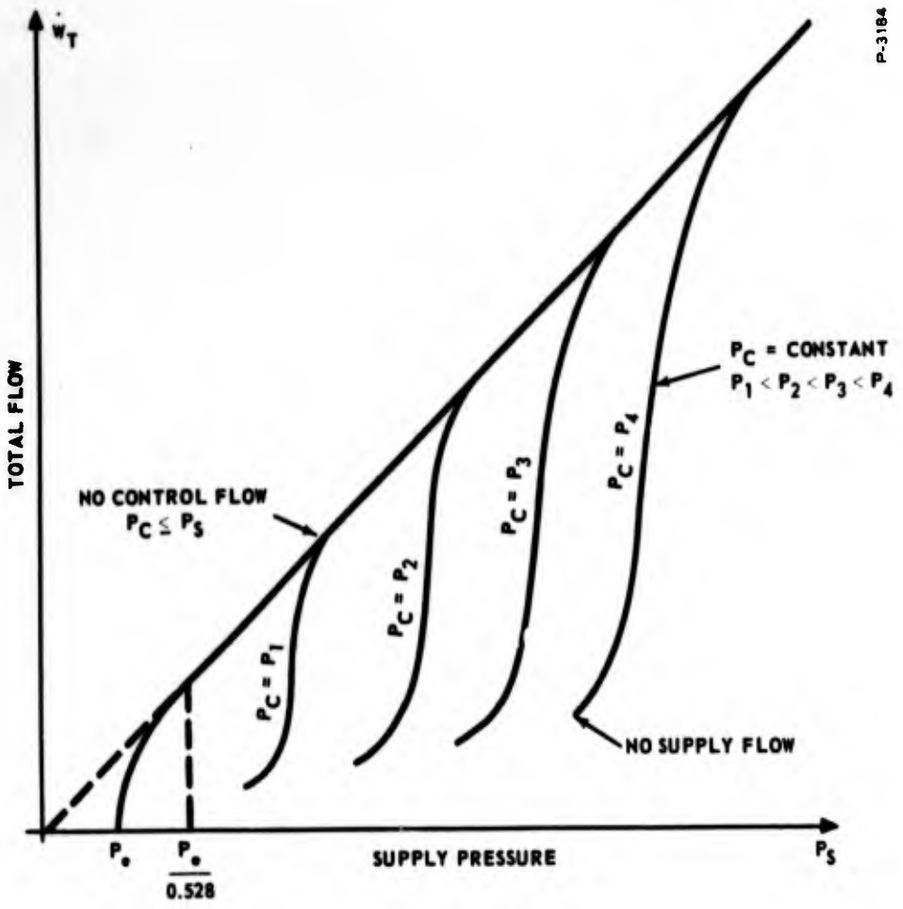

Figure 2-3 - Static Performance Characteristics of Vortex Valves

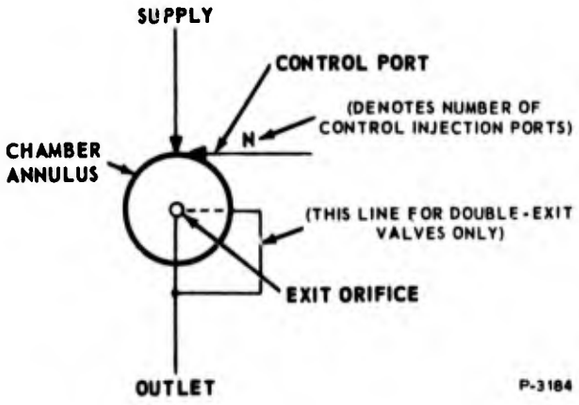

Figure 2-4 - Schematic Symbol for Vortex Valves

where P_{CSC} is the control pressure for supply flow cutoff at the given supply pressure. The turndown ratio is nearly independent of P_S for $P_S >> P_e$.

The schematic symbol for vortex valves is given to Figure 2-4. The valve configurations represented by this symbol are generally more complex than that shown in Figure 2-2, but the use of multiple-control ports and double-exit valves does not alter the fundamental concept of the vortex valve.

2.2.2 Vortex Valve Design

In a practical valve, the functional schematic form of Figure 2-2 is implemented as in Figure 2-5. The supply flow, instead of being admitted to the vortex chamber at one location, is introduced through an annular plenum formed by a button-shaped insert in the chamber. The flow distributes itself around the plenum and then enters the chamber through the annular restriction (with respect to the plenum area) formed by the button outside diameter and the chamber inside diameter. This configuration provides a uniform sheet of fluid around the chamber diameter in contrast to the non-uniform flow distribution of a signal supply hole chamber.

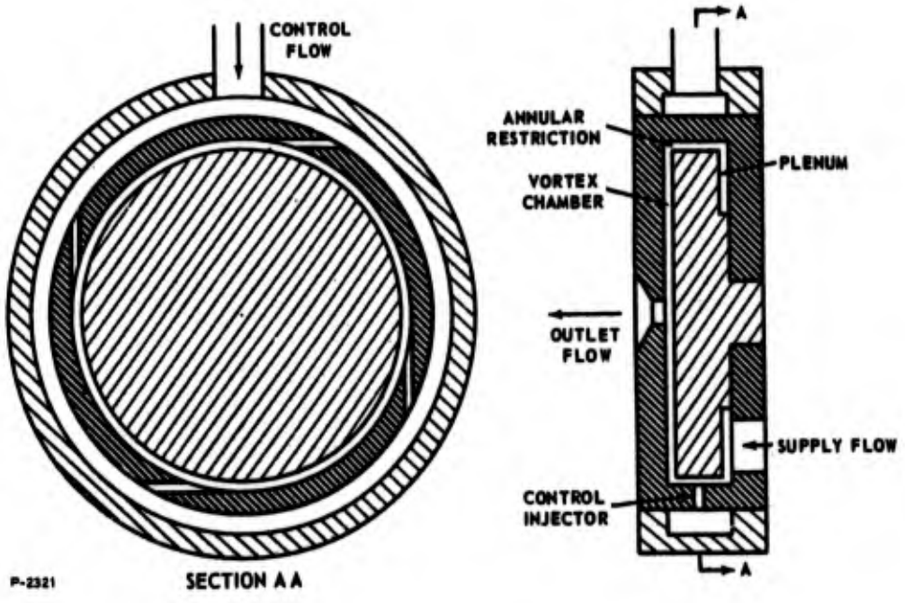

Figure 2-5 - Schematic of Vortex Valve Design

This configuration also allows the introduction of tangential control flow at several points around the periphery of the chamber or around the button outside diameter. In addition, the annular restriction forces the tangential flow to mix completely with the supply flow, resulting in maximum vortex efficiency.

The basic configuration described above may be altered or adjusted several ways to optimize performance. The most effective single modification is to provide a doublet exit hole by placing a second exit hole in the button. This reduces the losses at the exit hole, resulting in improved efficiency.

2.2.3 Vortex Valve Experimental Investigation

Several breadboard vortex valves were designed and fabricated to investigate vortex valve geometry and its effects on performance. A "building block" assembly was designed to provide maximum flexibility during experimental investigations and future circuit studies.

The vortex valves are assembled by sandwiching a button, injector manifold, injector plate, injector cover, and receiver between manifold blocks. Figure 2-6 shows a typical vortex valve assembly. Each component can be replaced or modified individually.

The injector plate design is shown in the close-up, Figure 2-7. When placed between the injector manifold and injector cover, and over the button, the injector plate forms the outside wall of the vortex chamber. Control ports A and B are common as are control ports C and D. Control ports A, B, C and D are on one side of the injector plate and are additive in the sense that they induce control swirl in the vortex chamber in the same direction. Control ports E and F (F is not visible in Figure 2-7) are located on the opposite side of the injector plate; they are common and induce swirl in opposition to control ports A, B, C and D. By choice of angular location of the injector plate, the vortex valve may be assembled with two sets of control ports that induce swirl in either the same or opposite directions. A thin (approximately 0.005 inch) teflon gasket bonded to the injector manifold and injector cover, seals the communicating passage between control ports.

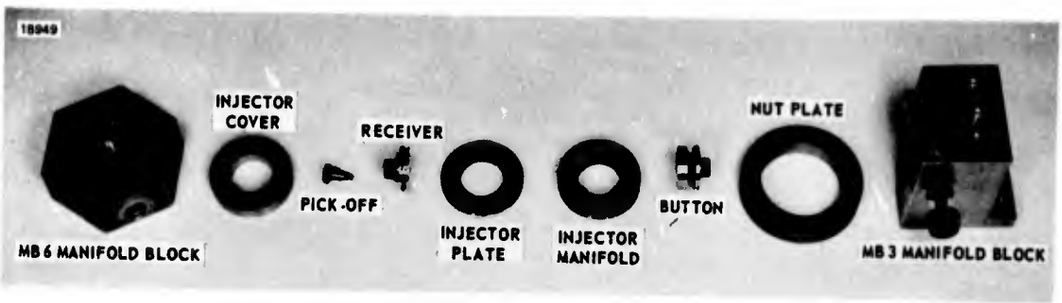

Figure 2-6 - Typical Vortex Valve Components

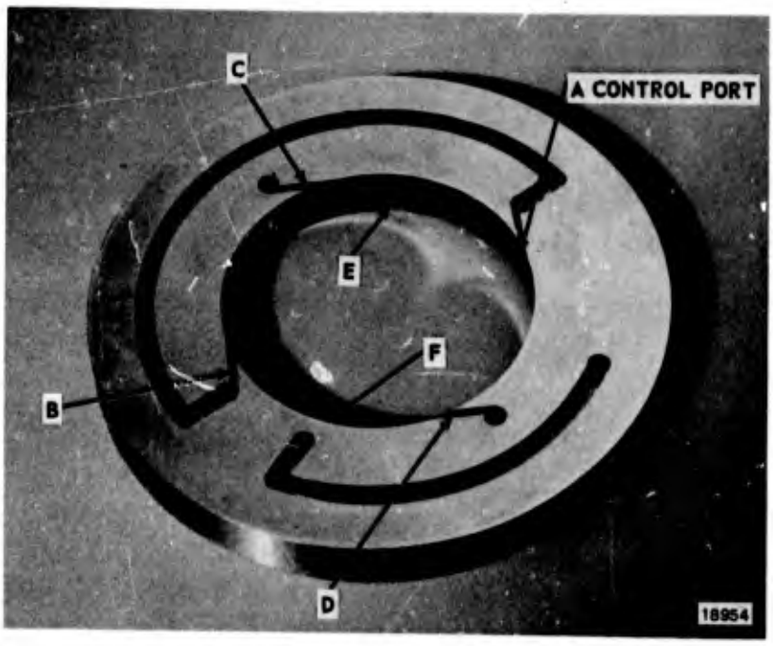

Figure 2-7 - Control Injector Plate

2.2.4 Vortex Valve Performance

2.2.4.1 Single Exit Vortex Valve

Both a 5/8 inch and a 1 inch vortex valve were studied to determine optimum turndown geometry for the required regulator flow. The best performance curve of a single-exit valve is shown in Figure 2-8. The characteristics of valves are obtained experimentally by plotting the pressure upstream of a load orifice; in Figure 2-8, the load area is equal to the required regulator load area. The pressure downstream of the load orifice is nearly atmospheric so

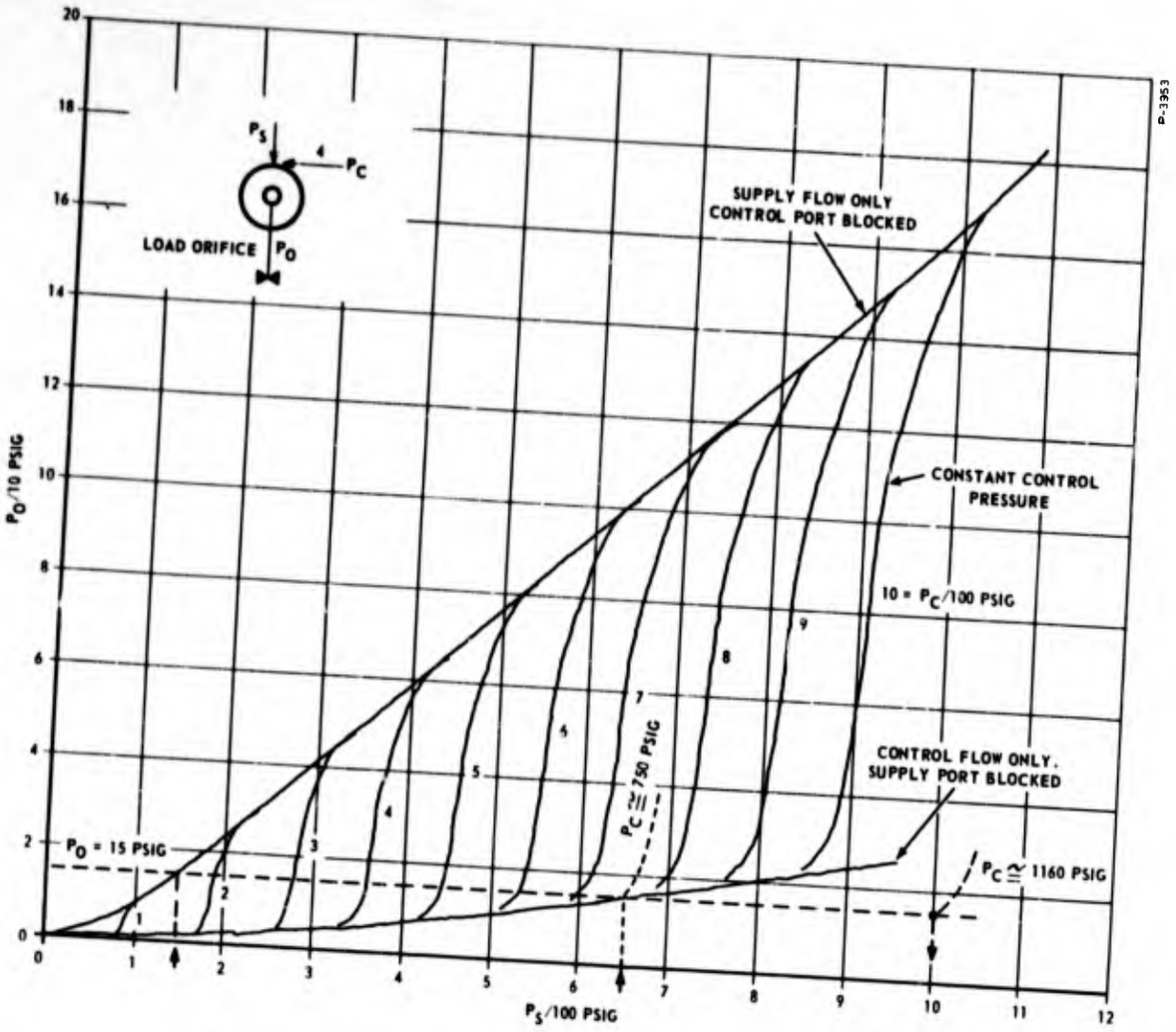

Figure 2-8 - Single Exit Valve Performance

the load flow is given approximately by (0.014) (P_O + 15) /30 where P_O is in psig and P_O is greater than 15. For P_O less than 15, the expression for the load flow is multiplied by f_1 (15/(P_O + 15). This valve has an exit orifice diameter of 0.08 inch, less than the 0.088 inch required to deliver the desired load flow at a supply pressure of 100 psig, but its performance characteristics are useful in studying the throttling function. We see that the valve will deliver the required load flow for supply pressures between 650 and 150 psig. The absolute supply pressure ratio 665/165 = 4.0 is the same as the turndown ratio for the valve; the turndown ratio, evaluated at P_S = 650 psig, is

(103 + 15)/30 = 3.94. It is evident that the supply flow must be cut off when P_S = 650 psig, and that a control pressure of P_C = 750 psig is required. The results of the tests established the following design guidelines:

1. Vortex chamber lengths between one quarter exit hole diameters and several exit hole diameters do not affect maximum turndown.
2. Exit hole diameter-to-chamber diameter ratio should be about one-eighth.
3. Control port area to exit hole area ratio should be about one-eighth.
4. The annular clearance around the button is very critical for "good mixing" and control port effectiveness and should be minimum. On the other hand, it must not be so small that a significant pressure drop occurs.
5. Control port configuration, i.e., round hole or square slot is not very critical.
6. Control port number, i.e., signal tangential hole or series of tangential ports is not critical.

2.2.4.2 Double-Exit Valve Performance

By adding an additional exit hole in the vortex valve button, the maximum flow capacity of the valve can be increased without a proportional increase in the control flow required to achieve full turndown. Figure 2-9 shows the performance of the valve with the characterisitcs of Figure 2-8.after conversion to a double-exit configuration. This makes the valve too large for the present application; it now delivers the required load flow between supply pressures of 125 and 500 psig. But the increased effectiveness of the double-exit configuration is demonstrated by the range of supply pressure over which the valve will deliver twice the required flow. The absolute supply pressure ratio is now 680/115 = 5.9 which is a 50 percent improvement in supply pressure range over the single exit configuration.

The full advantage of double-exit valves is not demonstrated in the above comparison because the modified valve did not realize the improvement in turndown capability that was expected. The turndown ratio evaluated at P_S = 640 psig in Figure 2-6 is 4.6

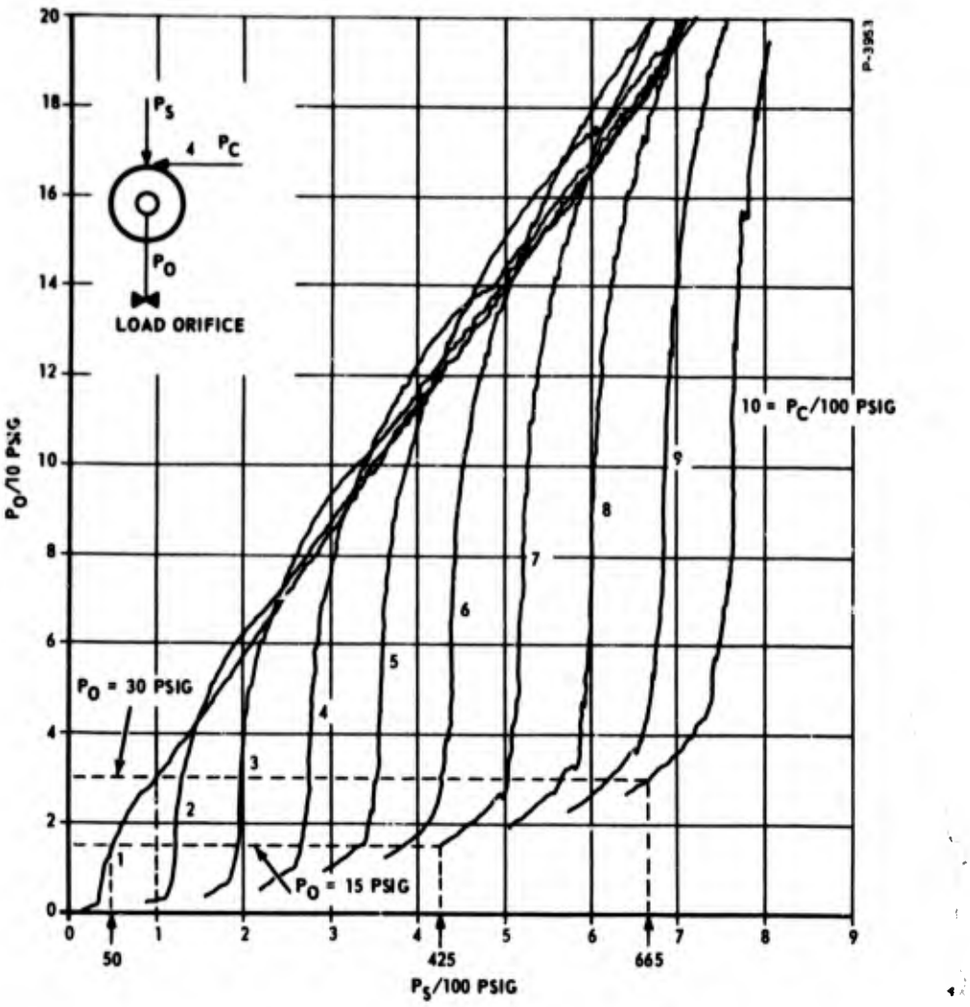

Figure 2-9 - Double Exit Vortex Valve Performance

which is to be compared with the turndown of 3.9 for the single exit valve. The slight improvement in turndown in this case is attributed to the loss of control port effectiveness that resulted when the annular clearance around the button was increased without a corresponding change in the control port. Another double-exit valve has demonstrated an 8.1/1 turndown ratio at a supply pressure of 80 psig, and there should be no change in its turndown ratio at higher pressures (no such change has been experienced in other valves). The 8.1/1 turndown ratio of this valve was confirmed prior to making the modifications in the original single exit valve button.

2.2.4.3 Tangential Control Performance

Both configurations above require control pressures equal to the supply pressure at full flow and control pressures above supply pressure at minimum flow. A third vortex throttling device controlled by a pressure less than supply is shown schematically in Figure 2-10. At P_c equal to zero, the flow is minimum and at P_c equal to P_s, the flow is maximum. This configuration was also experimentally investigated and the results are shown in Figure 2-11. We see that the valve will deliver the required load flow for supply pressures between 650 and 225 psig. The absolute supply pressure ratio 665/240 = 2.77 or the turndown ratio is 2.77. It is evident that the maximum flow occurs when P_s equals P_c.

A exit hole diameter to chamber diameter ratio of one-twelfth proved to be optimum in this case.

2.2.5 Multiple-Stage Vortex Throttling Valve

The problem of providing adequate turndown for the throttling valve suggests the possibility of one or more vortex valves acting as variable impedances, and turned the investigation toward the more general question of how to stage or combine vortex valves to realize throttling performance that cannot be achieved in a single valve alone.

Figure 2-12 shows a circuit consisting of two vortex valves connected in series and indicates the pressure and flow notation. The last subscript "i" refers to the initial conditions and the last subscript "f" refers to final conditions.

Figure 2-13 gives a representation of the normalized flow pressure characteristics of a variable pneumatic impedance. The upper curve AC represents the device "turned on," with the impedance a minimum. The lower curve BD represents the device "shut off" with the impedance a maximum.

The curves are plotted as w_o/w_N versus P_u/P_d where P_u/P_d is the pressure ratio, w_o is the outlet flow, and:

$$w_N \triangleq \frac{C_2 C_d A_e P_d}{\sqrt{T}} \qquad (2\text{-}5)$$

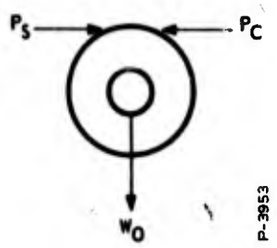

Figure 2-10 - Tangential Control Vortex Valve Schematic

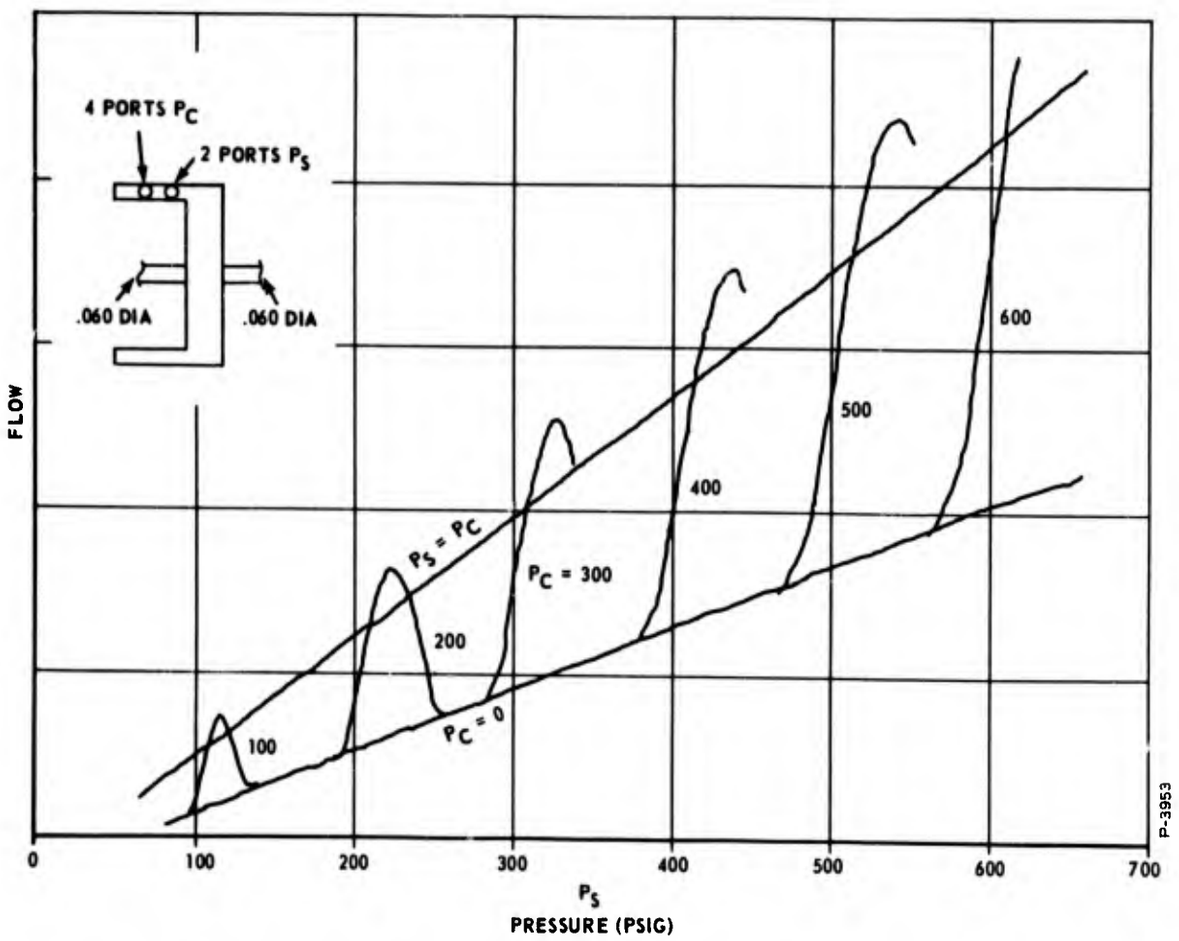

Figure 2-11 - Tangential Control Vortex Valve Performance

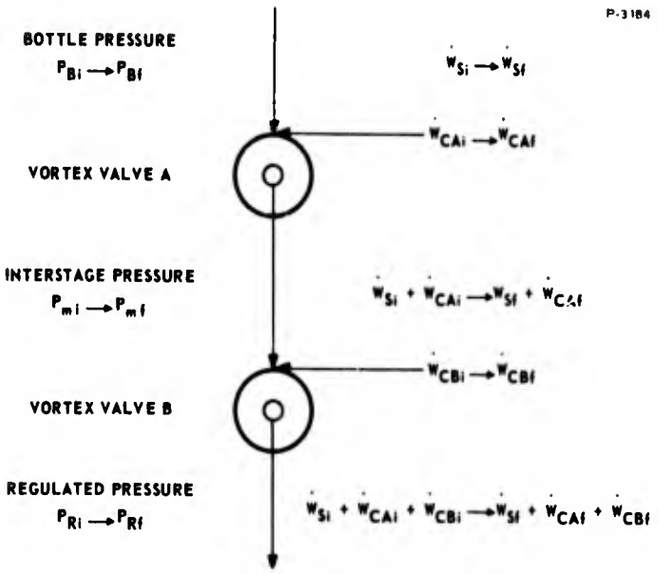

Figure 2-12 - Staging Analysis - Schematic and Notation

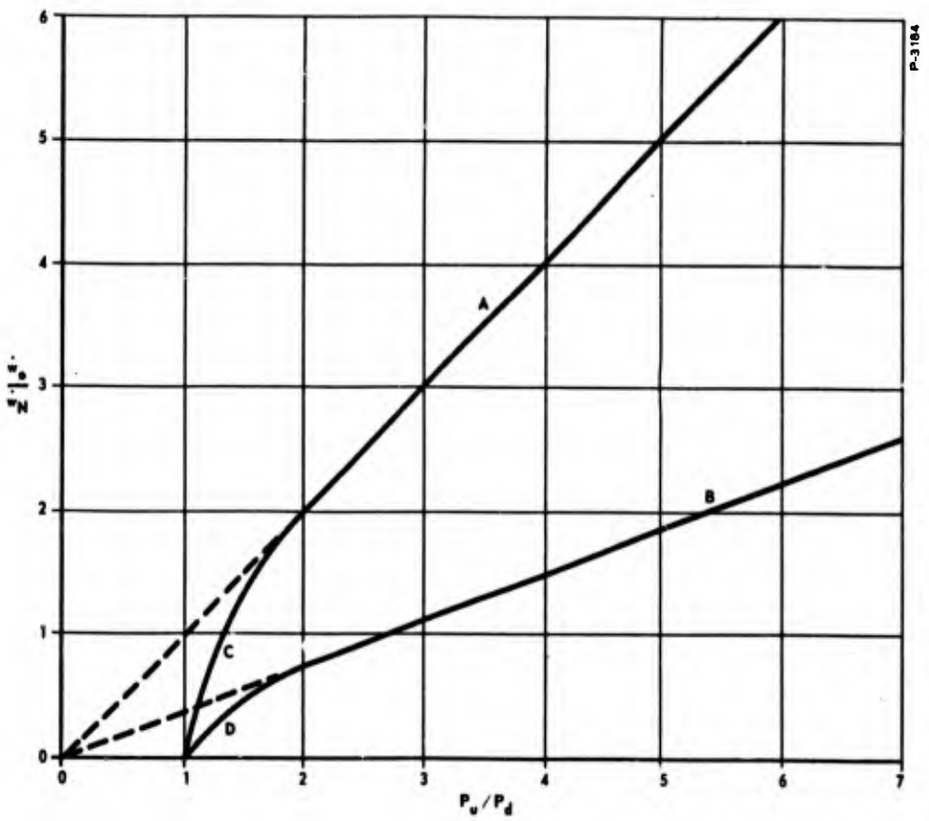

Figure 2-13 - Normalized Flow-Pressure Characteristics

where

$$C_2 = g\sqrt{\frac{k}{R\left(\frac{k+1}{2}\right)^{(k+1)/(k-1)}}} \qquad (2\text{-}6)$$

The equation of the straight line segment A is:

$$\frac{\dot{w}_o}{\dot{w}_N} = \frac{P_u}{P_d} \qquad (2\text{-}7)$$

The equation of the straight line segment B is:

$$\frac{R_t \dot{w}_o}{\dot{w}_N} = \frac{P_u}{P_d} \qquad (2\text{-}8)$$

where R_t is the turndown ratio (maximum impedance divided by minimum impedance) of the device.

A rigorous description of the curved line segments C and D would be based upon the equation for the flow of a compressible fluid through an orifice or nozzle. However, it is sufficiently accurate and much more convenient to use the elliptical approximation to the compressible flow equation credited to Fleigner.* Based on this approximation, the equation for the curved line segment C is:

$$1 + \frac{1}{4}\left(\frac{w_o}{w_N}\right)^2 = \frac{P_u}{P_d} \qquad (2\text{-}9)$$

Similarly, the approximate equation for the curved line segment D is:

$$1 + \frac{1}{1}\left(\frac{R_t w_o}{w_N}\right)^2 = \frac{P_u}{P_d} \qquad (2\text{-}10)$$

Equation (2-10) is only an approximate description of a vortex valve in the full turned down condition which will have a critical pressure ratio significantly greater than 2. However, the equation will be sufficiently accurate for use in the region $1 < P_u/P_d < 2$.

---

*"Thermodynamics," J. E. Emswiler, F. L. Schwartz, McGraw-Hill Book Company, Inc., New York and London, p. 302, 1943.

If the staged vortex valves of Figure 2-12 are part of a perfect pressure regulator supplying a fixed load we can say:

$$\dot{w}_{Si} + \dot{w}_{CAi} + \dot{w}_{CBi} = \dot{w}_{CAf} + \dot{w}_{CBf} + \dot{w}_{Sf} \qquad (2\text{-}11)$$

$$P_{Ri} = P_{Rf} = P_R \qquad (2\text{-}12)$$

If the downstream vortex valve B is to exercise any control over the flow through the staged impedances, the upstream vortex valve A must operate in a range of pressure ratios such that charges in the interstage pressure P_m will affect the flow through the vortex valve A. If the vortex valve A was an orifice, this would be approximately defined by $1 \leq P_B/P_m \leq 2$. Since a wide open vortex valve is an orifice and since $P_{Bi}/P_{mi} < P_{Bf}/P_{mf}$ we can say that $1 \leq P_B/P_m \leq 2$. That is, vortex valve A must operate in the region described by equations (2-11) and (2-12). For convenience we can assume that vortex valve B is described by equations (2-9) and (2-10).

If vortex valve A is in the fully turned down condition $\dot{w}_S = 0$ and the control flow $\dot{w}_{CA}$ will be the full flow through the valve. It will be impossible to operate vortex valve B in the fully turned down condition unless $\dot{w}_{CA} = 0$.

If we let R_{tA} be the turndown ratio of vortex valve A and R_{tB} be the turndown ratio of vortex valve B, we can write the following equations from equations (2-7) through (2-12) noting that the initial impedances must be a maximum if P_R and $\dot{w}_S + \dot{w}_{CA} + \dot{w}_{CB}$ are to be constant. This implies that $\dot{w}_{Si} = \dot{w}_{CAf} = \dot{w}_{CBf} = 0$.

$$R_{tB}\,(\dot{w}_{CAi} + \dot{w}_{CBi}) = \frac{C_2\, C_d\, A_B\, P_{mi}}{\sqrt{T}} \qquad (2\text{-}13)$$

$$\dot{w}_{Sf} = \frac{C_2\, C_d\, A_B}{\sqrt{T}}\, P_{mf} \qquad (2\text{-}14)$$

$$R_{tA}\, \dot{w}_{CAi} = \frac{2\, C_2\, C_d\, A_A\, P_{mi}}{\sqrt{T}} \sqrt{\left(\frac{P_{Bi}}{P_{mi}}\right) - 1} \qquad (2\text{-}15)$$

$$w_{Sf} = \frac{2\, C_2\, C_d\, A_A\, P_{mf}}{\sqrt{T}} \sqrt{\left(\frac{P_{Bf}}{P_{mf}}\right) - 1} \qquad (2\text{-}16)$$

We will define a parameter ψ :

$$\psi \triangleq \frac{\dot{w}_{CAi}}{\dot{w}_{CAi} + \dot{w}_{CBi}} = \frac{\dot{w}_{CAi}}{\dot{w}_{Sf}} \qquad (2\text{-}17)$$

Equations (2-5) and (2-13) through (2-17) may be combined to give:

$$\left(\frac{\psi R_{tA}}{R_{tB}}^2\right) = \frac{\left(\frac{P_{Bi}}{P_{mi}} - 1\right)}{\left(\frac{P_{Bf}}{P_{mf}} - 1\right)} \qquad (2\text{-}18)$$

We will define an overall turndown ratio for the staged vortex valves

$$R_{to} = \frac{\Delta P_{Bi}}{P_{Bf}} \qquad (2\text{-}19)$$

From equations (2-13) and (2-14) it can be seen that

$$R_{tB} = \frac{P_{mi}}{P_{mf}} \qquad (2\text{-}20)$$

Combining equations (2-18) through (2-20) gives:

$$R_{to} = \left(\frac{P_{mf}}{P_{Bf}}\right) \left(\frac{R_{tB}^2 - \psi^2 R_{tA}^2}{R_{tB}}\right) + \left(\frac{\psi^2 R_{tA}^2}{R_{tB}}\right) \qquad (2\text{-}21)$$

The limiting cases are:

$$\text{If } \frac{P_{mf}}{P_{Bf}} = 1,\ R_{to} = R_{tB} \qquad (2\text{-}22)$$

$$\text{If } \frac{P_{mf}}{P_{Bf}} = \frac{1}{2}, \; R_{to} = \frac{R_{tB}^2 + \psi^2 R_{tA}^2}{2 R_{tB}} \qquad (2\text{-}23)$$

From the above equation, it can be seen that unless $\psi R_{tA} > R_{tB}$, $< R_{to} < R_{tB}$. Furthermore, it will be impossible to operate vortex valve B in the fully turned down conditions, since provision must be made for the flow $\dot{w}_{CA}$. Thus the value for R_{tB} in the staged configuration will be less than the maximum R_{tB} possible. Permitting even small amounts of supply flow to enter a vortex valve significantly decreases turndown ratio.

Since the overall turndown ratio of the two vortex valves connected in series will in general be less than the turndown ratios of the individual valves, and since the effective turndown ratios of the individual valves will be less than the maximum possible value, it may be concluded that staging valves will give no improvement in turndown. In certain cases, there will be an improvement in the value of P_C/P_S required to obtain a given turndown. This will be discussed in the next Section.

2.2.6 Vortex Throttling Valve with Vortex Pilot Valve

Another method of cascading vortex valves is to use a "pilot" valve (Figure 2-14) which feeds the control and supply ports of a second valve as shown in Figure 2-15. The "pilot" valve pickoff

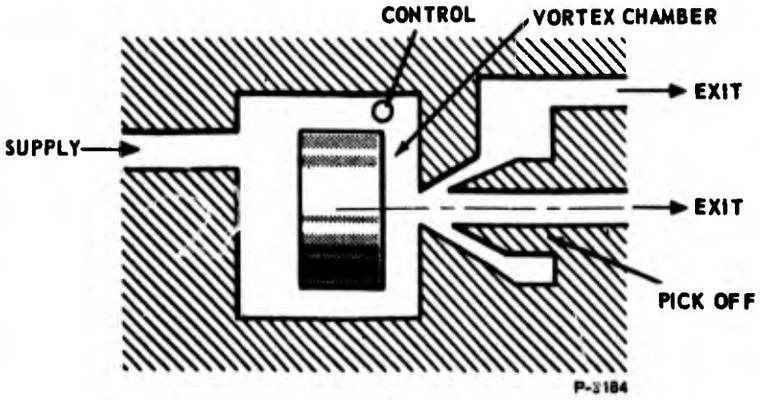

Figure 2-14 - Output Configuration for Vortex Pilot Valve

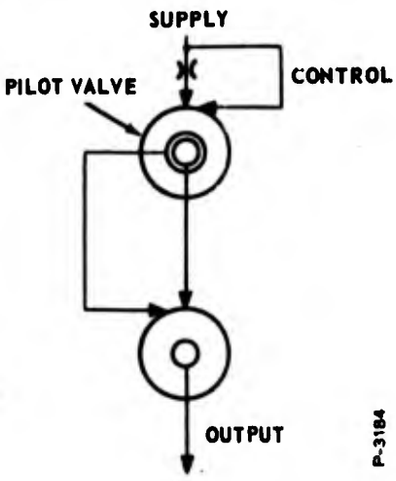

Figure 2-15 - Pilot Configuration of Cascaded Vortex Valve

converts the vortex valve into an amplifier. The differential pressure change between the two pickoff exits (Figure 2-14) changes much more rapidly than the control pressure. Furthermore the central exit of the pickoff see almost 98 percent of the supply pressure with no control or swirl flow exits and almost zero pressure when the valve is turned down. The annular exit around this center pickoff serves to capture the diverted flow from the pickoff when it is shut off by full control flow. The characteristics of valves connected in this way were determined experimentally and the effect of the pickoff location was investigated over a range of 0.25 to 1.75 outlet hole diameters. When the pickoff is 0.25 diameter from the outlet hole, the valve combination requires a minimum P_C/P_S for full turndown, but the throttling can not be controlled over the complete throttling range. A jump phenomenon with hysteresis occurs at the most sensitive operating point until the pickoff is moved to about 1.25 diameters from the outlet hole. When the pickoff is more than 1.25 diameters from the outlet hole, the turndown ratio is reduced. Performance characteristics for the pilot configuration of cascaded valves, with what appears to be the best location for the pickoff, are shown in Figures 2-16 and 2-17. From Figure 2-16, the inlet pressure range where the combined valves will satisfy the regulator throttling requirement is from 900 to 200 psig.

2.3 FEEDBACK METHODS

2.3.1 Performance of Confined-Jet Amplifiers

The feedback amplifier must operate with output bias pressure higher than the input bias pressure. The confined-jet amplifier shown in Figure 2-18 is the only available element with characteristics that satisfy this requirement, so the performance of individual confined-jet amplifiers must be well understood before an attempt is made to combine them in a staged feedback amplifier.

The test schematic diagram and the confined-jet receiver configurations that have been investigated are shown in Figure 2-19. Figures 2-20 to 2-23 show the output pressure versus control pressure with various constant supply pressures. For these tests, the receiver was positioned two nozzle diameters from the nozzle and load orifice area was one-half of the nozzle area. Note that the noisy operation in the high gain region of receiver A is reduced by the internal cone of receiver B. The noise is further reduced by the coned configurations

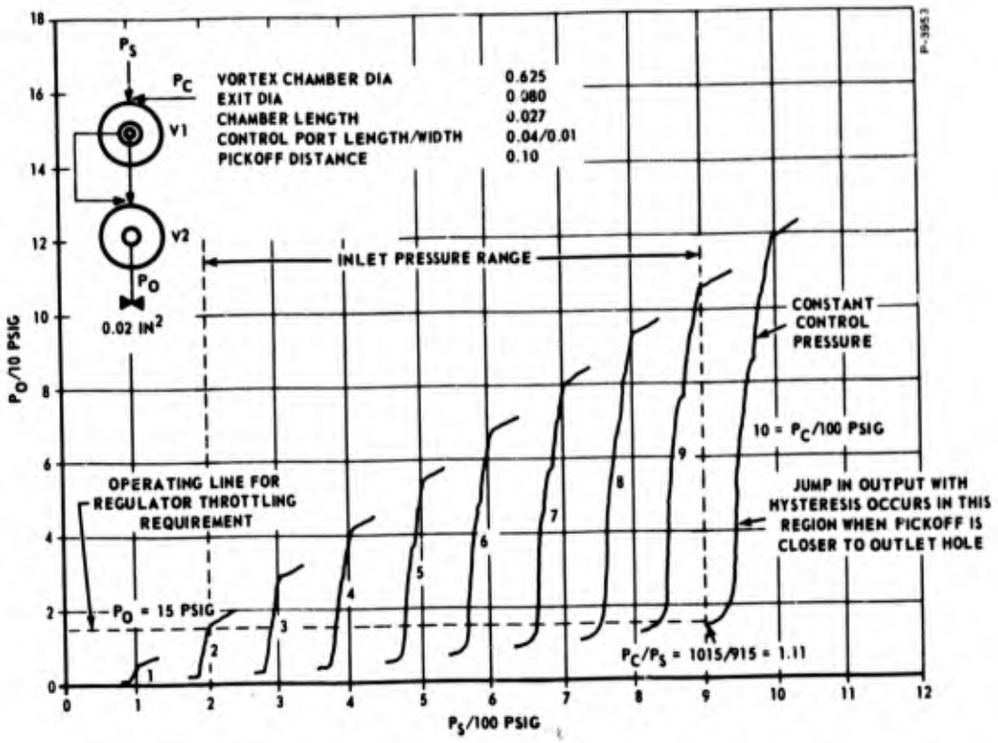

Figure 2-16 - Two-Stage Piloted Vortex Valve Performance

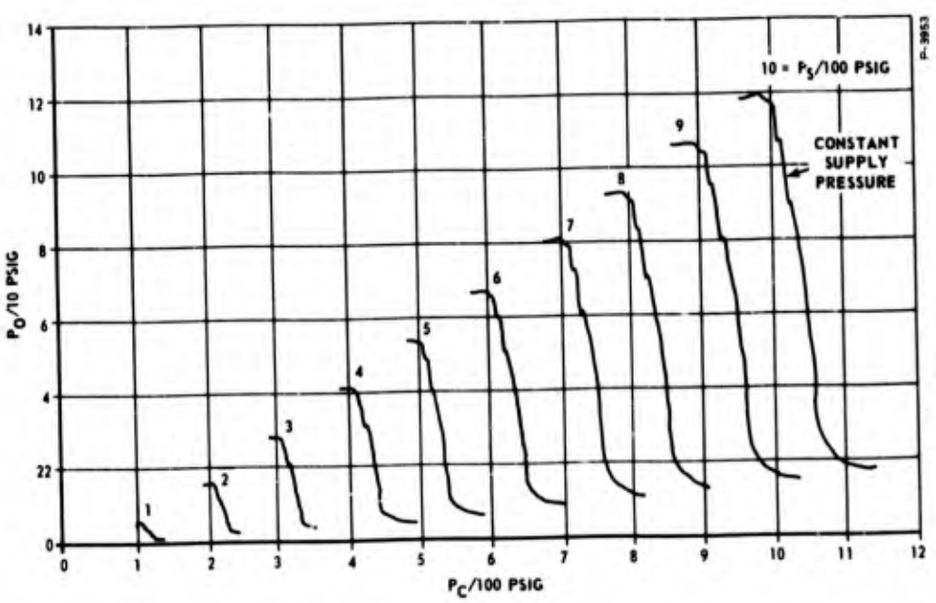

Figure 2-17 - Two-Stage Piloted Vortex Valve Performance

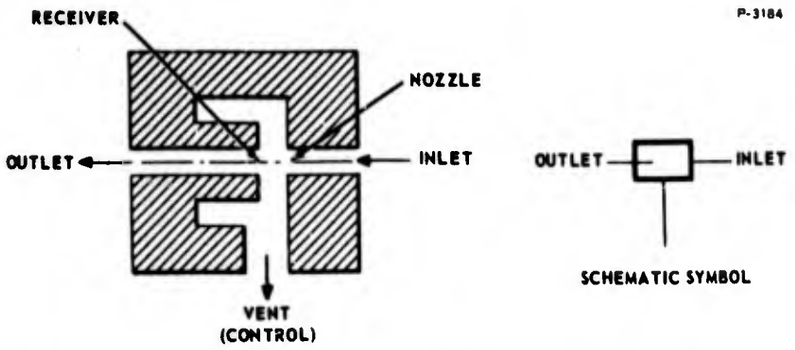

Figure 2-18 - Confined-Jet Amplifier Configuration and Schematic Symbol

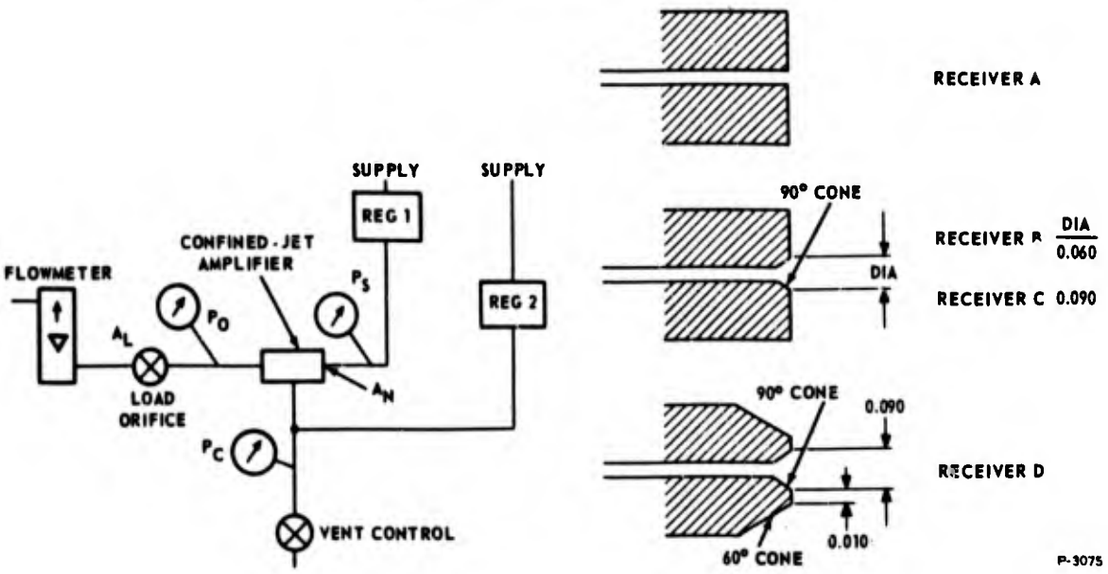

Figure 2-19 - Confined-Jet Amplifier Test and Receiver Configurations

of receiver C and D. Forty variations of receiver spacing from L/D = 0.5 to 3 were investigated, using the four receiver configurations. Of these, the performances of receivers B and D (Figure 2-21 and 2-22) offer the highest incremental gain and operating range with comparatively low noise. The useful operation appears to be in the range P_C/P_S = 0.15 to 0.25, and the maximum output pressure is about 70 percent of the supply pressure.

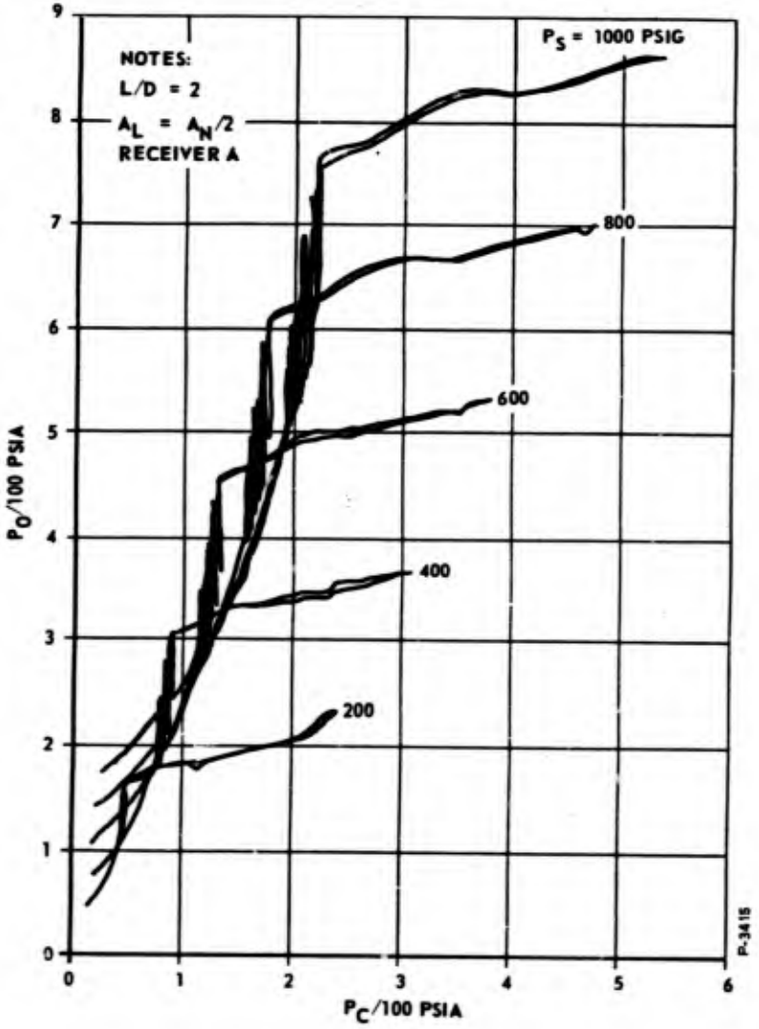

Figure 2-20 - Confined-Jet Amplifier Performance - Receiver A

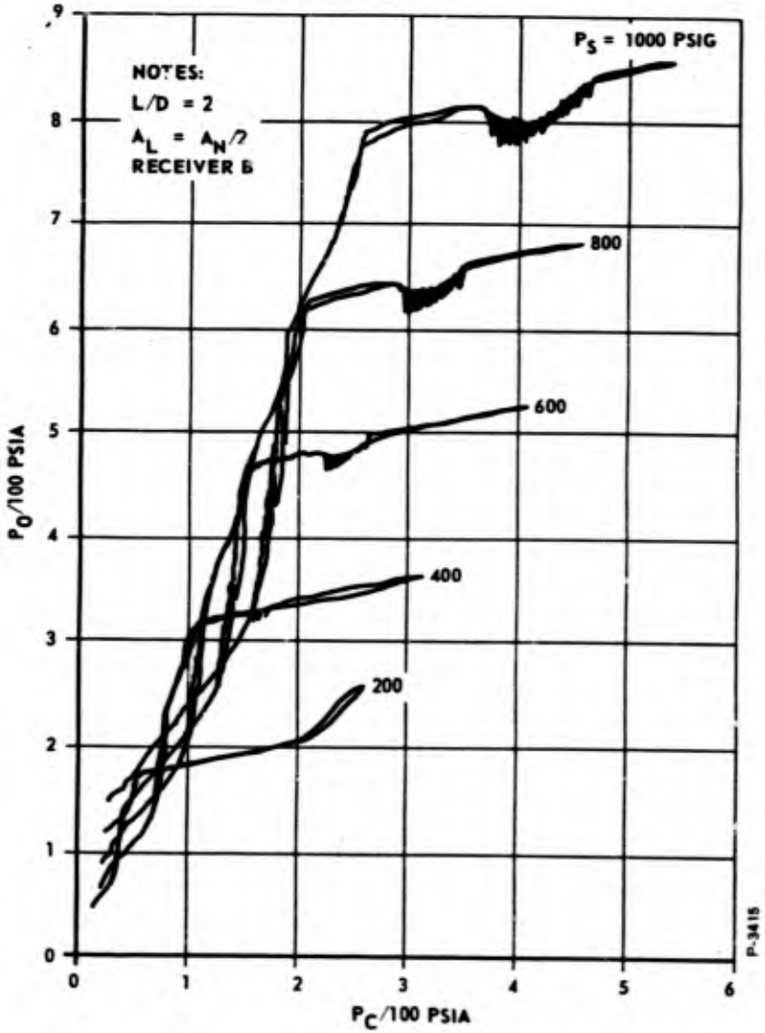

Figure 2-21 - Confined-Jet Amplifier Performance - Receiver B

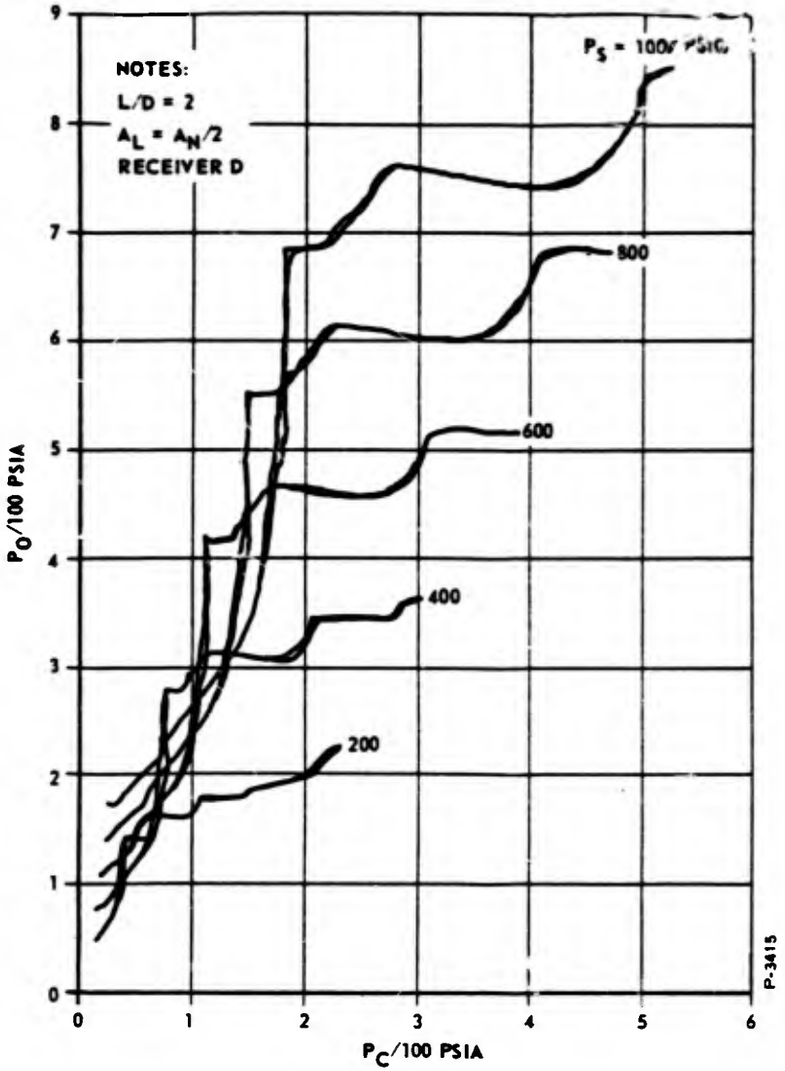

Figure 2-22 - Confined-Jet Amplifier Performance Receiver D

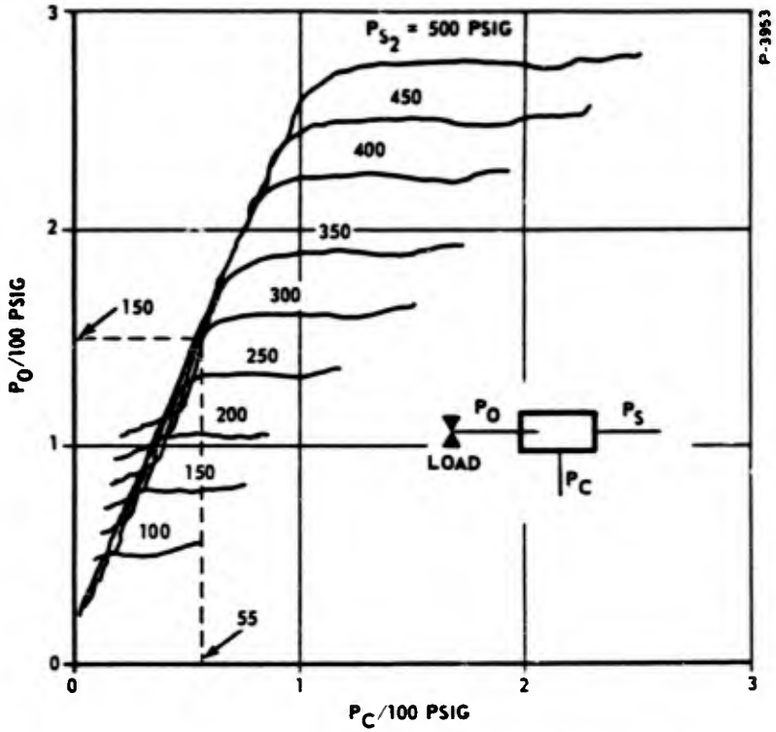

Figure 2-23 - Confined-Jet Amplifier Performance Receiver A

An interesting, and possibly useful property of confined-jet amplifiers is illustrated in the test results shown in Figure 2-23. For this test, a type-A receiver was used with L/D = 1.4 and the load area was equal to the nozzle area. We observe that, if the control pressure is held at 55 psig, the output pressure is very nearly independent of the supply pressure for $300 < P_S < 500$. This property, a result of the over-lapping characteristics for different supply pressures, seems to hold for the type-A receiver more than the others, and the range of the supply pressure independence seems to increase with the load area. The output pressure recovery falls off with increasing load area, so there is a limit to the supply pressure range that can be obtained by loading.

2.3.2 Confined-Jet Amplifiers with Vortex Control Valves

A single-stage feedback amplifier is formed by using a vortex valve to control the vent flow (or pressure) of the confined-jet amplifier as shown in Figure 2-24. The output pressure recovery of the confined-jet amplifier is greater than the control pressure required for the vortex valve, so the output can be used directly to provide either positive or negative feedback around the amplifier. The performance of this circuit is shown in Figures 2-25 and 2-26. The use of positive feedback increases the output pressure recovery and reduces the control pressure required to deliver the maximum output pressure.

2.3.3 Parallel-Staged Confined-Jet Feedback Amplifiers

The parallel-staged feedback amplifier configuration is shown in Figure 2-27. The input-output characteristics of this amplifier are shown in Figure 2-28 and the corresponding interstage pressures are shown in Figure 2-29. These characterisitcs were obtained without positive feedback around either stage; it does not appear that positive feedback will be required to get high incremental gain. The characteristics with the load area set to produce output pressure saturation at about 70 percent of the supply pressure are shown in Figure 2-30.

2.4 REFERENCE METHODS

2.4.1 Single Versus Multiple-Orifice Bridge

The pneumatic flow characteristics of a series of equal area orifices have been developed in Appendix D; these results can be normalized by means of the following equation.

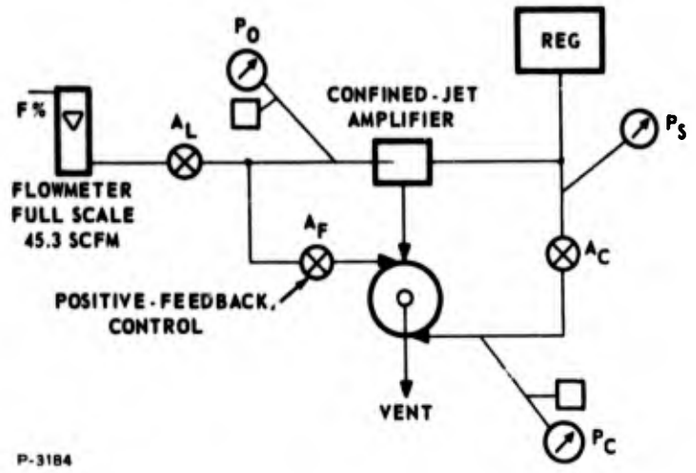

Figure 2-24 - Single-Stage Feedback Amplifier Test Schematic

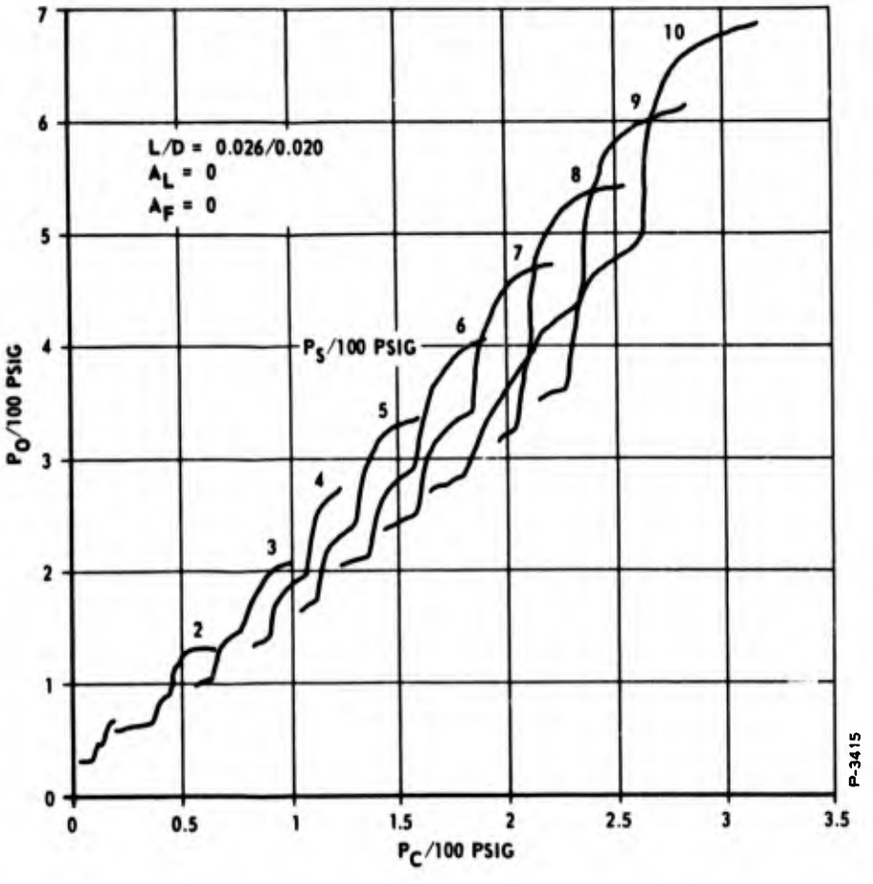

Figure 2-25 - Single-Stage Feedback Amplifier Performance; No Feedback

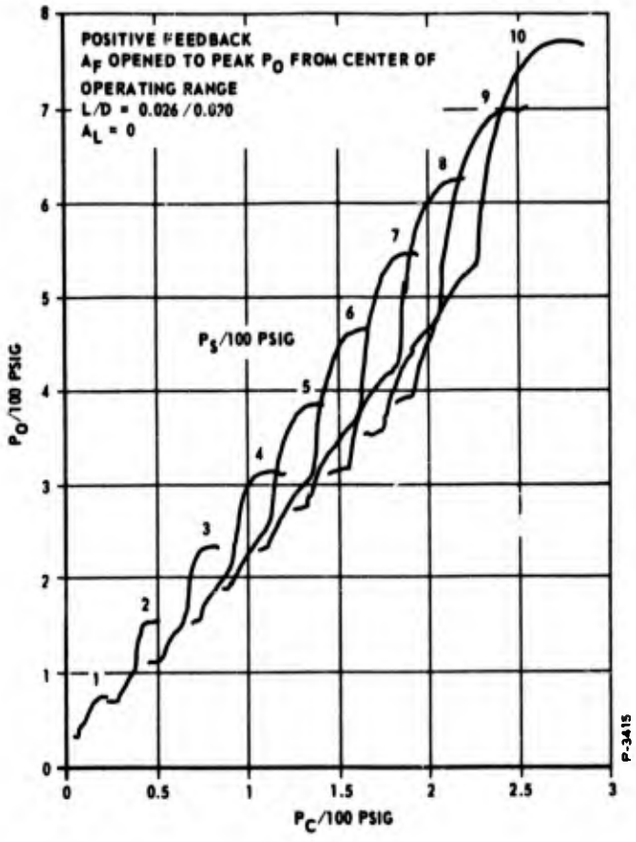

Figure 2-26 - Single-Stage Feedback Amplifier Performance; Positive Feedback

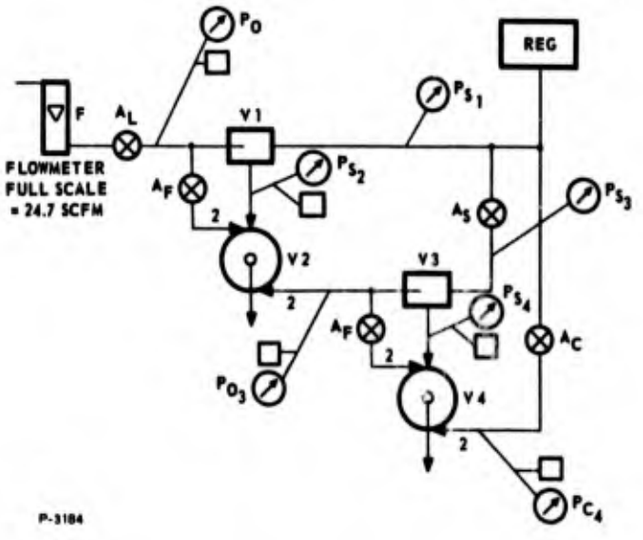

Figure 2-27 - Parallel-Staged Feedback Amplifier Test - Two Stages

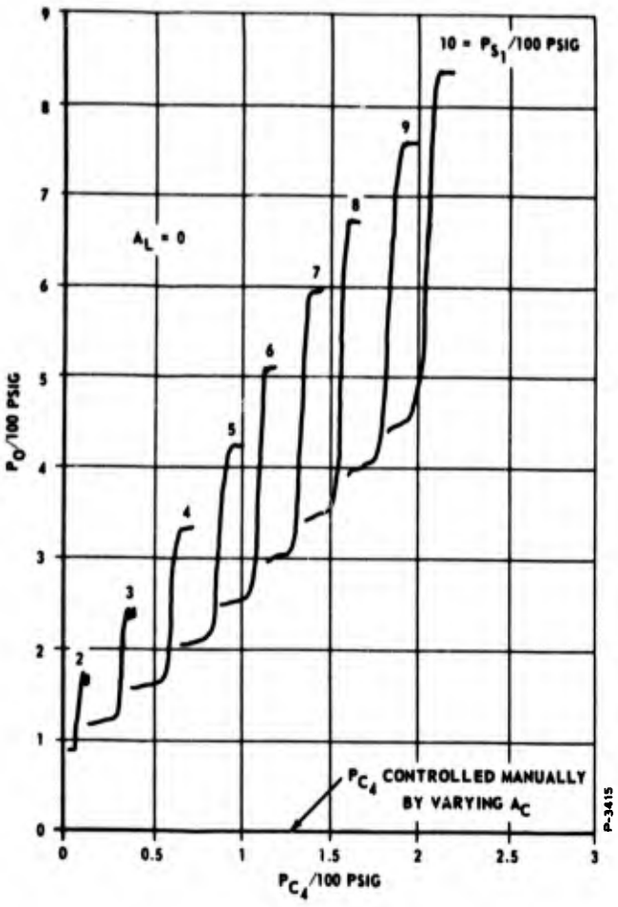

Figure 2-28 - Two-Stage Feedback Amplifier Performance

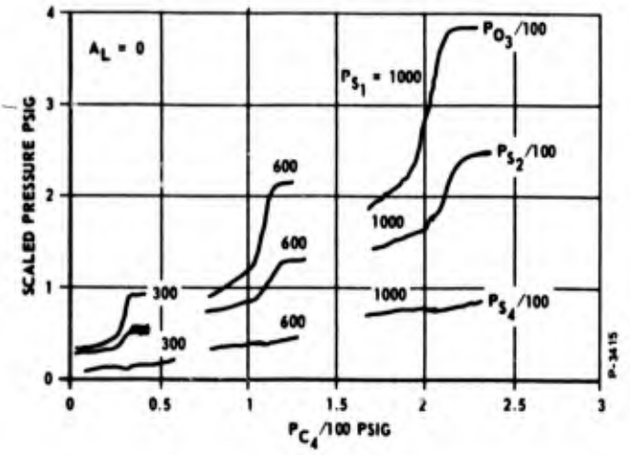

Figure 2-29 - Two-Stage Feedback Amplifier Interstage Pressure Corresponding to Figure 2-28

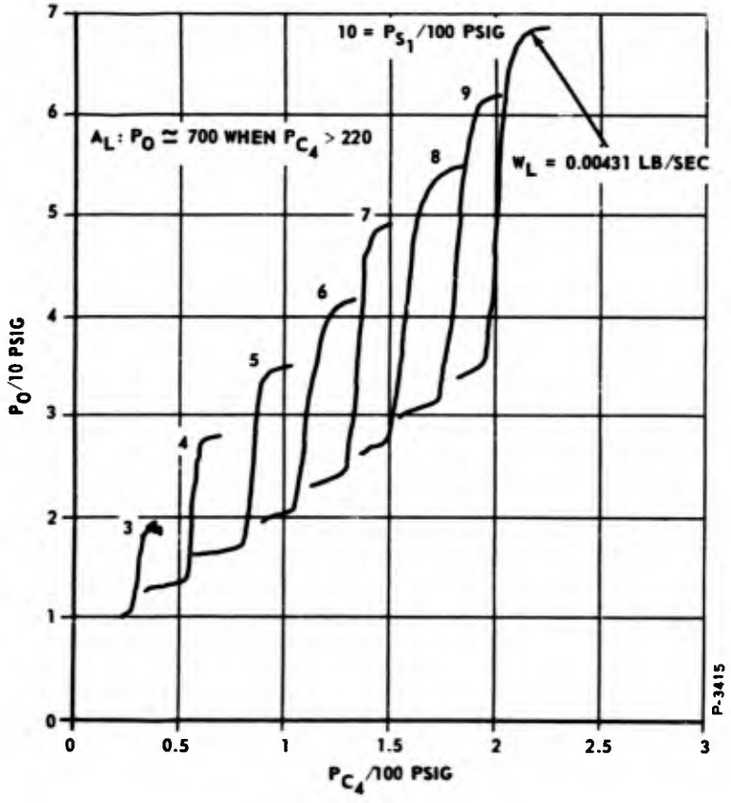

Figure 2-30 - Two-Stage Feedback Amplifier Performance with Output Load

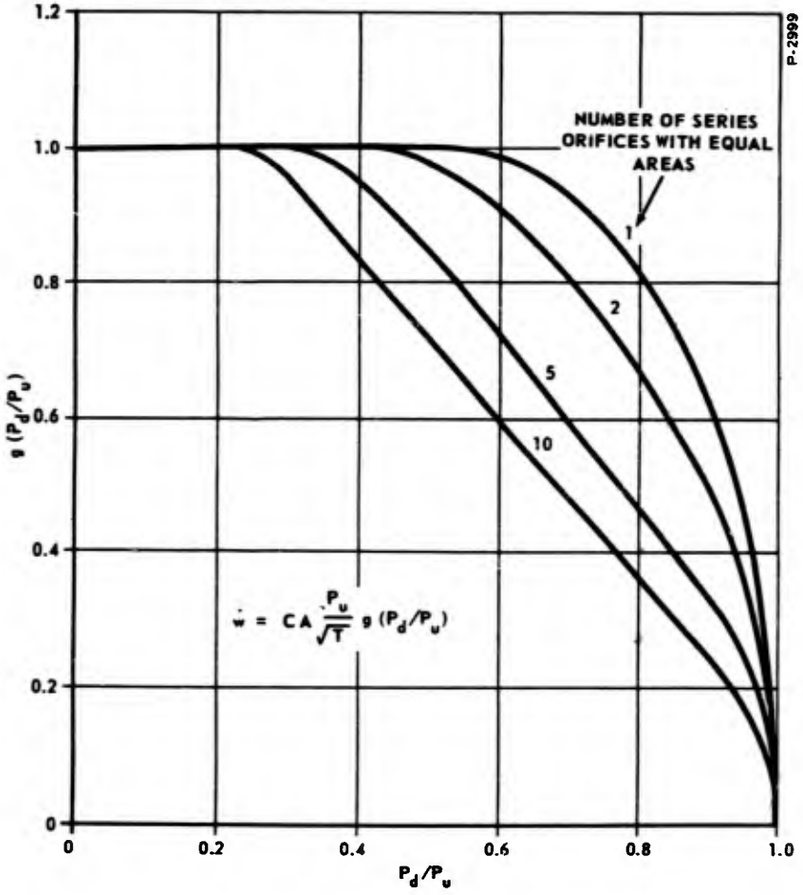

Figure 2-31 - Flow Function for Orifices in Series

$$g\left(\frac{P_d}{P_u}\right) = \frac{\left(\frac{A_m}{A_1}\right)\left(\frac{P_d}{P_u}\right)^{1/k}\sqrt{1-\left(\frac{P_d}{P_u}\right)^{(k-1)/k}}}{\left(\frac{A_m}{A_1}\right)\left(\frac{P_d}{P_u}\right)^{1/k}\sqrt{1-\left(\frac{P_d}{P_u}\right)^{(k-1)/k}}}_{\max} \qquad (2\text{-}24)$$

If n=1, the above equation gives the f_1 function which is frequently used to calculate the flow of gases through restrictions. The function g (P_d/P_u) is plotted in Figure 2-31 for n=1, 2, 5, and 10 and k = 1.4.

As can be seen from the Figure 2-31, increasing the number of orifices makes g (P_d/P_u) a more nearly linear function of P_d/P_u and also decreases the critical pressure ratio. For n = 10, the critical pressure ratio is approximately 0.250 compared to 0.528 when n = 1.

This change in shape of the flow function curve as pressure ratio changes appears to have application as a method of measuring changes in regulated pressure. If a series of n orifices is flowed in parallel with a single orifice, the relative quantities of flow in each branch will be a function of pressure ratio across them. The changes in flow in the two branches may be detected if the branches are in the supply and control lines of a vortex pressure amplifier as is indicated in Figure 2-32.

One restriction is that the outlet orifice of the vortex pressure amplifier must be flowing at a nonsonic pressure ratio. This is a consequence of the fact, as is shown in Appendix D, that settling the pressure ratio across an orifice sets the pressure ratio across any other orifice in series with it. If the outlet orifice of the vortex pressure amplifier is at a sonic pressure ratio, its pressure ratio will be effectively independent of changes in the sensed pressure. As a consequence, the pressure ratio across the parallel orifice branches will be fixed and the relative flows through the branches will be fixed, locking the operating point of the pressure amplifier.

In all fluid state systems, it is important that the various components be properly matched. Thus, the pressure amplifier must be capable of supplying flow to the components it controls. The ability of a pressure amplifier to deliver flow decreases as its gain increases.

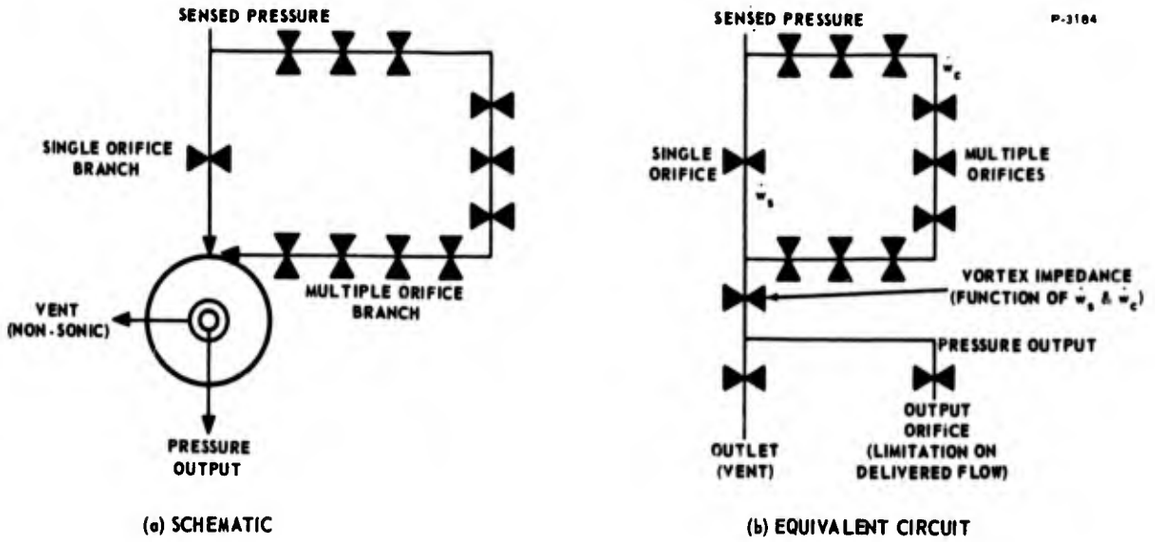

Figure 2-32 - Single Versus Multiple Orifice Bridge

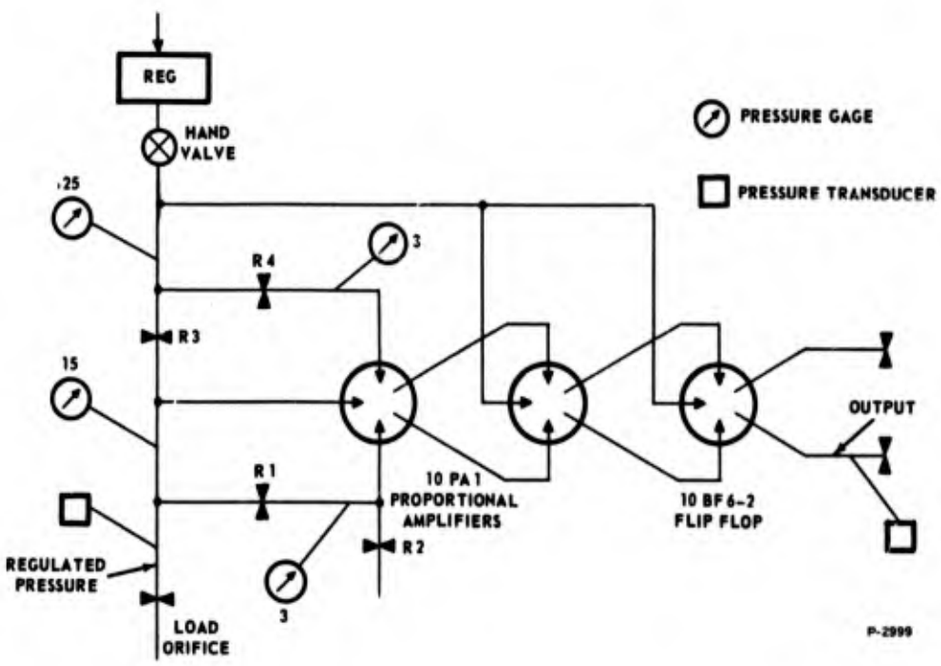

Figure 2-33 - Reference Circuit Test Schematic

Furthermore, the output of the pressure amplifier is at a lower level than the sensed pressure. These factors impose restrictions upon this approach which will require further investigation.

2.4.2 Reference Circuit Using Jet-on-Jet Amplifiers

The use of a sonic versus subsonic-orifice bridge circuit has been demonstrated using jet-on-jet amplification as shown in Figure 2-33. In this circuit, orifice R4 is sonic and R1 is subsonic at the quiescent operating pressures indicated on the Figure. The pressures downstream of orifices R1 and R4 are set equal at quiescent conditions so there is zero differential output from the proportional amplifiers; these pressures do not change symmetrically with small variations of the throttling valve (hand valve), so a differential input signal is applied to the control ports of the first proportional amplifier when the regulated pressure changes as a result of a change in the throttling valve flow. The input differential pressure signal is amplified by the proportional amplifiers to drive a flip-flop output device.

The performance of this reference circuit is shown in Figure 2-34 where several traverses of regulated pressure were made

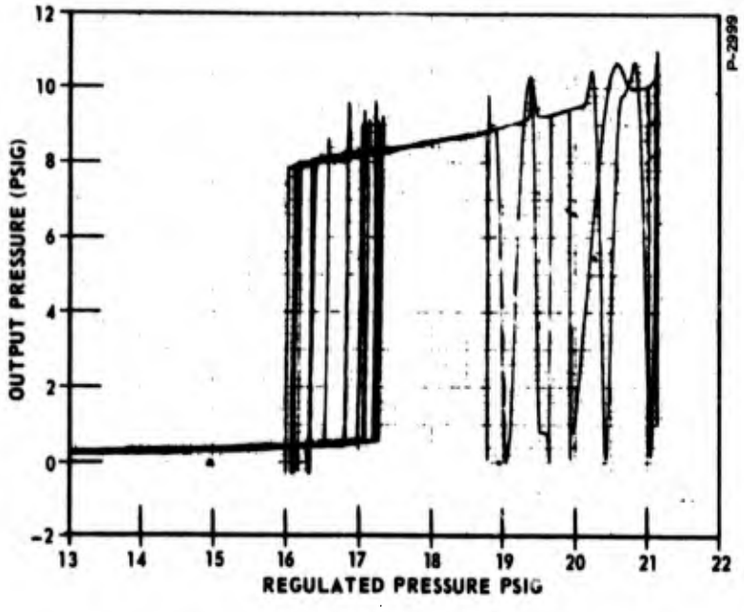

Figure 2-34 - Reference Circuit Switching Characteristic

to examine repeatability. The maximum total hysteresis is less than 1.5 psi, but there is some erratic switching at regulated pressures above 19 psig. This test was intended only to demonstrate the feasibility of orifice reference bridges and not the method of reference signal amplification.

2.4.3 Inherent Reference of Feedback Amplifiers

The two preceeding reference schemes have been based upon the detection of shifts in the regulated pressure by means of orifice bridge circuits and the amplification of the output of the bridge by means of fluid amplifiers. The output of the reference circuit is then further amplified in the feedback circuit to furnish a signal which is capable of controlling the throttling element.

Since the feedback circuit is required to amplify the output of the reference circuit in any event, the question arises as to the need for amplification in the reference circuit. Elimination of the reference circuit amplifier has one desirable feature, the drop in pressure across the reference circuit is eliminated, reducing the magnitude of the pressure ratio across the feedback circuit.

Elimination of a separate reference circuit implies that the difference between atmospheric pressure and the regulated pressure can be applied directly to the input of the feedback circuit. Or, the complete regulator can be a closed system with only the output pressure open to atmospheric pressure. Such a regulator would be an "absolute" pressure regulator as it would tend to keep the output pressure at a level independent of atmospheric pressure.

BLANK PAGE

SECTION 3

INVESTIGATION OF REGULATION CONCEPTS

3.1 CONTROL OF THE THROTTLING VORTEX VALVE

3.1.1 General

To control the valve in Figure 2-8 along the line of P_0 = 15 psig, the control pressure must be at least equal to the control pressure ratio P_C/P_S = 1.15 times the supply pressure when P_S = 650 psig and decreases to the supply pressure as the supply pressure decreases to 150 psig.

The simplest control scheme would be to store part of the gas at higher pressure for control purposes as illustrated in Figure 3-1. P_{BC} must be greater than P_B if the programming, reference, and feedback elements are to provide the control pressure P_C required along the line P_R = 15 psig in Figure 2-8. Extending this line to the right,

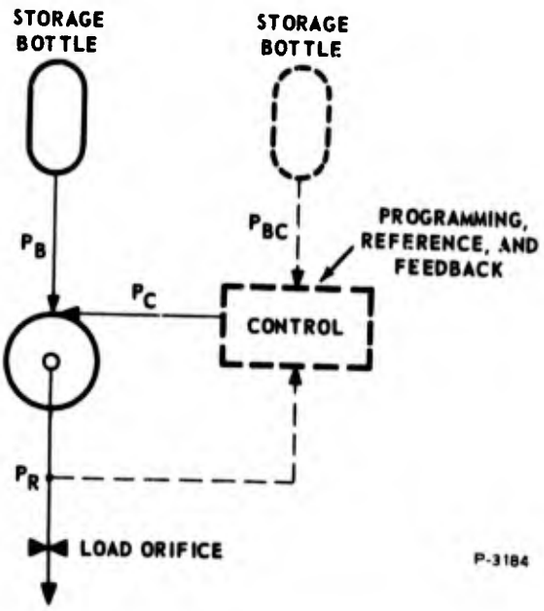

Figure 3-1 - Single-Stage Vortex Throttling Element with Part of the Gas Supply Stored at Higher Pressure for Control Purposes

beyond the range of the single-exit valve, we estimate the control pressure required for supply flow cutoff would be 1160 psig when the storage bottle pressure P_B is 1000 psig. If the feedback amplifier can then deliver a P_C up to about 80 percent at P_{BC}, a storage pressure of 1500 psig would be enough for the supply cutoff point at P_B = 1000 psig in Figure 2-8. We see that a valve with turndown ratio 181/30 = 6.0 would provide the throttling range from P_B = 1000 to 150 psig. This dual storage bottle concept will be discussed further in another section.

Another potential method of obtaining the P_C/P_S ratio required to shut off the throttling vortex valve at the higher levels of P_B would be to use a pressure dropping orifice in the supply line of the vortex valve. However, this approach can be eliminated from consideration for this application by the following analysis.

A large signal vortex valve characteristic similar to the characteristic shown in Figure 2-8 was programmed on a digital computer. This characteristic was then applied to the circuit shown in Figure 3-2.

3.1.2 Load Line Analysis

Figure 3-3 shows the general characteristics of a typical vortex valve. In the top figure, 3-3(a), the supply flow characteristic of the valve is shown at zero control flow and at four fixed control pressures, P_{c1}, P_{c2}, P_{c3} and P_{c4}. The orifice characteristic may be superimposed on this map. This representation is helpful when the characteristics of the circuit shown in Figure 3-2 are to be evaluated at a constant value of P_{in}. This is the case when the orifice is used to generate the difference between supply and control pressure necessary

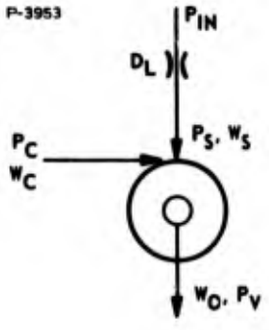

Figure 3-2 - Circuit Schematic

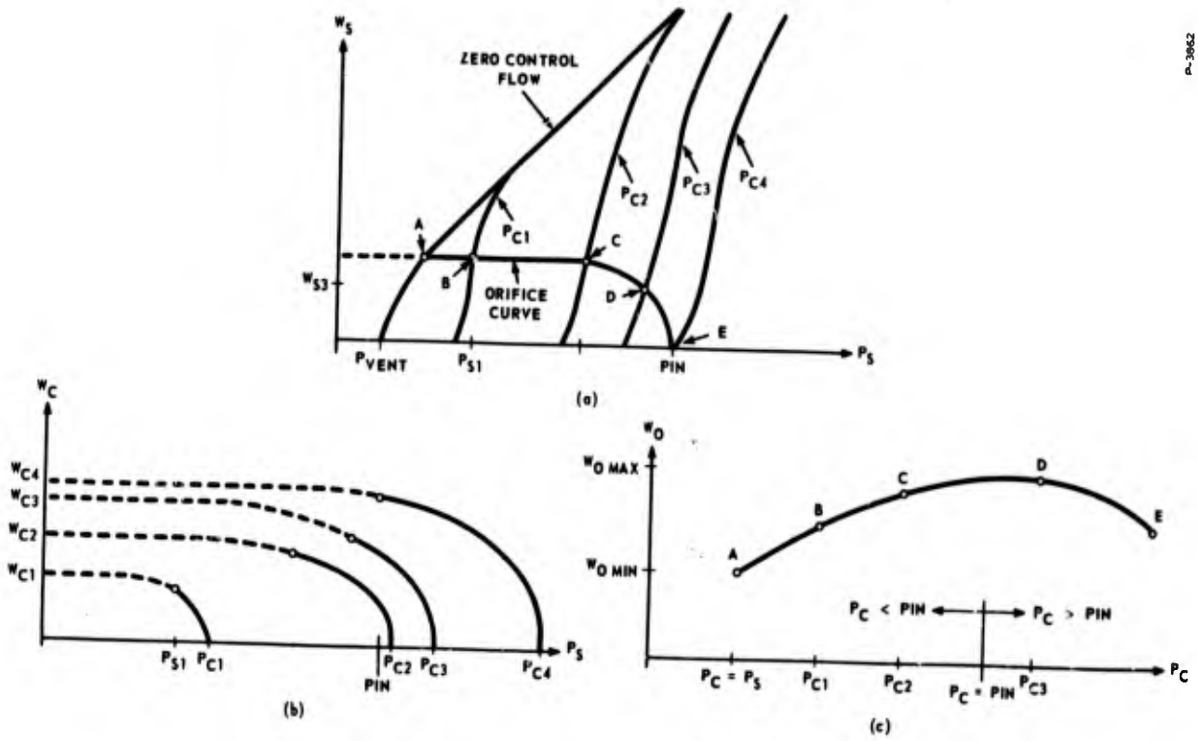

Figure 3-3 - Typical Load Line Analysis

to operate a vortex valve from a single pressure source. The middle plot, Figure 3-3(b) gives the control flow curves at the corresponding control pressures P_{c1} through P_{c4}. In the bottom plot, Figure 3-3(c), the total flow through the valve, $W_o = W_s + W_c$, as given by the sum of the upper two curves is shown.

Zero control flow occurs at $P_s = P_c$ for the vortex valve. At this condition, the value of W_s is defined by the size of the series orifice and the size of the vortex valve for a fixed P_{in}. For the conditions shown, the pressure drop across the orifice is sufficiently high to develop sonic flow through the outlet of the vortex valve. Thus, the supply flow is dependent only on the size of the upstream orifice and the value of P_{in}. The supply pressure is defined by the intersection of the two flow curves at point A.

Increasing the control pressure to the value P_{c1} is shown by the constant control pressure characteristic curve in the top figure, 3-3(a). The supply flow is still the same, as the intersection point B is still on the sonic portion of the orifice load line. The supply pressure

is P_{s1} at the intersection; the corresponding control flow is W_{c1} as given in the middle graph, Figure 3-3(b). The total flow is greater at this point than at the initial condition with zero control flow. Further increase in the control pressure results in a general increase of the outlet flow as long as the flow through the series orifice is sonic, point C. Only after the flow becomes subsonic in the orifice, point D, will the total flow gradually decrease by increasing the swirl within the vortex valve. At the end, if the control pressure is increased sufficiently, P_{c4}, the supply flow becomes zero, point E.

The above discussion indicates the general behavior of the vortex valve with a series orifice in the supply line:

(1) Flow turndown takes place only in the subsonic range.

(2) The turndown will be significantly reduced if the control pressure is not allowed to exceed P_{in}, as shown in Figure 3-3(c).

(3) The maximum and the minimum flow conditions do not occur at the end points.

(4) The relative size of control port and series orifice will significantly influence the exact behavior of the circuit.

(5) The most promising operation zone is in the highly nonlinear range.

The last point is illustrated in Figure 3-4, giving the effect of both the series orifice size and the control port size. The operation of the circuit with two sizes of control port and two sizes of series orifice is shown. Only the two end conditions are defined by the load lines: the condition at zero control flow, and the condition where $P_{in} = P_c$ is used for the minimum flow. The total flow through the circuit is again shown on the bottom graph, Figure 3-4(c) for the four combinations. The optimum flow turndown is dependent on the value of the maximum flow that occurs at an intermediate control pressure. Thus, if a reasonably accurate prediction of the ratio of maximum to minimum flow is desired, end point analysis will not be satisfactory. The load line technique will result in accurate prediction only when the nonlinear characteristics of the vortex valve in the area are well-defined.

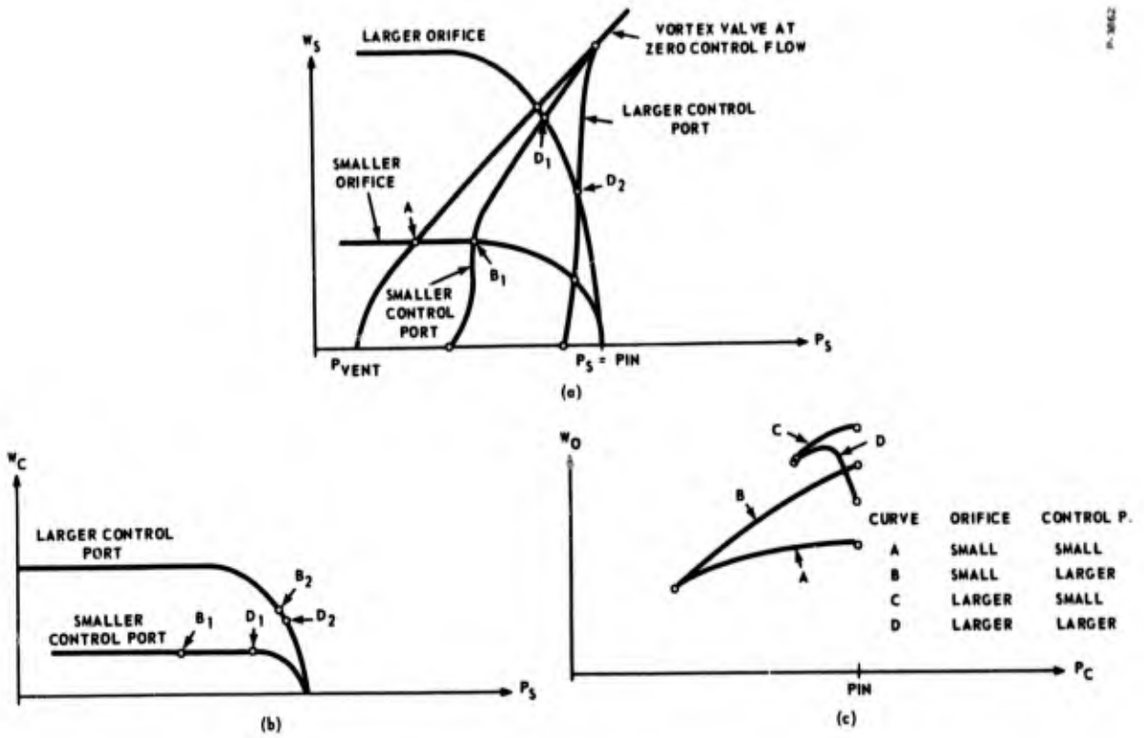

Figure 3-4 - Load Line Analysis Effect of Port Sizes

3.1.3 Computer Analysis

In addition to the vortex valve characteristics, the series orifice flow is described by

$$W_S = \frac{\pi}{4} D_L^2 C_{d_3} \frac{1}{\sqrt{T_S}} P_{in} C_1 f_1 \left(\frac{P_S}{P_{in}} \right) . \qquad (3\text{-}1)$$

Figures 3-5, 3-6, and 3-7 indicate that the general character of the circuit is as anticipated from the load line analysis. Figure 3-5 represents the results with a vortex valve using a 0.030-inch control port, Figure 3-6 with a 0.055-inch control port and Figure 3-7 with a 0.086-inch control port. In each of the three figures, the results with 0.312-, 0.208-, 0.104-, 0.073- and 0.052-inch load orifices are shown corresponding to flow area ratios of 9, 4, 1, 0.5 and 0.25 between the load orifice and the vortex valve outlet orifice areas. From the curves, the turndown ratio may be calculated for various conditions. The maximum turndown possible if P_c can not exceed P_{in} is of interest representing the operation of the circuit from a single pressure source.

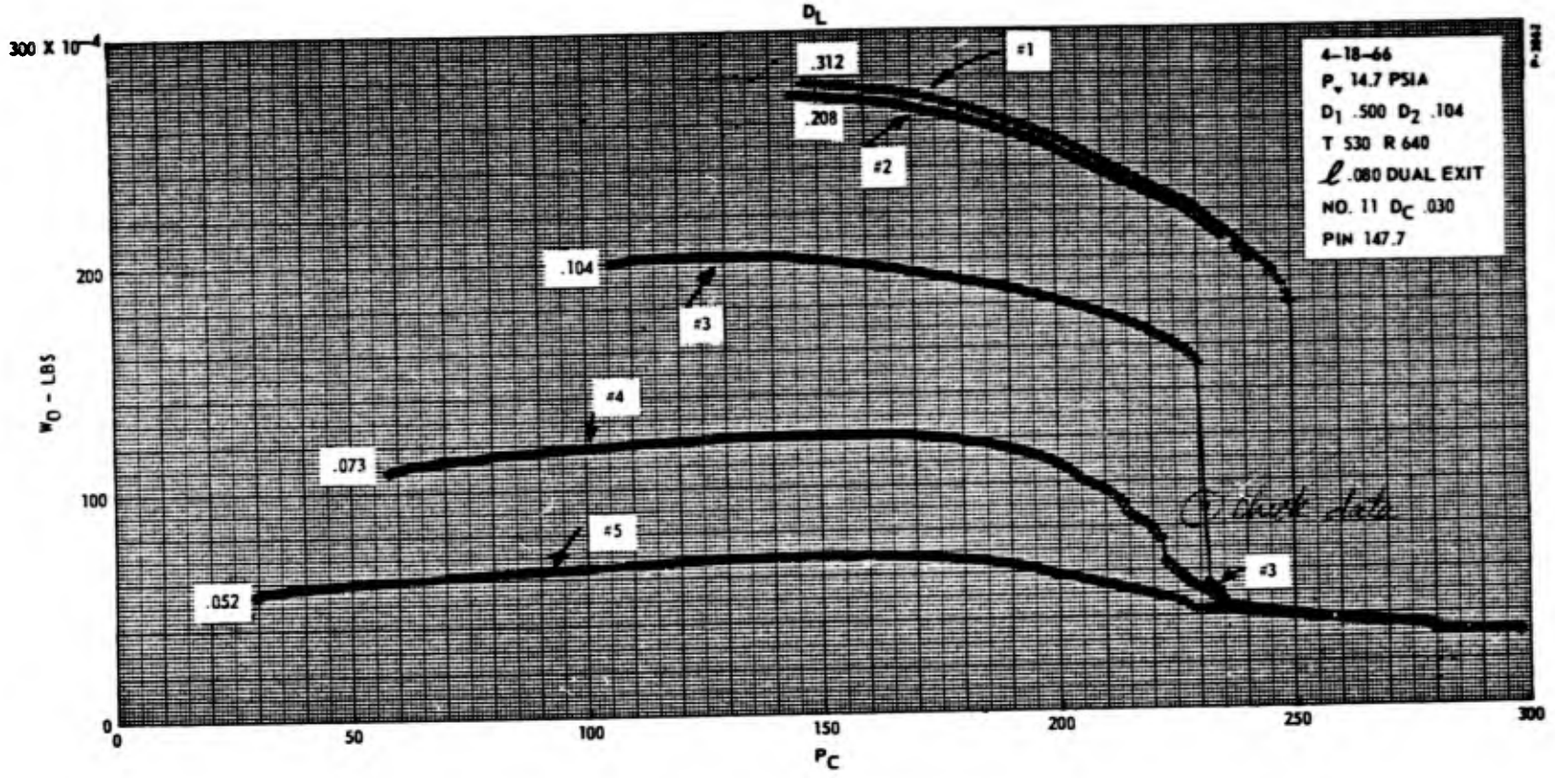

Figure 3-5 - Effect of Load Orifice D_c = 0.030

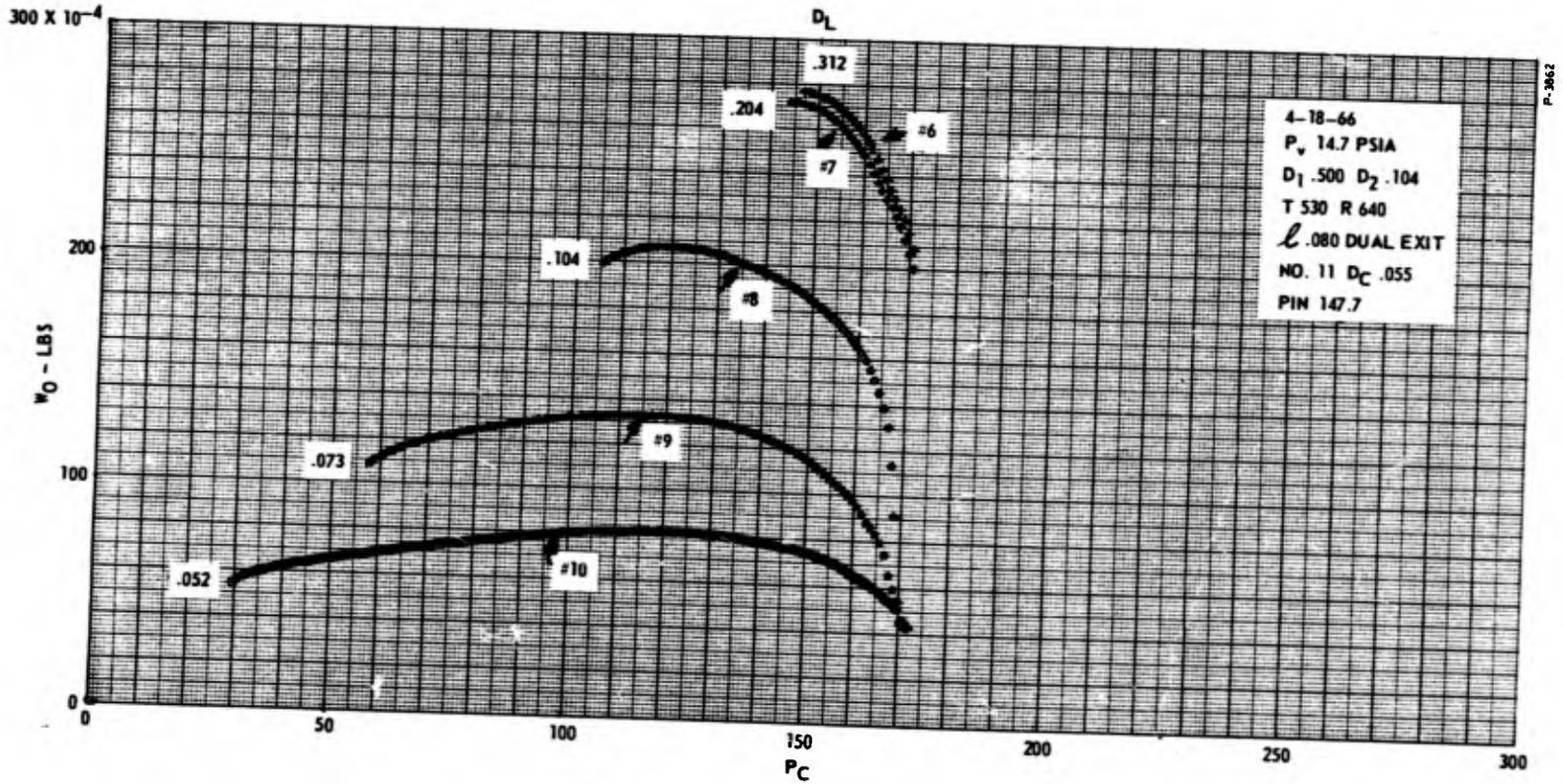

Figure 3-6 - Effect of Load Orifice D_C = 0.055

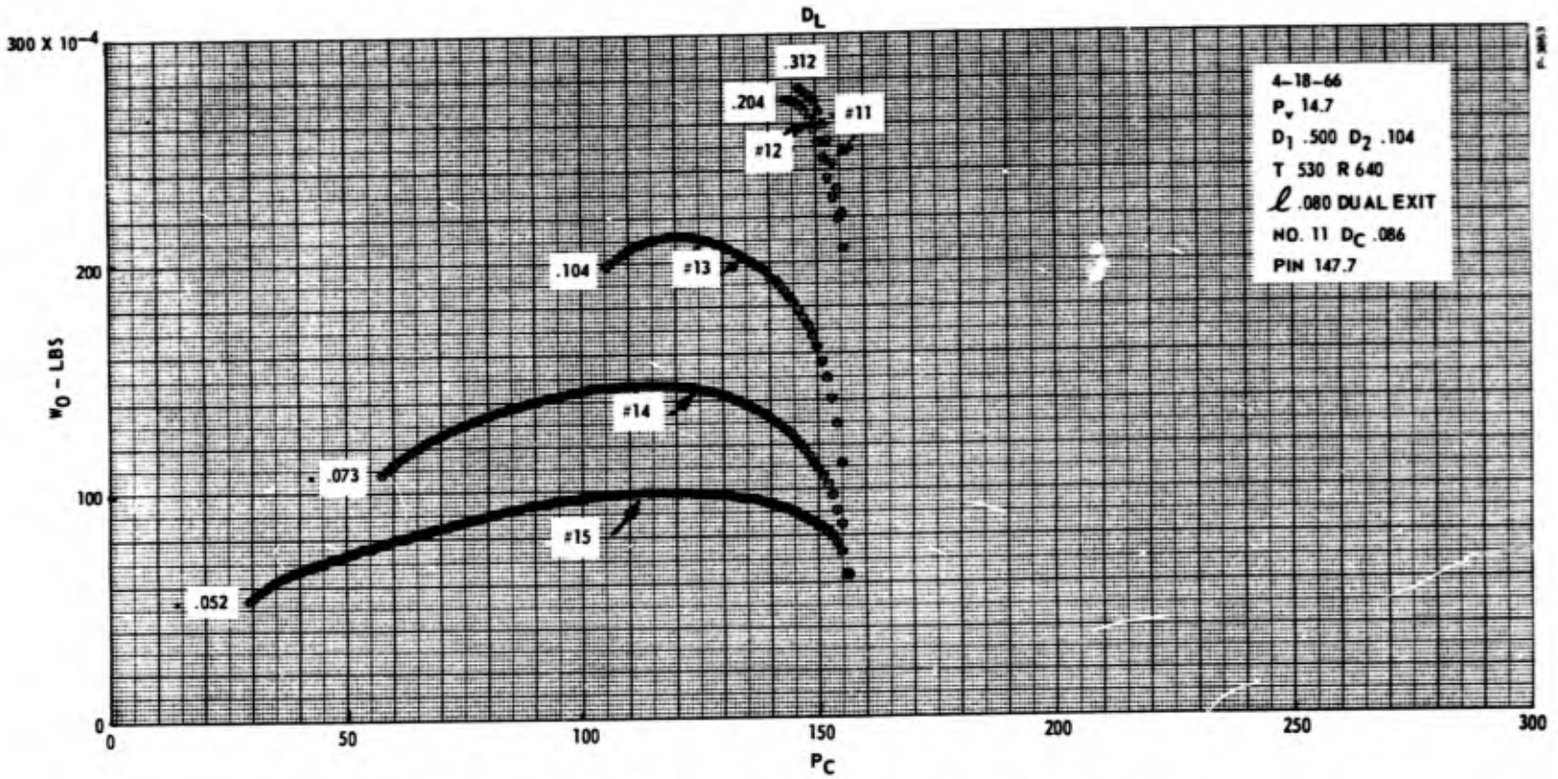

Figure 3-7 - Effect of Load Orifice D_c = 0.086

One-hundred percent pressure recovery of the control element that would regulate the flow resistance between P_{in} and P_c is assumed. From the curves, performance with other limits, such as $P_{cmax} \leq 0.8\ P_{in}$, can be evaluated. In the following, the turndown possible with $P_c \leq P_{in}$ will be discussed.

For smaller control ports, $D_c = 0.030$, Figure 3-5, no turndown occurs in the area $P_c \leq P_{in}$. As D_c is increased to 0.055 in Figure 3-6, the turndown is improved. Further improvement is observed by increasing D_c to 0.086 as shown in Figure 3-7.

A summary of the turndown ratio is shown in Figure 3-8, indicating the best turndown at the largest control port and a load orifice size of about 0.070. The best turndown for the circuit was only 1.22.

The turndown was evaluated as a function of the series orifice size for additional control port sizes. The best turndown for each combination is shown in Figure 3-9 as a function of control port size. The best turndown for the circuit is 1.28 and occurs when the control port size equals the outlet size of the vortex chamber. The turndown for the circuit does not have a very sharp peak, indicating that several combinations of control port size and series orifice size give near maximum flow turndown.

3.1.4 Experimental Verification

The basic experimental curve used to describe the vortex chamber in the analysis was a curve representing the X-19 vortex valve. Thus, some of the results of the analytical calculation may be compared with available test data on the X-19 valve, also the series orifice circuit performance can be evaluated at the calculated operating conditions using the X-19 vortex valve.

The turndown ratio of the vortex valve as a function of control port area is shown in Figure 3-10. The experiments were performed at 54.7 psia supply pressure, the calculations were based on 147.7 psia supply pressure. The agreement between the calculated and experimental flow turndown ratio is good. The same turndown ratio curves are given as a function of control port to outlet diameter ratio in Figure 3-11.

Using all four control ports of the X-19 vortex valve in parallel, the total effective control port size is 0.086 inch. In the double outlet configuration, the effective outlet flow area is that of a

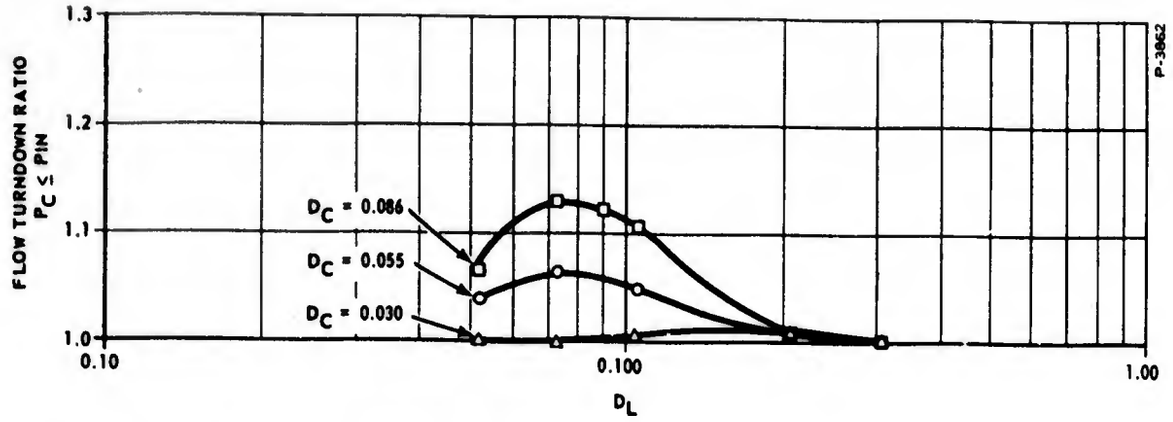

Figure 3-8 - Effect of Series Orifice on Turndown Ratio

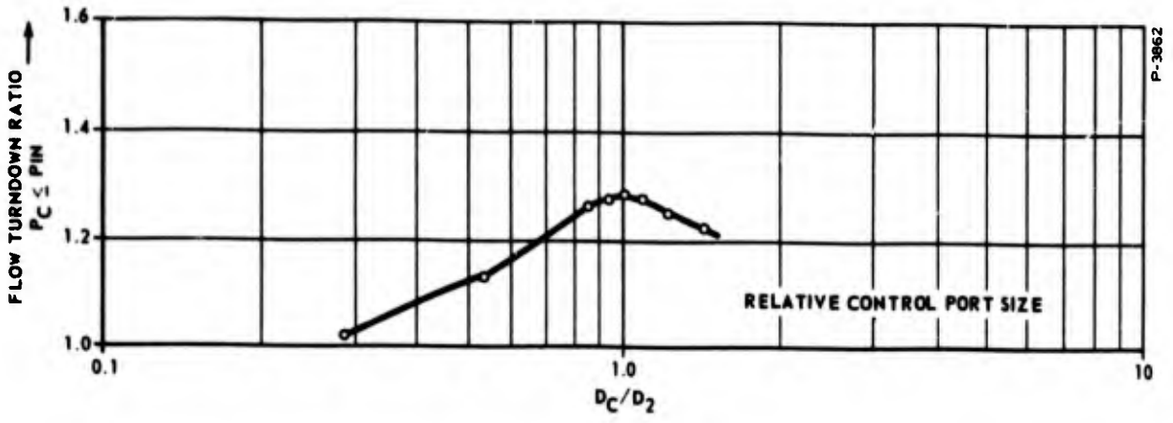

Figure 3-9 - Effect of Control Port Size on Turndown Ratio

0.104-inch diameter port, the dimensions used in the calculations presented in Figure 3-7. The total flow through the valve and the control pressure was recorded on a X-Y plotter as shown in Figure 3-12. In addition to the flow curves at constant P_{in}, the maximum flow at zero control flow and the minimum flow at zero supply flow is shown. The flow turndown at 147.7 psia supply pressure is 4.4 and agrees well with the calculations shown in Figure 3-11.

The four turndown curves representing different series orifice sizes were obtained by adjusting valve "A" with valve "B" closed until the starting value of P_c for each of the calculated curves given in Figure 3-7 were established. From the starting point, valve "B" was gradually opened and the total flow recorded as a function of

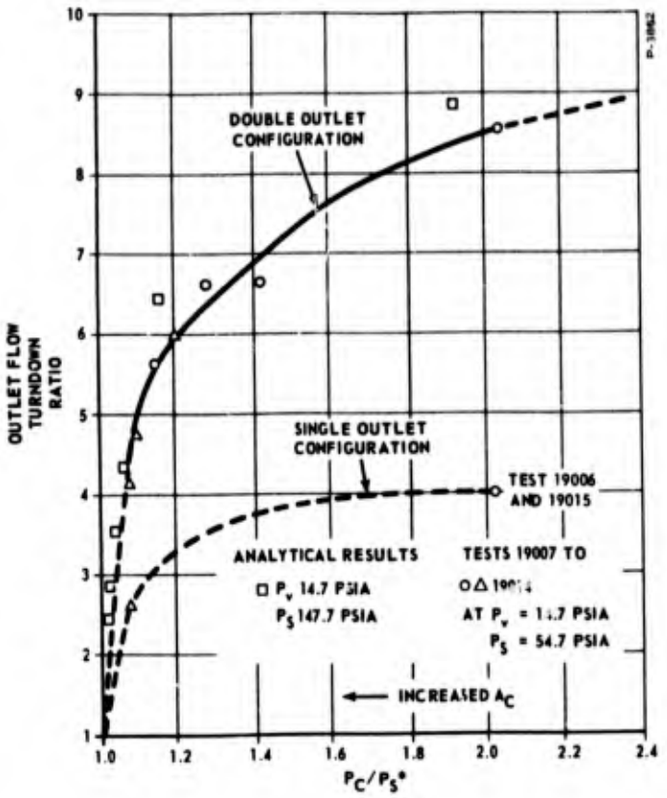

Figure 3-10 - Turndown Ratio Versus Control Port Size

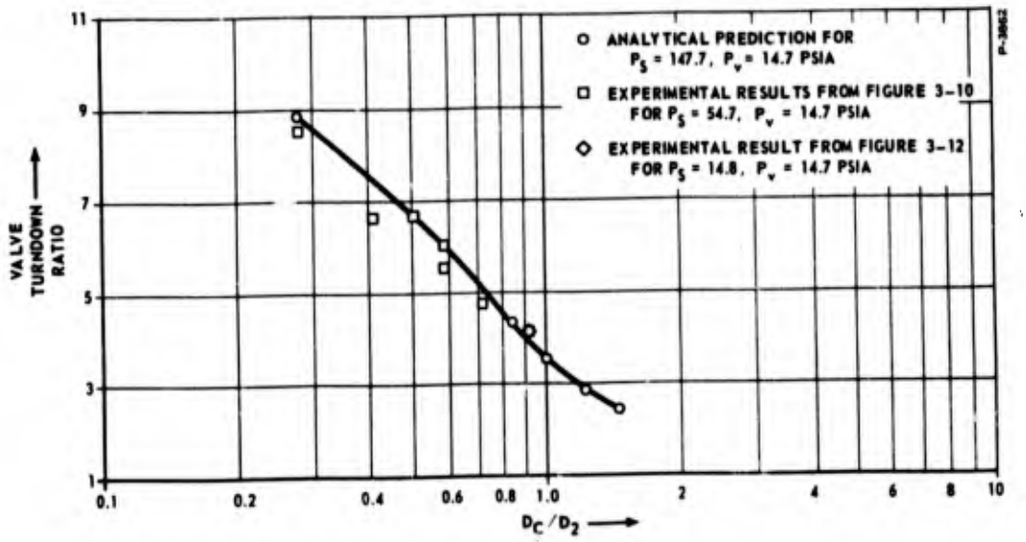

Figure 3-11 - Flow Turndown as a Function of Relative Control Port Size

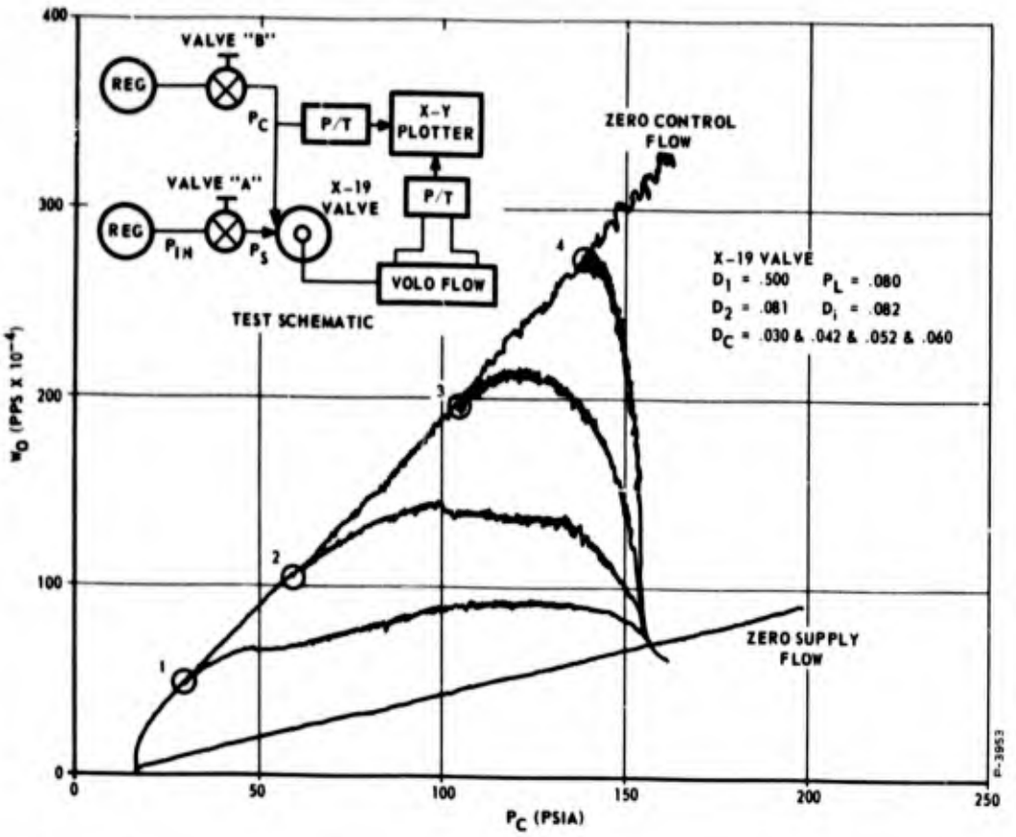

Figure 3-12 - Experimental Evaluation of Series Orifice Circuit

control pressure. The agreement between the analytical prediction of Figure 3-2 and the experimental results shown in Figure 3-12 is excellent. The use of actual fixed orifices instead of valve "A" in the experiment was not considered worth the additional complexity, as the orifice sizes must be usually adjusted experimentally to compensate for variations in the contraction coefficient of the orifice.

Some improvement in operating range is obtained by using a series of orifices in place of a single orifice for the restriction. This is a consequence of the fact that the critical pressure ratio of a series of orifices is less than that of a single orifice. This is discussed in Appendix D. The effect of the multiple orifices can be analyzed by determining the function of P_S/P_B corresponding to f_1 (P_S/P_I) used in the preceding discussion. The advantage of increasing the number of orifices n decreases rapidly for n > 10 so we have approximated f_{10} (P_S/P_B) in Figure 3-13 to illustrate the control range obtained by using

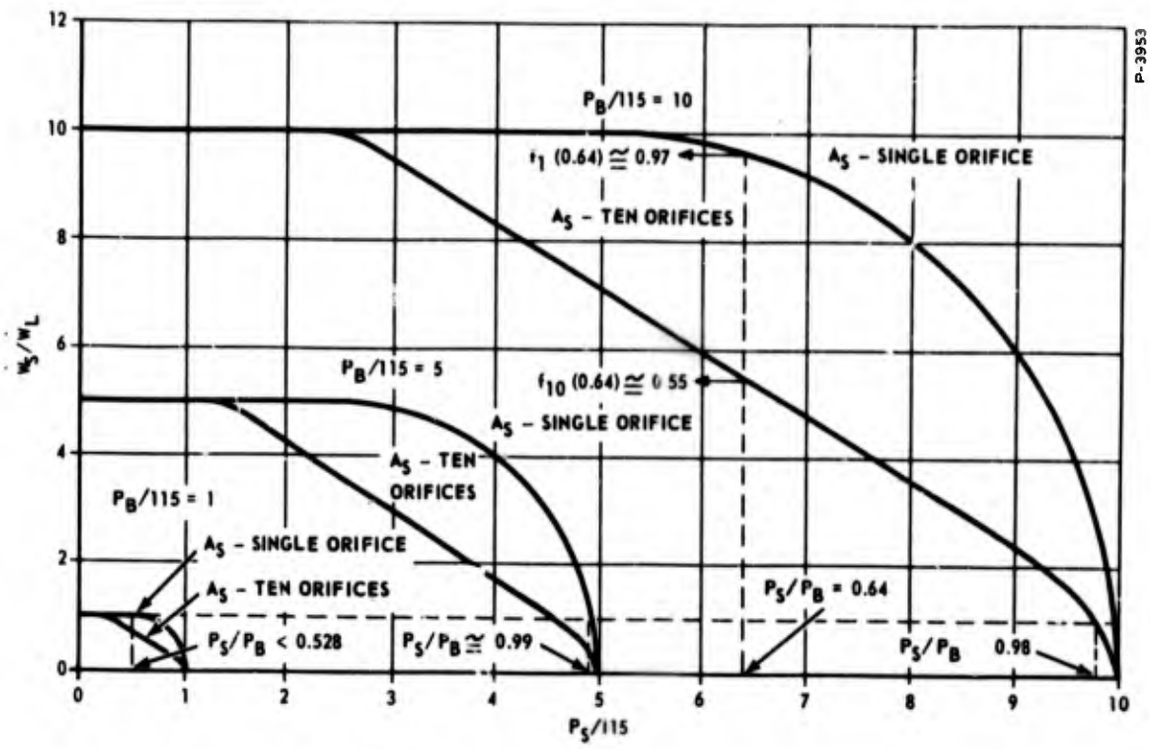

Figure 3-13 - Determination of Supply Pressure Requirements for Single and Multiple Orifice Restriction in Supply Line of a Vortex Throttling Valve

ten orifices in series. If the series of orifices is sized for an initial $P_S/P_B = 0.64$, the inlet pressure can drop to about one half of its initial value before the series of orifices begins to limit the supply flow. To obtain the throttling range required for the regulator, the pressure ratio across the series of orifices must be $P_S/P_B \cong 0.98$ when P_B is ten times its minimum value.

Although there is some advantage in using a series of orifices instead of a single orifice, a restriction in the vortex valve supply line can not be used to drop the supply pressure to the valve for control purposes in this application.

3.2 CONTROL OF THE PILOT VORTEX VALVE

3.2.1 General

The pilot vortex valve configuration provides a reduction in the ratio P_C/P_S required for maximum impedance sensitivity and full turndown, but putting a restriction in the supply line of the pilot valve to obtain even this P_C/P_S requirement is still impractical.

From Figure 2-9, $P_C > 1120$ psig is required for full turndown when $P_S = 1000$ psig. We must provide a pressure source greater than the supply pressure to obtain effective throttling control. For the throttling tests shown in Figure 3-14, P_{S_3} was set at 1.5 P_{S_1} psig. The throttling performance with A_{F_2} (positive feedback path) closed is shown in Figure 3-15. The circuit will not throttle to the required load flow above $P_{S_1} = 700$ psig, but the operating line $P_0 = 21$ psig shows that a properly sized valve would operate to a minimum inlet pressure of about 225 psig.

It is not necessary to size the valve perfectly, however, because the positive feedback path A_{F_2} can be used to lower the throttling saturation for $P_{S_1} > 700$ psig as shown in Figures 3-16 and 3-17. The positive feedback reduces the control pressure P_{F_3} required to throttle the load flow to the required value without significantly increasing the minimum inlet pressure.

3.2.2 Dual Volume Gas Bottle

In a previous section, an approach to the throttling element was discussed which involved the use of a dual volume gas storage bottle shown in Figure 3-1. One of these gas volumes is pressurized to a higher level than the other and serves as a source of control pressure for the throttling of the flow from the lower pressure bottle. The discussion was concerned with the throttling element requirements; the discussion here will be primarily concerned with gas storage requirements.

It can easily be shown that for single compartment spherical pressure vessels or for single compartment cylindrical pressure vessels having spherical ends and identical L/D ratios, the pressure vessel weight for a given factor of safety and weight of gas is theoretically independent of the storage pressure. Although practical constraints may alter this conclusion somewhat in certain applications, it can generally be considered to hold in the real case.

Storage volume, on the other hand, decreases inversely as initial storage pressure. Ullage is also reduced. As a result, as pressure vessel technology improves, the trend has been for gas storage bottle pressures to increase, especially in military and aeronautical applications.

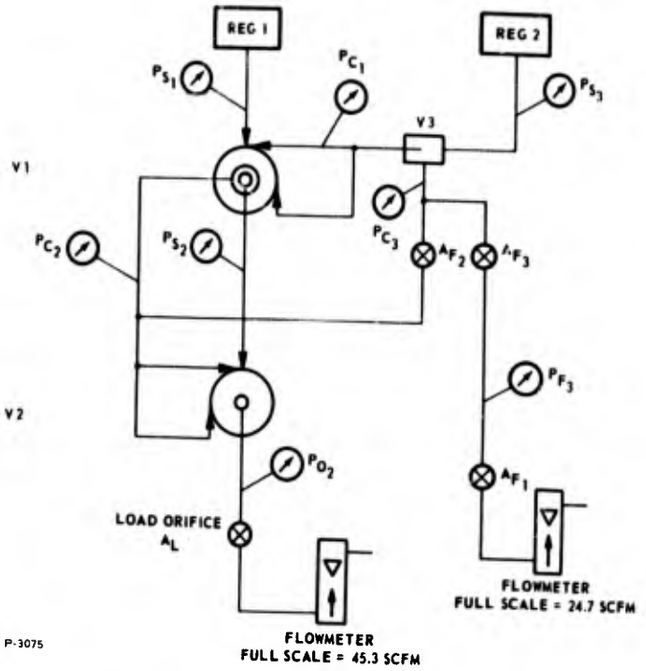

Figure 3-14 - Throttling Circuit Test

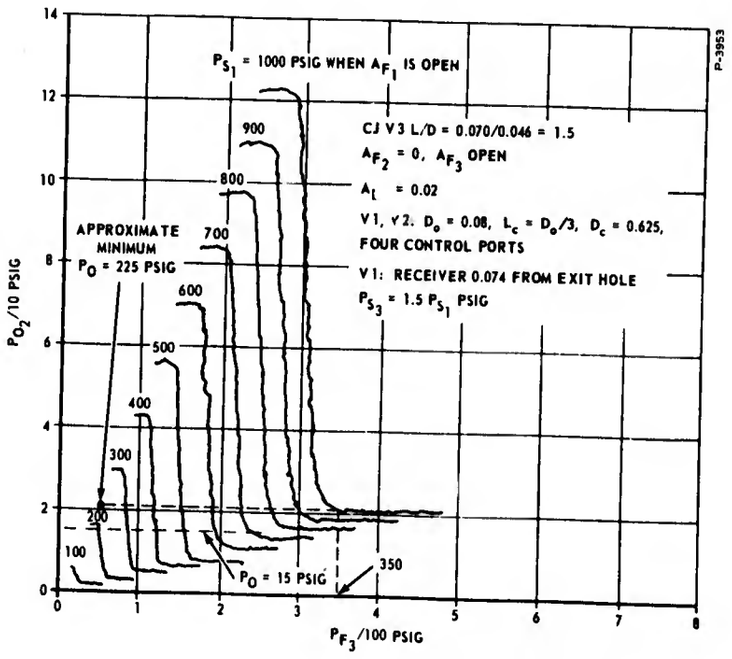

Figure 3-15 - Two-Stage Piloted Vortex Valve Performance

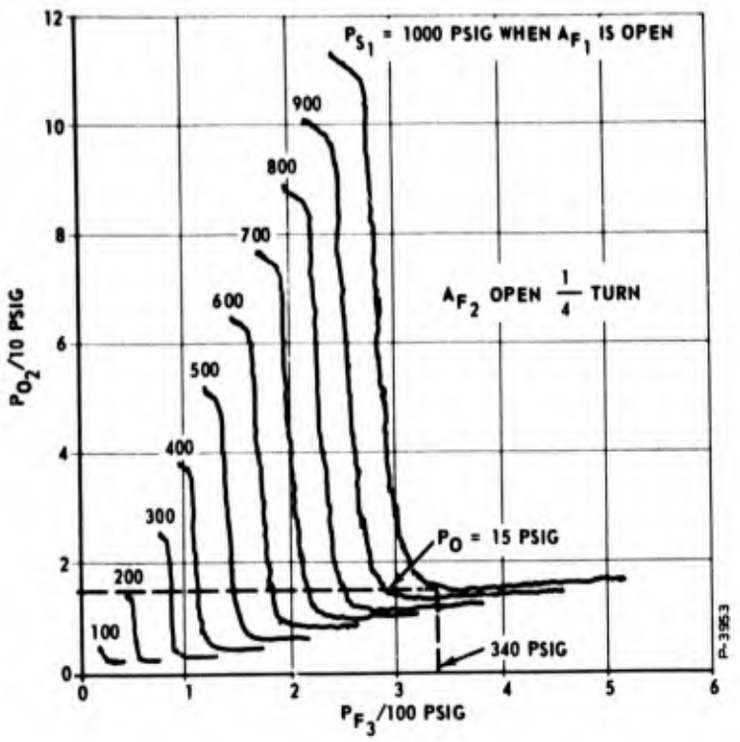

Figure 3-16 - Two-Stage Piloted Vortex Valve Performance (Positive Feedback)

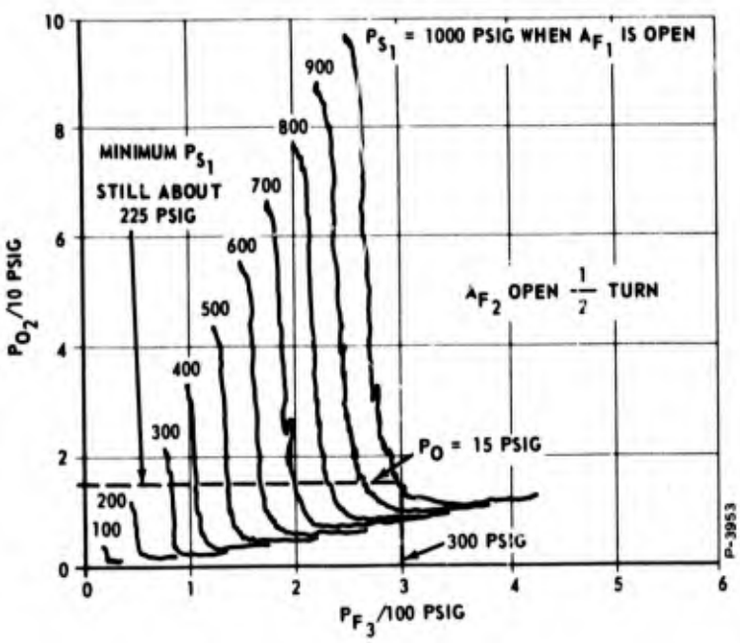

Figure 3-17 - Two-Stage Piloted Vortex Valve Performance (Positive Feedback)

In view of the above, the necessity of having to store the pressurizing gas at two different levels must be considered a disadvantage. Furthermore, the possibility of leakage disturbing the required balance between the weights of gas stored in the two volumes must be considered. On the other hand, the dual volume approach has the out standing advantage of producing an all-fluid system of the purest form. Since this corresponds to the goal of this project, the dual volume approach thus deserves investigation.

One of the first questions which occurs during such an investigation is to determine the ratio of the volumes of the two tanks. This may be approached by the following reasoning:

Consider the dual bottle system indicated in Figure 3-18. At the initial conditions, the vortex valve will be shut off and the flow from the low pressure bottle will be zero. At the final conditions, it

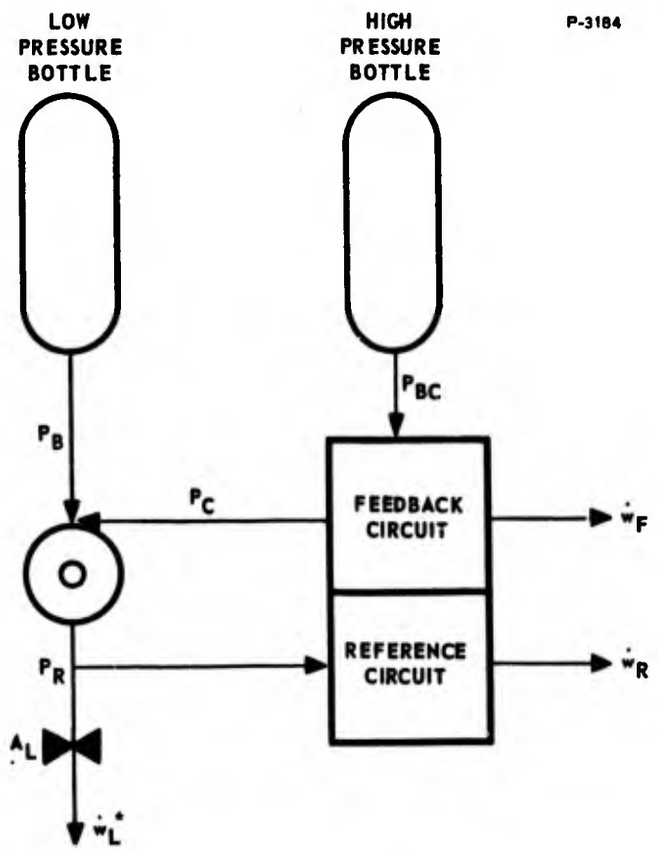

Figure 3-18 - Dual Pressure Bottle System

may be assumed that the low pressure bottle supplies the total demand of the load and the reference circuit. In other words

$$\dot{w}_{Bi} = 0 \tag{3-2}$$

$$\dot{w}_{bf} = \dot{w}_L^* + \dot{w}_R \tag{3-3}$$

Assuming that pressure P_B decays as a linear function of time, we can say

$$W_B = \left(\frac{\dot{w}_L^* + \dot{w}_R}{2} \right) t_o \tag{3-4}$$

At the initial conditions, the high pressure bottle will supply the total flow demand of the system. It may be assumed that all flow from the high pressure bottle passes through confined-jet amplifiers which, viewed from the input, act as sonic orifices. Therefore if $P_{BCf}/P_{BCi} = 0.1$, we can say:

$$\dot{w}_{B_{Ci}} = \dot{w}_L^* + \dot{w}_R + \dot{w}_{Fi} \tag{3-5}$$

$$\dot{w}_{BCf} = \frac{\dot{w}_L^* + \dot{w}_R + \dot{w}_{Fi}}{10} \tag{3-6}$$

We will also assume that P_{BC} decays as a linear function of time:

$$W_{BC} = 0.55 \, (\dot{w}_L^* + \dot{w}_R + \dot{w}_{Fi}) \, t_o \tag{3-7}$$

Defining the efficiency of the feedback circuit as $\eta_F = 1 - w_{Fi}/(\dot{w}_L^* + \dot{w}_R^* + \dot{w}_{Fi})$ and dividing equation (3-7) by equation (3-4) gives:

$$\frac{w_{B_C}}{w_B} = \frac{1.1}{\eta_F} \tag{3-8}$$

The volumes of the two tanks are:

$$\frac{V_{BC}}{V_B} = \frac{1.1\ P_{Bi}}{\eta_F\ P_{BCi}} \qquad (3\text{-}9)$$

The P_C/P_B ratio required to shut off the vortex valve will range from perhaps 1.1 to 1.4, depending upon the final configuration selected. The pressure recovery of a confined-jet amplifier supplying a flowing load will be approximately 70 percent. Thus the ratio P_{BCi}/P_{Bi} = 1.6 to 2.0. The feedback efficiency η_F is not expected to be greater than 50 percent. Then equation (3-9) shows that the volumes of the two tanks will be approximately equal with the high pressure tank being possibly the larger. If the two volumes are equal and P_{BCi}/P_{Bi} = 2 the volume of the two tanks will be 33-1/3 percent greater than the volume of a single tank initially at pressure P_{BCi} and holding the same weight of gas.

One approach to a dual compartment pressure vessel which might have merit in this application is described in "Chrysler-Type Oxygen Pressure Vessel Calculations, Designs, and Testing" by H. R. Greenlee, WADD Technical Report 60-365, May 1960. This describes a pressure vessel concept, consisting of a continuously-wound high-pressure tube fitted and brazed to the inside of a cylindrical shell. The tube reinforces the cylinder and permits the use of a thinner cylindrical wall. However, this saving depends upon the two volumes being in the proper proportion, which does not necessarily hold in this application.

3.3 LAG CIRCUIT REGULATOR

An inherent disadvantage of the Dual Volume storage bottle is the fact that both volumes must be precharged to a prescribed level for proper regulator operation. If the higher pressure volume should leak prior to operation, the regulator could be rendered useless. This presents a reliability factor tending to nullify the advantages of an all-fluid no-moving-part regulator.

A more reliable all-fluid regulator using only one storage bottle is shown in Figure 3-19. It utilizes the tangential vortex valve requiring a control pressure less than supply pressure and a delay or lag circuit to provide this control pressure.

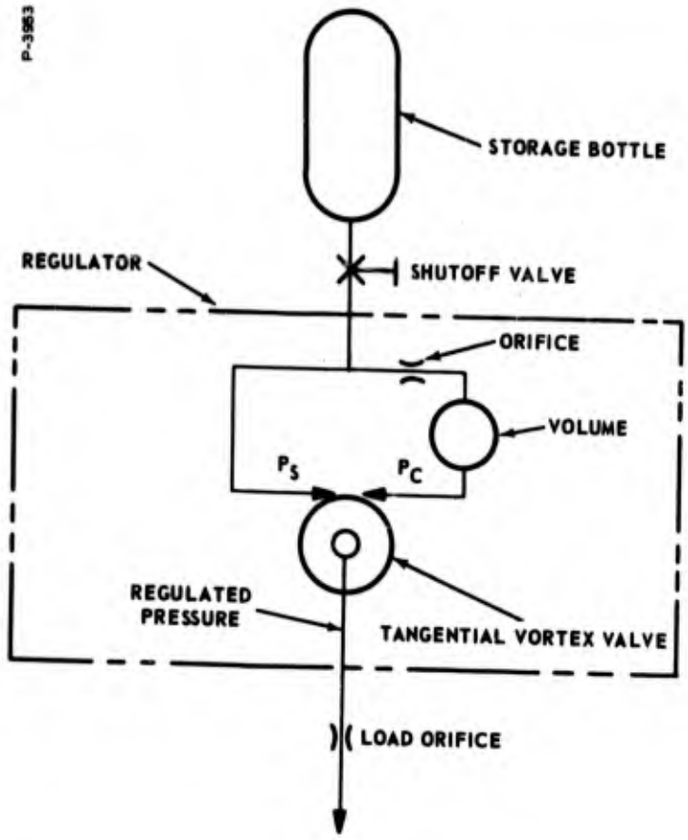

Figure 3- 19 - Lay Circuit Regulator

The vortex throttle is connected to a fixed volume supply bottle through a normally closed valve. A small orifice and control volume is provided in the P_c line. The blowdown is started by instantaneously opening the valve. Initially, all flow passes through the P_s port and turnds down the vortex throttle. The orifice and control volume causes P_s pressure to build up slowly while the bottle pressure drops. As P_c increases, the throttle opens and the total flow remains constant. Finally, P_c equals P_s and the throttle is fully open.

This concept will only work on bottle supplies.

This regulation circuit was implemented using the breadboard tangential amplifier and several different sized pressure tanks. The results are shown in Figure 3-20 and the regulated pressure falls within the pressure requirements over a two and one-half to one blow-down. The storage tank was charged to different pressure levels from 600 to 1,000 psig without affecting the performance of the device. The

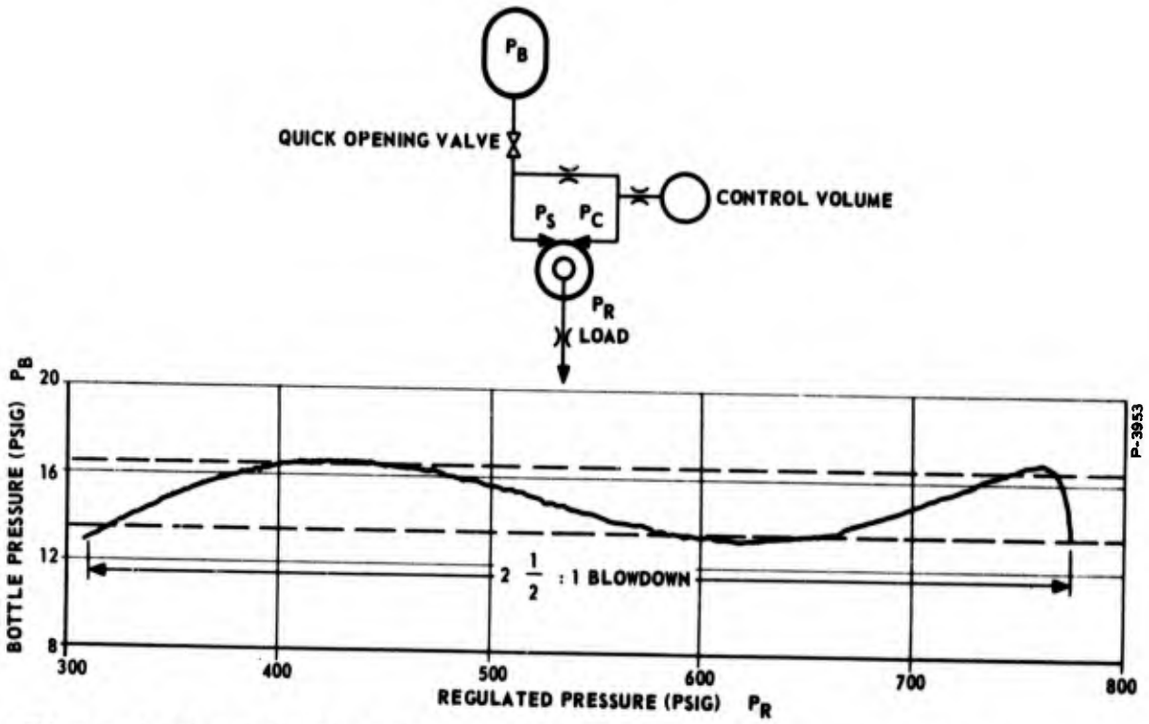

Figure 3-20 - All-Fluid Blowdown Pressure Regulator Performance

slope changes of the regulated pressure curve can be reduced by altering the control volume. In designing a regulator of this type for a given load the volume would be optimally sized for the load required flow. However, by using different loads, the size did not appear very critical as the fixed orifice could be used to adjust the regulator's output pressure performance.

The required volume ratio to storage volume is about one-third. Again, the fixed orifice can be used to compensate for different volume ratios.

An integrated tangential vortex valve with dual exit holes was fabricated into a volume tank fitting and is shown in Figures 3-21, 3-22 and 3-23. The unit is sized to meet the flow requirements with a 150 in^3 supply bottle. The lag volume is 50 in^3 and the vortex valve unit screws into the 50 in^3 volume. Different control volumes can easily be used with this regulator to accommodate different supply bottle volumes.

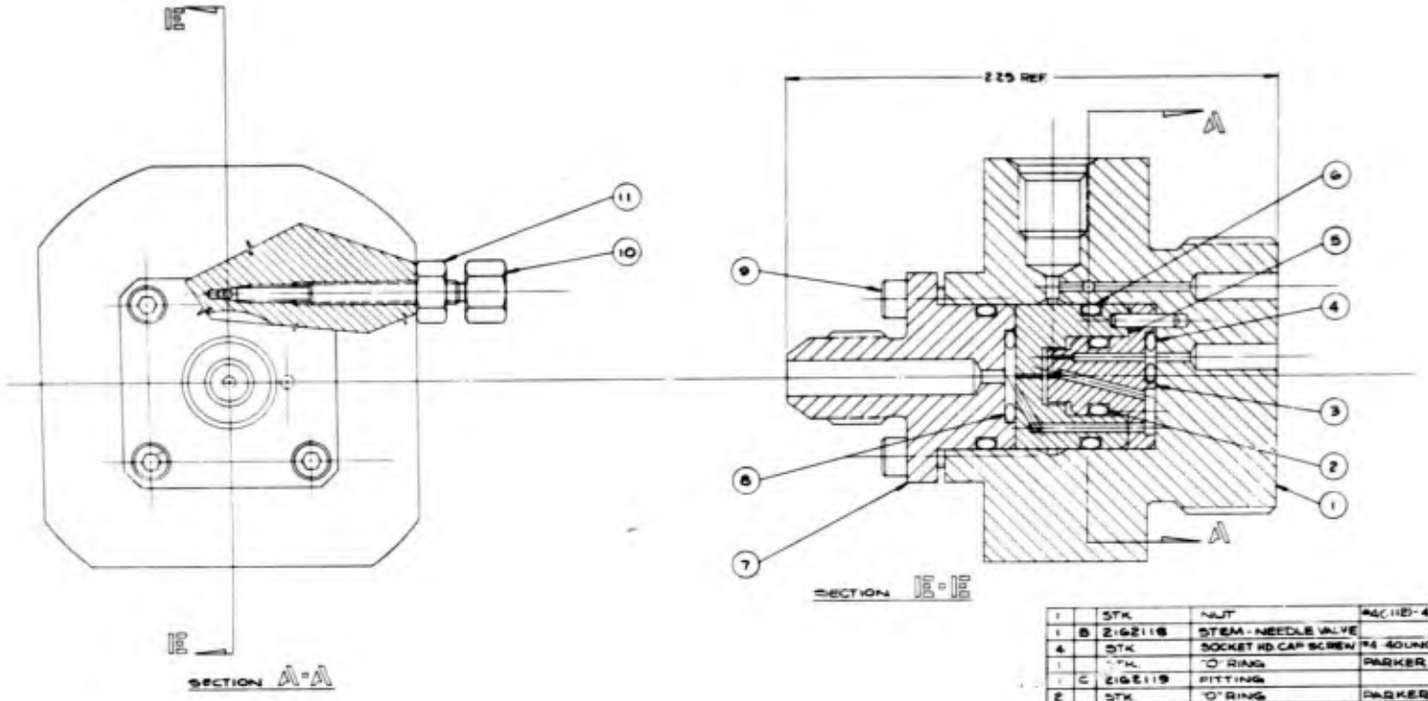

1		STK	NUT	#4C(12)-40UNC-2B SST	11
1	B	2162116	STEM - NEEDLE VALVE		10
4		STK	SOCKET HD CAP SCREW	#4-40UNC-2A x 3/8 LG	9
1		STK	"O" RING	PARKER #2-11	8
1	C	2162119	FITTING		7
2		STK	"O" RING	PARKER #2-15	6
1	C	2162120	BUTTON HOLE PLUNGER		5
1		STK	"O" RING	PARKER #2-5	4
1	C	2162121	BUTTON FR INJECTOR		3
1		STK	"O" RING	PARKER #2-10	2
1	D	2162122	INJECTOR HOUSING		1
QTY REQD	ITEM NO	PART NO.	DESCRIPTION	MATERIAL DESCRIPTION & SPECIFICATION	ITEM NO.

LIST OF MATERIAL

Figure 3-21 - Tangential Vortex Valve Assembly for Lag Circuit Regulator

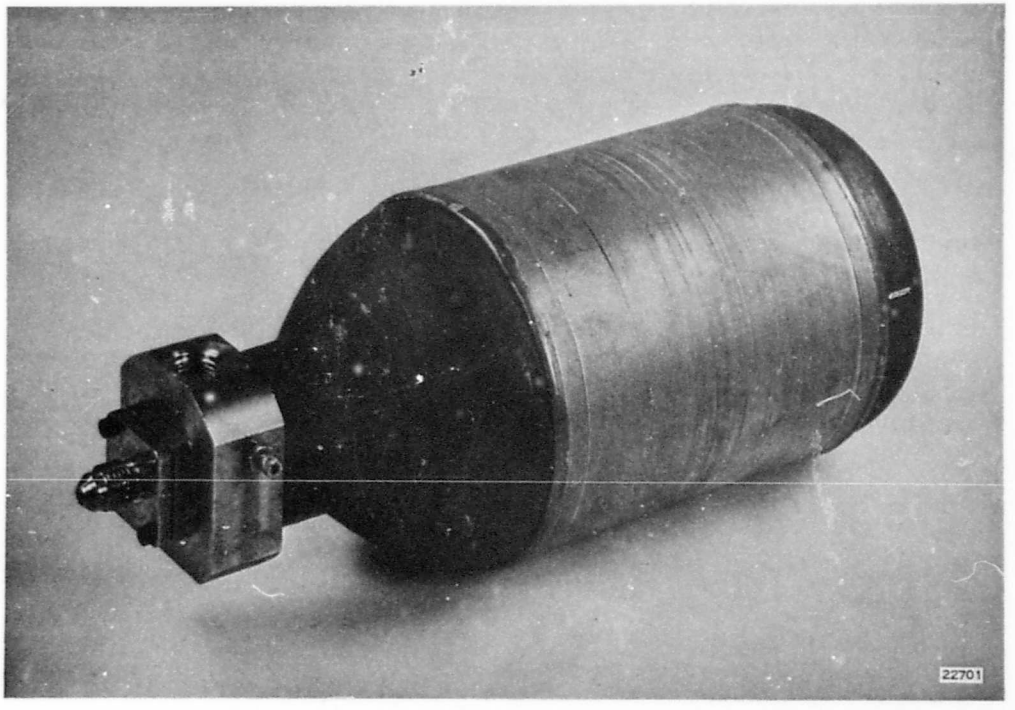

Figure 3-22 - Assembled View of Lag Circuit Regulator

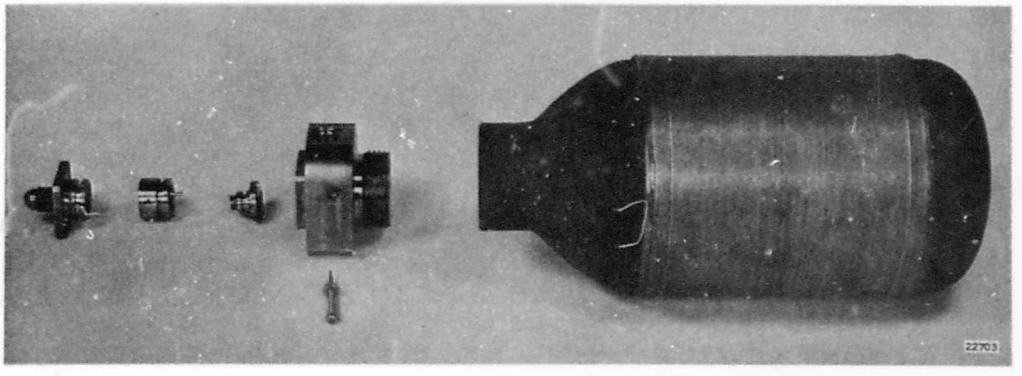

Figure 3-23 - Exploded View of Lag Circuit Regulator

3.4 DOUBLE LAG CIRCUIT REGULATOR

The lag circuit regulator in the previous section has a turndown limitation, due to the limited turndown characteristics of the tangential vortex control valve. A similar approach, using a conventional vortex valve is shown in Figure 3-24. This circuit is similar to the two bottle regulator, except that fluid is only stored at one initial pressure in the storage volume V. Also, the turndown range is greater than the two bottle approach because of the unique operation requirement of the vortex valve.

As the quick opening valve is opened, fluid flows through fixed orifices A_1 and A_2 and begins to charge volumes V_1 and V_2. Area A_2 and volume V_2 are set to charge at a faster rate than volume V_1 to provide control pressure to the confined-jet amplifier, which in turn controls the vortex valve. Initially as the pressure in volume V_1 is low,

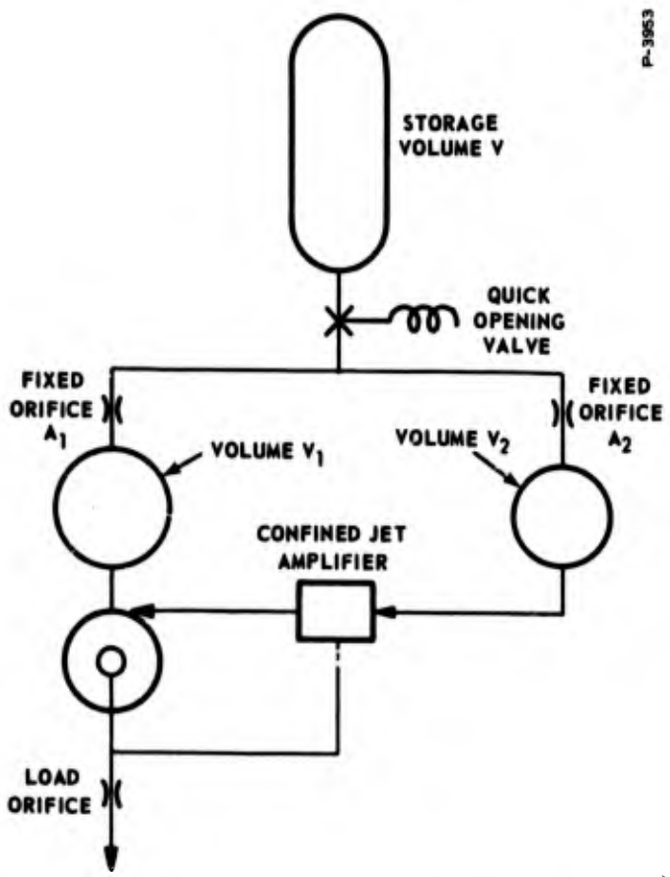

Figure 3-24 - Double Lag Circuit Regulator

the vortex valve must be fully open. As this pressure builds up, the vortex valve must turn down until it becomes fully closed. At this point, if the volumes and areas are correctly sized, the pressure in volume V_1 will have reached its peak and will then decay with the storage bottle pressure. The vortex valve will then have to reopen because its supply pressure is dropping. Thus, a vortex valve with a turndown ratio of 5 used in this manner could operate over almost a 20 to 1 turndown range.

The load pressure must be fed back to the confined-jet amplifier to control the valve and keep the output pressure constant.

To determine the required volume sizes in relation to the storage volume, the following analysis was performed.

Referring to Figure 3-24, all orifices are assumed to operate "sonic," so that flow is proportioned to upstream pressure. Secondly, it is assumed that the confined-jet amplifier is also a sonic load orifice A_c and the output flow is constant and the sum of the confined-jet amplifier, plus the vortex valve flow. The differential equations relating flows to pressure are:

Storage Volume,

$$\frac{dP}{dt} + \frac{CC_d (A_1 + A_2) \sqrt{T_R}}{V} P = 0 \qquad (3\text{-}10)$$

where P is to storage volume pressure at time t.

Confined-Jet Supply Volume;

$$\frac{dP_2}{dt} = (W_2 - W_c) \frac{RT}{V_2} = \left\{ \frac{CC_d A_2 P}{\sqrt{T}} - \frac{CC_d A_c P_2}{\sqrt{T}} \right\} \frac{RT}{V_2} \qquad (3\text{-}11)$$

where W_2 is the flow through A_2, W_c is the flow through A_c, and P_2 is the pressure in volume V_2 at time t.

Vortex Valve Volume,

$$\frac{dP_1}{dt} = (W_1 - W_S) \frac{RT}{V_1}$$

$$W_S = W_{c_{max}} = W_c = W_{c_{max}} - \frac{CC_d A_c P_2}{\sqrt{T}}$$

$$\frac{dP_1}{dt} = \left[\frac{CC_d A_1 P}{\sqrt{T}} - W_{c_{max}} + \frac{CC_d A_c P_2}{\sqrt{T}}\right]\frac{RT}{V_1} \qquad (3\text{-}12)$$

where W_1 is the flow through A_1, W_S is the vortex valve supply flow, and $W_{c_{max}}$ is the required load flow when P_2 is maximum. This sets up the condition that W_S is zero at this time.

Integrating equations (3-10), (3-11), and (3-12), yields:

$$\frac{dP}{dt} + \frac{CC_d(A_1 + A_2)\sqrt{T}\,R}{V} P = 0$$

Let

$$a = \frac{CC_d(A_1 + A_2)\sqrt{T}\,R}{V}$$

$$\frac{dP}{dt} + aP = 0$$

$$C_1 e^{-at} = P$$

$$t = 0 \quad P = P_o$$

$$P = P_o e^{-at} \qquad (3\text{-}13)$$

$$\frac{dP_2}{dt} = (W_2 - W_c)\frac{RT}{V_2} = \left\{\frac{CC_d A_2 P}{\sqrt{T}} - \frac{CC_d A_c P_2}{\sqrt{T}}\right\}\frac{RT}{V_2}$$

$$\frac{dP_2}{dt} + \beta P_2 = \beta \frac{A_2}{A_c} P_o e^{-at}$$

where

$$\beta = \frac{CC_d A_c R\sqrt{T}}{V_2}$$

$$P_2 = C_2 e^{-\beta t} + C_3 e^{-\alpha t}$$

$$\frac{dP_2}{dt} = -C_2 \beta e^{-\beta t} - C_3 \alpha e^{-\alpha t}$$

$$-C_2 \beta e^{-\beta t} - C_3 \alpha e^{-\alpha t} + C_2 \beta e^{-\beta t} + C_3 \beta e^{-\alpha t} = \beta \frac{A_2}{A_c} P_{oe}^{-\alpha t}$$

$$-C_3 \alpha + C_3 \beta = \beta \frac{A_2}{A_c} P_o$$

$$C_3 = \frac{\beta A_2}{(\beta - \alpha) A_c} P_o$$

$$P_2 = C_2 e^{-\beta t} + \frac{\beta A_2}{(\beta - \alpha) A_c} P_o e^{-\alpha t}$$

$$t = 0 \; P_2 + P_{20}$$

$$P_{20} = C_2 + \frac{\beta A_2 P_o}{(\beta - \alpha) A_c} \qquad C_2 = P_{20} - \frac{\beta A_2 P_o}{(\beta - \alpha) A_c}$$

$$P_2 = P_{20} e^{-\beta t} + \frac{\beta A_2 P_o}{(\beta - \alpha) A_c} \left\{ e^{-\alpha t} - e^{-\beta t} \right\} \qquad (3\text{-}14)$$

$$\frac{dP_1}{dt} = (W_1 - W_S) \frac{R'T}{V_1}$$

$$W_S = W_{c_{max}} - W_c = W_{c_{max}} \frac{CC_d A_c P_2}{\sqrt{T}}$$

$$\frac{dP_1}{dt} = \left[\frac{CC_d A_1 P}{\sqrt{T}} - W_{c_{max}} + \frac{CC_d A_c P_2}{\sqrt{T}} \right] \frac{RT}{V_1}$$

$$\frac{dP_1}{dt} = \frac{CC_dA_1R\sqrt{T}}{V_1} P_o e^{-\alpha t} - \frac{RT}{V_1} W_{c_{max}} + \frac{CC_dA_cR\sqrt{T}}{V_1} \left\{ X \right\}$$

$$X = \left[P_{20} e^{-\beta t} + \frac{\beta A_2 P_o}{(\beta - \alpha) A_c} \left\{ e^{-\alpha t} - e^{-\beta t} \right\} \right]$$

Let

$$\frac{CC_dA_1R\sqrt{T}}{V_1} = \gamma$$

$$\frac{dP_1}{dt} = \left[\gamma P_o + \gamma \frac{A_cA_2}{A_1A_c} \frac{\beta P_o}{(\beta-\alpha)} \right] e^{-\alpha t} + \left[-\gamma \frac{A_cA_2}{A_1A_c} \frac{\beta P_o}{(\beta-\alpha)} + \gamma \frac{A_c}{A_1} P_{20} \right] e^{-\beta t} - \frac{RT}{V_1} W_{c_{max}}$$

$$\frac{dP_1}{dt} = \gamma P_o \left[1 + \frac{A_2\beta}{A_1(\beta - \alpha)} \right] e^{-\alpha t} + \frac{\gamma}{\beta} \left[\frac{A_cP_{20}}{A_1} - \frac{A_2\beta P_o}{(\beta - \alpha)A_1} \right] e^{-\beta t} - \frac{RT}{V_1} W_{c_{max}}$$

$$P_1 = -\frac{\gamma}{\alpha} P_o \left[1 + \frac{A_2\beta}{A_1(\beta-\alpha)} \right] e^{-\alpha t} - \frac{\gamma}{\beta} \left[\frac{A_cP_{20}}{A_1} - \frac{A_2\beta P_o}{(\beta-\alpha)A_1} \right] e^{-\beta t} - \frac{RT}{V_1} W_{c_{max}} t + C_4$$

$$t = 0 \quad P_1 = P_{10}$$

$$P_{10} + \frac{\gamma}{\alpha} P_o \left[1 + \frac{A_2\beta}{A_1(\beta - \alpha)} \right] + \frac{\gamma}{\beta} \left[\frac{A_cP_{20}}{A_1} - \frac{A_2\beta P_o}{(\beta - \alpha) A_1} \right] = C_4 \quad (3\text{-}15)$$

By inserting the following constants into equations (3-13), (3-14) and (3-15), we obtain,

$CC_dA_1R\sqrt{T}$	0.075
$CC_dA_2R\sqrt{T}$	0.125
$CC_dA_2R\sqrt{T}$	0.075
V	1

V_1 2

V_2 0.2

P_{10} 0.06

P_{20} 0.06

P_o 1

$$p = e^{-0.188t} \tag{3-16}$$

$$p_2 = 0.308\,e^{-0.188t} - 0.248\,e^{-t} \tag{3-17}$$

$$p_1 = 2.076 + 0.124e^{-t} - 0.178t - 2.14e^{-0.188t} \tag{3-18}$$

which is plotted in Figure 3-25.

An experimental check on these equations was made, using volumes and orifices and a conventional pressure regulator and is shown in Figure 3-26.

Although the above analyses and experimental data verifies that the concept works (as predicted), the large lag volumes make the circuit impractical where space is at a premium. However, if space is a minor limitation, this regulator circuit would be very useful.

3.5 HYBRID REGULATOR

3.5.1 Description

One approach which avoids the limitations imposed by the use of a signal storage pressure bottle is to use a mechanically-variable area as the primary pressure dropping element. The use of a variable area deviates from the idealized goal of having an all-fluid system with no-moving-parts. However, the scheme appears to represent an extremely practical solution to the problem of producing the required pressure regulator performance with a minimum of moving parts while retaining the high reliability and other desirable characteristics of a completely all-fluid system.

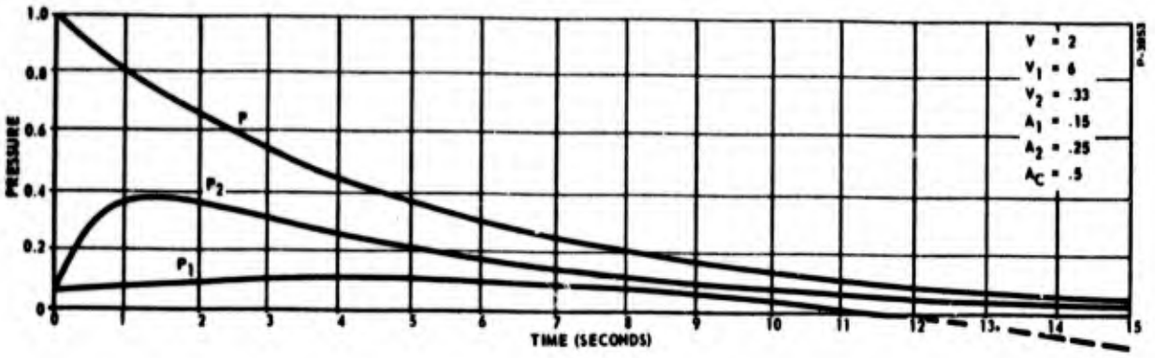

Figure 3-25 - Plot of Pressures P, P_1 and P_2 For a Blowdown of Volume V

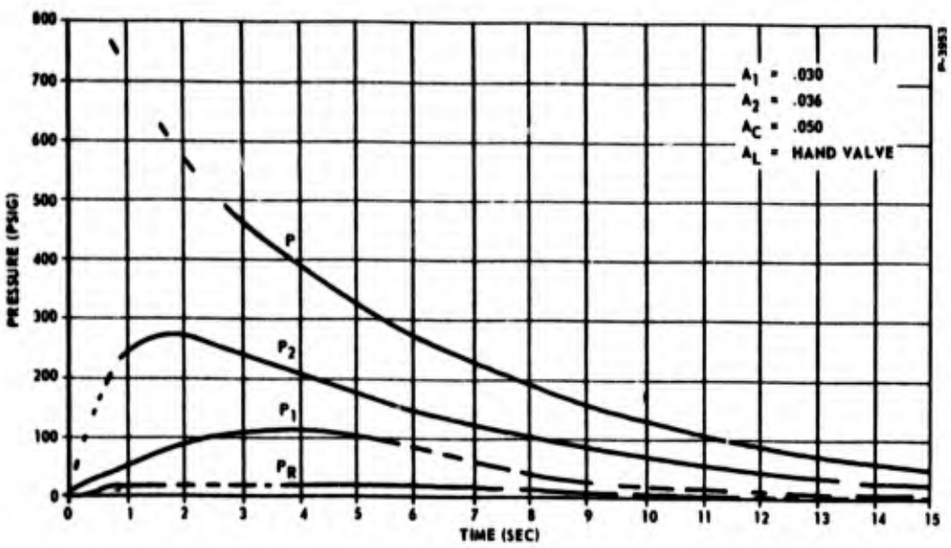

Figure 3-26 - Experimental Blowdown of Double Lag Circuit

Figure 3-27 is a schematic of this hybrid regulator concept. Supply pressure is dropped to about 100 psig by the variable mechanical orifice. This mechanical valve may take the shape of a spool valve as shown in the figure. A fluid-state sensing and control circuit controls the variable area. The vortex valve provides the control pressure and a confined-jet amplifier senses the output pressure and feeds it back to the vortex valve. In addition to being simple, this circuit has the advantage of being efficient, since all flow passes through the load.

A breadboard of the circuit shown in Figure 3-27 was assembled, using a mechanical element which was originally designed for a servo-valve-type application. This mechanical element did not have the shut-off capability that is required for a pressure regulator type application.

Hence, the breadboard pressure regulator did not have the ability of maintaining regulation over an extended range of supply pressures. However, within a limited range of supply pressures, regulation is quite accurate and the device appeared to be superior to conventional spring-reference pressure regulators. Typical regulation is shown in Figure 3-28. The various levels of regulation are obtained by changing the spring preload.

3.5.2 Design

The two hybrid regulators were fabricated. Figure 3-29 is an enlarged (2 times size) assembly view of the regulators. Figure 3-30 is a schematic of the regulator components. Flow enters the input and must pass by the poppet and seat. The poppet is suspended on two flexure disks and cannot physically contact any surface. The corrugated disk serves only as a suspension member for the poppet and is free to flex the required travel. The main disk suspends the poppet and also serves as the spring. It is many times stiffer than the corrugated disk.

Flow is metered by the poppet and seat and divides into two paths. The first path branches off and supplies the flow required by the confined-jet amplifier. The remaining gas flows around the poppet stem which forms a fixed orifice as a result of the limited clearance between the poppet and the bore. This flow passes into a chamber formed by the spring disk and continues into the vortex valve. The valve is controlled by the confined-jet amplifier by tangential ports located in the button. The controlling action varies the valve apparent exit area and therefore its pressure. This pressure in turn acts against the spring disk, closing or opening the poppet as required.

The output port contains the confined-jet amplifier such that the regulated or output pressure becomes the confined-jet amplifier vent pressure and provides the required control signal. It would be possible to locate the confined-jet amplifier externally to the regulator for remote sensing. The regulated pressure is adjusted by the spanner nut at the input end. By screwing the nut in or out, the spring disk preload is varied to provide the necessary reference. The back of the spring disk is vented to the outlet port, thus, "sees" the regulated pressure. This results in the regulator being insensitive to ambient conditions. A dynamic analysis of the regulator is presented in Appendix C.

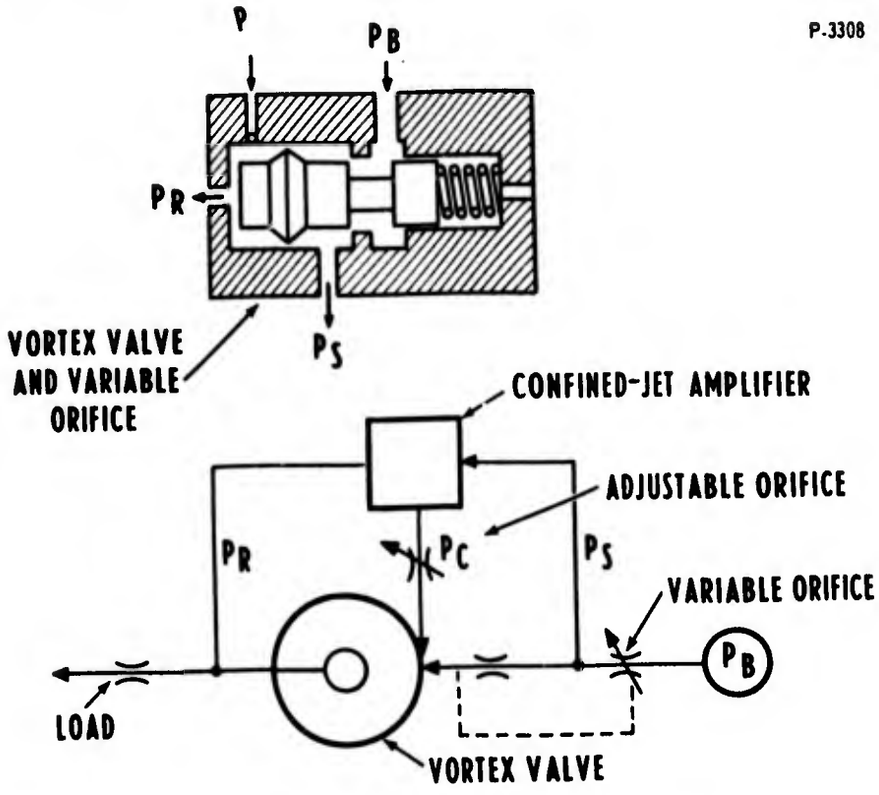

Figure 3-27 - Mechanical Element Pressure Regulator Schematic

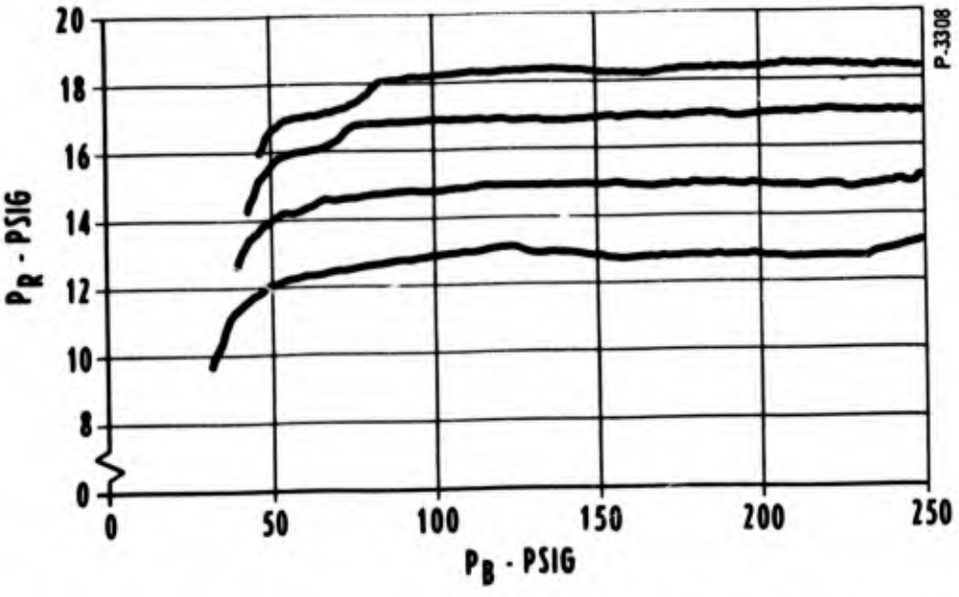

Figure 3-28 - Breadboard Pressure Regulator Performance

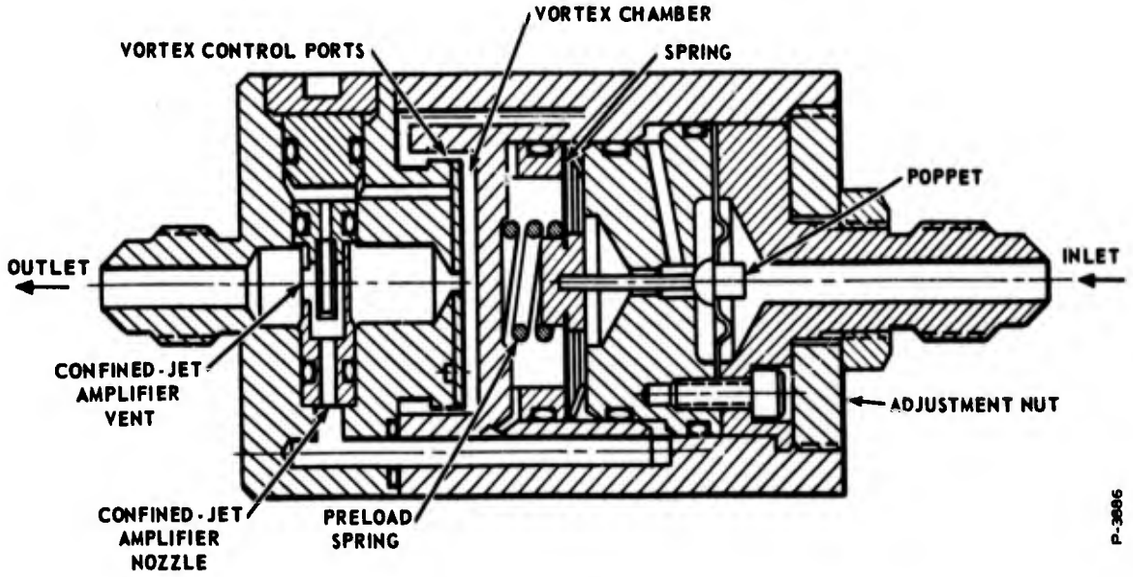

Figure 2-29 - Hybrid Regulator Assembly

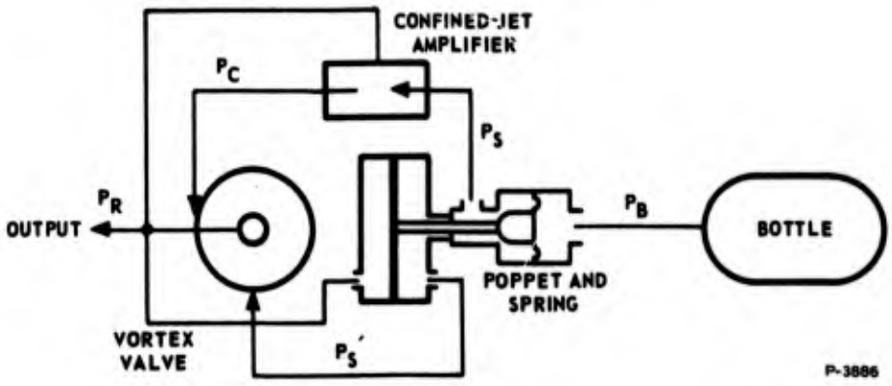

Figure 3-30 - Hybrid Regulator Schematic

The critical parts are made of stainless steel and the body is of anodized aluminum. All parts can be disassembled and inspected or replaced with different sizes, if desired. "O" rings are used for most of the seals, with the exception of the seal upstream of the poppet, which is formed by the corrugated disk. The vortex valve button containing the tangential control ports is a diffusion-bonded assembly and, therefore, does not present leakage problems typical of unbonded vortex injectors.

Figures 3-31 and 3-32 are photographs of one regulator assembly. The fluid state sensing and control circuit, consisting of the vortex valve and confined-jet amplifier assembly is located in the downstream end cap and fitting. The mechanical poppet and spring assembly are inserted into the housing and adjusted with the upstream end cap. The poppet is suspended between the diaphragm spring assembly and an upstream combination gasket and suspension diaphragm. The poppet cannot physically contact or slide against any surface and therefore, is free from friction. The regulator is easy to disassemble for maintenance or repair although neither function should be required.

3.5.3 Testing

The confined-jet amplifier used to sense the regulated pressure and provide the feedback signal to the vortex valve input-output characteristics are shown in Figure 3-33. It is interesting to note that its operation is very good and noise-free. The data in Figure 3-33 represents a significant improvement compared with most of the breadboard data obtained with the breadboard hardware. The design of the confined-jet amplifier which represents a considerable improvement in size and complexity compared to the breadboard models, probably accounts for this performance improvement. The unit is only one inch long by one-quarter inch in diameter and is a single assembly.

Testing of the hybrid regulator uncovered several design problems. The first problem that developed was in the flexure support and spring combination. The spring rate curve for the original supported design was about three times stiffer than predicted. This was caused by a nonlinear spring rate curve that increased with large deflections. A re-examination of the equations indicated that the required travel of the spring was much larger than used in the development of the equations.

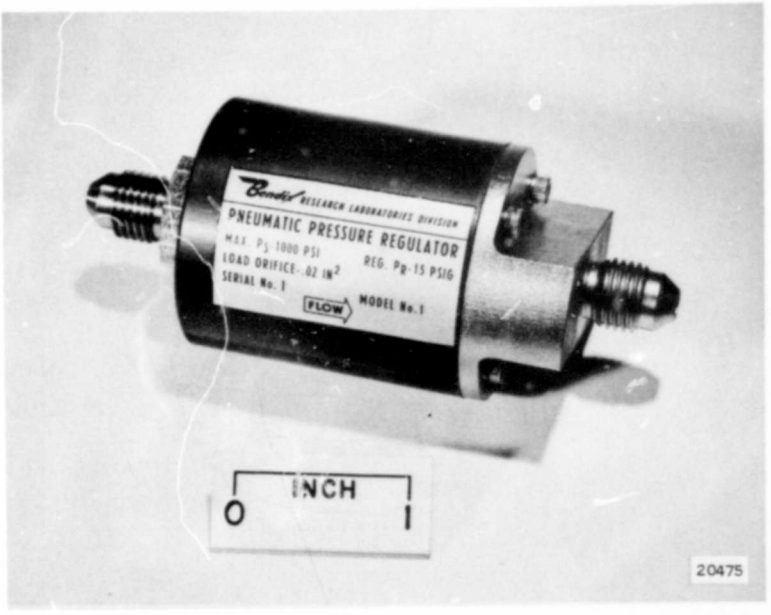

Figure 3-31 - Hybrid Regulator Assembly

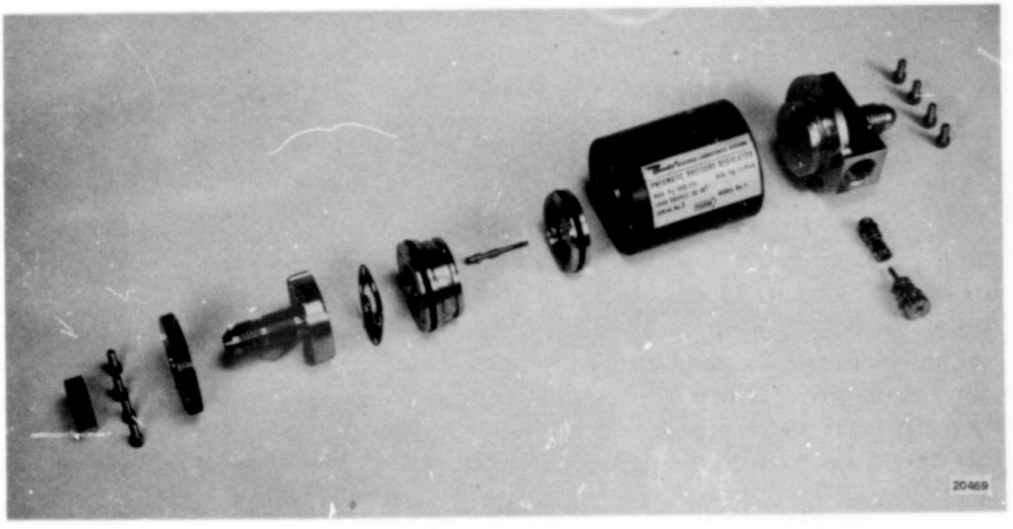

Figure 3-32 - Hybrid Regulator Assembly (Exploded View)

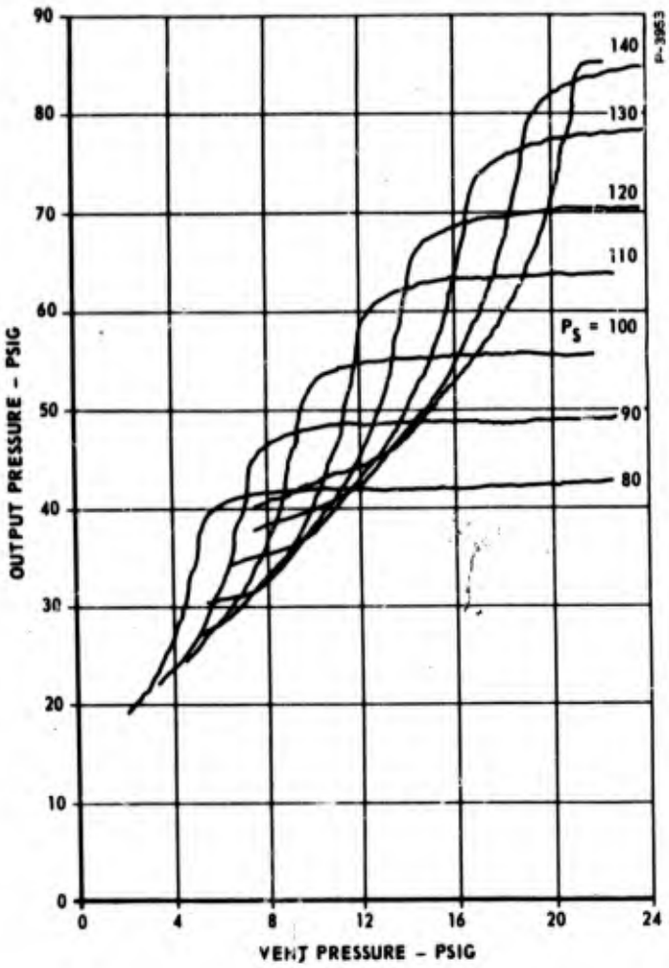

Figure 3-33 - Hybrid Regulator (Confined-Jet Amplifier)

It was decided to remove the outer support around the spring and convert this to a pivot point. The spring rate curve obtained for this configuration is shown in Figure 3-34. It has desired characteristics in the range of zero to 0.030-inch deflection and has excessive spring rate at larger deflections. This range of travel is adequate for regulator operation, but the operating pressure on the spring shown in the regulator schematic, Figure 3-30, P'_s, will initially deflect the spring into the excessive spring rate range.

To reduce this initial deflection, an attempt was made to reduce the pressure differential between P'_s, which is about 50 psig, and P_R, the regulated pressure which is on the other side of the spring. An internal pressure pickoff was placed in the vortex amplifier as shown schematically in Figure 3-35. Its pressure would be much closer to P'_s

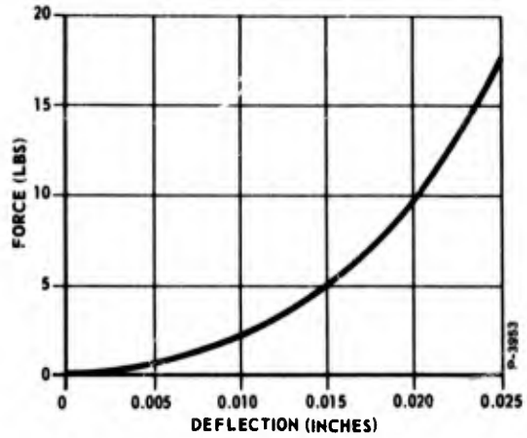

Figure 3-34 - Suspension Risk Sprint Rate

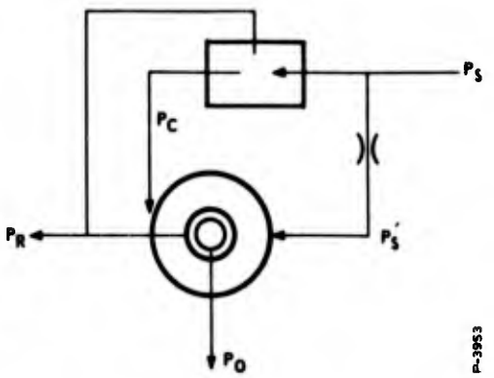

Figure 3-35 - Modified Fluid Stale Feedback Circuit Schematic

and, being transmitted from an amplifier pickoff, it would be a function of the tangential control flow coming from the feedback amplifier. The characteristics of this circuit are shown in Figure 3-36. Large gains with an operating range near zero differential pressure across the spring could be obtained if this pickoff pressure, instead of output pressure P_R, is placed behind the spring. However, upon study of these characteristic curves, they reveal another problem. Although the differential pressure $P_s' - P_o$ across the spring increases as the output pressure increases and would close the mechanical poppet, this same differential pressure will decrease when the supply pressure P_s increases. This would open the poppet, increasing P_s further, and would result in an unstable loop. This loop would oppose the feedback loop and the net result would be very low gain or possibly instability.

One of the regulators was modified to this configuration to check operation and it verified the poor gain and instability characteristics. The regulator would operate at the two extreme ends of the characteristic curves shown in Figure 3-36. Varying the output flow rate would (at certain levels) cause the unit to oscillate between these two points.

It was then decided that the original configuration must be used and the preload, due to the differential pressure between P_s' and P_R, would have to be eliminated. A coil spring was fabricated and inserted behind the support spring as shown in Figure 3-31. Its position was set to absorb the preload and place the disk spring in the desired operating or deflection range. This coil spring does not change the

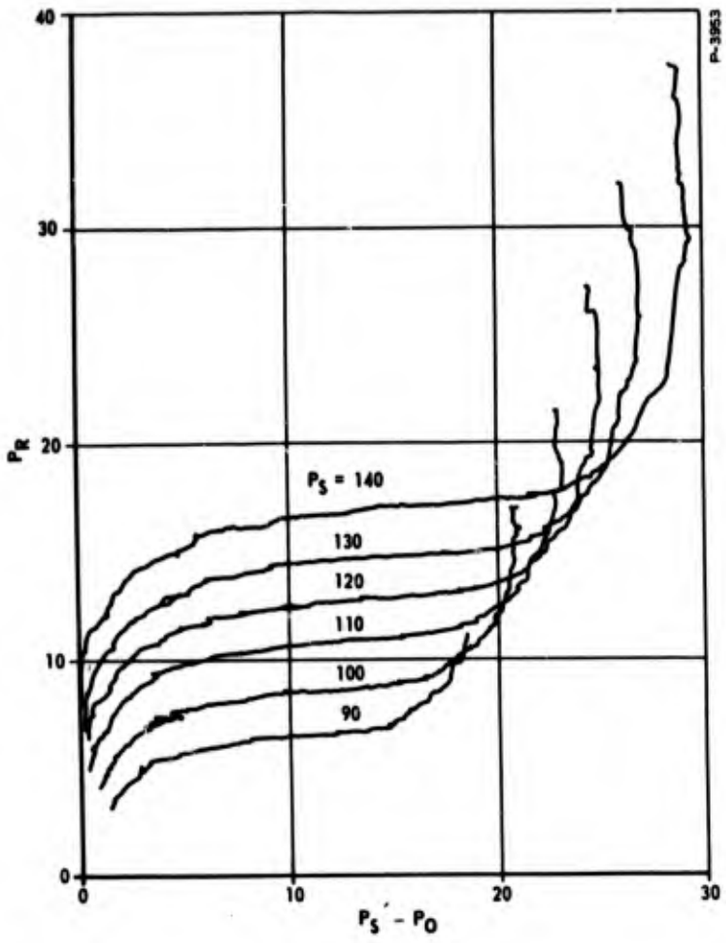

Figure 3-36 - Characteristic Curve for Circuit of Figure 3-35

design of the poppet in any way and it remains fully supported on the two support disks. Therefore, it cannot contact or drag on any surface and remains fully supported. In order to insure that the disk spring remains in contact with the support ring and forms a seal between P_s' and P_R, a retainer was added as shown in Figure 3-31 to maintain the disk against the ring. This retainer is flexible and allows the regulator poppet seat to be adjusted by the adjustment nut.

3.5.4 Performance

A typical performance curve of the modified regulator with a fixed orifice load is shown in Figure 3-37. The unit is useful over a 10-to-1 pressure range and initial supply pressure may be

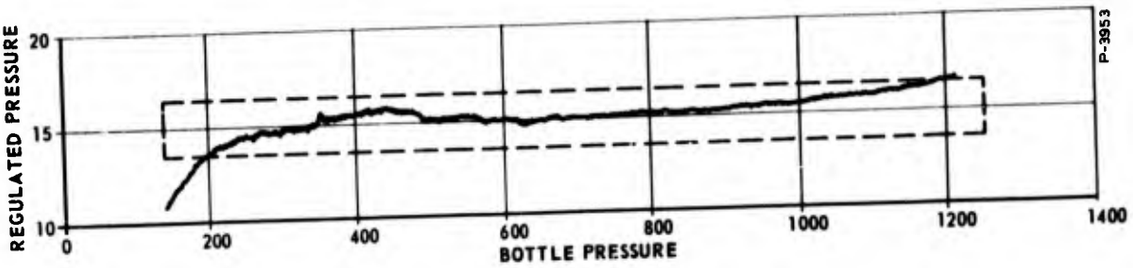

Figure 3-37-- Typical Hybrid Regulator Performance Curve

adjusted between 1000 and 2000 psi, resulting in different load flows. The regulator is adjusted by noting at what bottle pressure upper limit the poppet hits its stop. This point occurs when the output pressure begins to rise proportionally with the bottle pressure. When this point is set at 2000 psi bottle pressure, the regulator will supply a larger load flow at 15 psi than it will supply with the 1000 psi setting. Although the regulator is rated at 1000 psi, bottle pressures up to 2000 psi may safely be used. Lack of regulation, poor regulation, or oscillation may occur if the load is improperly matched to the regulator. These conditions are caused by small loads, whereas large loads will only result in pressures lower than 15 psig at the output, since the outlet hole will become restricted.

BLANK PAGE

SECTION 4

SUMMARY OF RESULTS, CONCLUSIONS, AND RECOMMENDATIONS

4.1 SUMMARY OF RESULTS

4.1.1 Throttling Methods

Vortex valves are variable impedance fluid state devices. Operation of vortex valves requires that a control pressure greater than the supply pressure be available. The turndown ratio which can be obtained and the P_C / P_S ratio required depend upon the exact configuration. The double exit valve can deliver turndown ratios of greater than 8 to 1 with high pressure nitrogen gas.

It can be demonstrated that the use of a fixed area orifice to drop the vortex valve supply pressure below the bottle storage pressure in order to obtain the necessary P_C / P_S ratio is impractical. This is a consequence of the fact that the pressure-dropping orifice becomes sonic during bottle blowdown and becomes incapable of being controlled by the downstream vortex valve when the bottle pressure has decreased only slightly.

It can be shown that no significant increase in turndown will result from connecting vortex valves in series. However, a significant decrease in the maximum P_C / P_S ratio required to achieve maximum turndown of a vortex valve will be realized by connecting it in series with a vortex pilot valve.

The problem of obtaining a control pressure higher than the supply pressure can be solved either by using a mechanically-variable area at the outlet of the pressure bottle or by using a pressure bottle with two compartments charged to different pressure levels. The first approach has a moving part in the system and hence is not strictly a fluid state device. While the weight of the dual volume tank is not appreciably greater than a single volume tank for the same weight of gas, it will occupy a greater volume.

4.1.2 Feedback Methods

The confined-jet amplifier is a fluid state device which permits a low pressure source to control a high pressure source. By varying the geometry and spacing of the nozzle and receiver, several gain characteristics can be achieved. Useful operation in the range of $P_C / P_S = 0.15$ has been obtained. Output pressure recoveries up to 70 percent of the supply pressure have been achieved with a flowing load. One highly useful property of the device is that it can be designed so that output pressure is insensitive to supply pressure changes over a wide range. Control of a confined-jet amplifier by means of a vortex valve which throttles the confined-jet amplifier vent has been demonstrated.

4.1.3 Reference Methods

Changes in the regulated pressure can be detected and amplified by means of orifice bridge circuits and either jet-on-jet or vortex pressure amplifiers. Although the change in regulated pressure is amplified, the level of the output is lower than the regulated pressure. The confined-jet amplifier can provide an absolute pressure reference by venting its vent flow directly into the load.

4.2 CONCLUSIONS

The following conclusions have been drawn from the results:

(1) No fixed area orifice having any appreciable pressure drop can be placed in the main flow path if the pressure regulator is to throttle flow over a wide range.

(2) No known fluid state device, other than the vortex valve, is capable of throttling a flow with acceptable efficiency. The vortex valve requires a source of control pressure higher than the supply pressure.

(3) Conclusions (1) and (2) jointly lead to the conclusion that either a mechanically variable orifice or a dual volume pressure bottle are required to implement a throttling pressure regulator.

(4) The feedback amplification circuit must be based on the confined-jet amplifier. No other fluid state component has the high pressure recovery and low P_C / P_S ratio associated with this device.

(5) For fixed orifice loads and blowdown applications, fluid state regulators operating on a programmed blowdown by use of pressure lag circuits can be implemented.

4.3 RECOMMENDATIONS

On the basis of the above conclusions, it is evident that either a system based on the dual valume tank or a mechanically-variable orifice must be used for minimum space, large-blowdown range operation. The hybrid regulator developed offers an excellent practical solution to the problem of producing the required pressure regulator performance with a minimum of moving parts while retaining the high reliability and other desirable characteristics of a completely all-fluid system.

On the other hand, if space is not at a premium, the two all-fluid approaches: (1) single lag circuit, (2) dual lag circuit, offer solutions to the problem. The dual lag circuit offers the longest blowdown range, but requires the largest amount of space. The single lag circuit requires little additional space, but is limited in blowdown range.

BLANK PAGE

APPENDIX A

NOTATION FOR SECTIONS 1 THROUGH 3

NOTE: Pressures will be in absolute units (psia) unless otherwise specified in text.

A = Flow area - in^2

A_A = Exit hole area of vortex valve A - in^2

A_B = Exit hole area of vortex valve B, also cross-sectional area of button - in^2

A_d = Mean effective area of diaphragm - in^2

A_e = Exit hole area - in^2

A_F = Feedback orifice area - in^2

A_L = Load orifice area - in^2

A_m = Effective area of a series of orifices - in^2

A_N = Confined jet amplifier nozzle area - in^2

A_S = Supply orifice area - in^2

C_d = Orifice discharge coefficient - dimensionless

C_2 = Characteristic gas coefficient - $\sqrt{°R}/sec$

D = Diameter - in

F_d = Diaphragm spring force - lbs

f_n = Natural frequency - cps

g = Standard sea level acceleration of gravity = 386 in/sec^2

k = Ratio of specific heats of gas - dimensionless

K = Spring rate - lbs/in

L = Length - in

m = Mass - $lb\text{-}sec^2/in$

n = Number of orifices in series - dimensionless

P = Pressure - psia or psig

P_B = Bottle pressure - psia or psig

B_{BC} = Control bottle pressure - psia or psig

P_C = Control pressure - psia or psig

P_{CSC} = Control pressure for supply flow cutoff - psia or psig

P_d = Pressure downstream of a pneumatic component - psia or psig

P_e = Exit pressure - psia or psig

P_F = Feedback pressure - psia or psig

P_m = Interstage pressure - psia or psig

P_R = Regulated pressure - psia or psig

P_S = Supply pressure - psia or psig

P_u = Pressure upstream of a pneumatic component - psia or psig

P_V = Mean vortex chamber pressure - psia or psig

P_O = Inlet pressure to a series of orifices (Used in Appendix D), also outlet pressure - psia or psig

P_1 through P_n = Pressure downstream of first through nth orifices in a series of orifices - psia or psig

R = Ideal gas constant - lb-in/lb°R

R_t = Turndown ratio of a valve - dimensionless

R_{tA} = Turndown ratio of valve A - dimensionless

R_{tB} = Turndown ratio of valve B - dimensionless

R_{to} = Overall turndown ratio - dimensionless

T = Absolute temperature of gas at zero velocity - °R

t_o = Total operating time - sec

$\dot{w}$ = Weight flow of gas - lbs/sec

$\dot{w}_B$ = Flow from bottle at pressure P_B - lb/sec

$\dot{w}_{BC}$ = Flow from bottle at pressure P_{BC} - lbs/sec

$\dot{w}_{C}$ = Control flow - lbs/sec

$\dot{w}_{CA}$ = Control flow for vortex valve A - lbs/sec

$\dot{w}_{CB}$ = Control flow for vortex valve B - lbs/sec

$\dot{w}_{F}$ = Vent flow of feedback circuit - lb/sec

$\dot{w}_{L}^{*}$ = Flow through load - lb/sec

$\dot{w}_{N}$ = Normalizing flow - lb/sec

$\dot{w}_{o}$ = Outlet flow - lb/sec

$\dot{w}_{R}$ = Vent flow of reference circuit - lb/sec

$\dot{w}_{S}$ = Supply flow - lbs/sec

$\dot{w}_{T}$ = Flow through throttling element - lbs/sec

W_{B} = Weight of gas initially stored at pressure P_{B} -lbs

W_{BC} = Weight of gas initially stored at pressure P_{BC} - lbs

V_{B} = Volume of W_{B} lbs of gas - in^3

V_{BC} = Volume of W_{BC} lbs of gas - in^3

η_{F} = Feedback system efficiency expressed as a fraction - dimensionless

Subscripts

1 through n - Refers to first through nth orifices in a series of orifices

i - Refers to initial conditions

f - Refers to final conditions

j - Refers to jth orifice in a series of n orifices

min - Refers to minimum value

max - Refers to maximum value

BLANK PAGE

APPENDIX B

THEORETICAL ANALYSIS OF VORTEX VALVES

This appendix provides a summary of an analysis accomplished for the purpose of describing vortex valve performance. It has been abstracted from "Phenomenology of Vortex Flow and Its Application to Signal Amplification" by L. B. Taplin and presented at Pennsylvania State University; Summer Engineering Seminars, Fluid Control Systems; July 6-16, 1965.

B.1 EXPERIMENTAL OBSERVATIONS OF PANCAKE VORTEX CHAMBERS

If a simple chamber is constructed as shown in the schematic, Figure B-1, some simple experiments will easily show the various amplifying properties which the vortex flow field possesses. The chamber is constructed so that the supplied radial flow component enters the chamber as uniformly as possible. One method, as shown, for accomplishing uniform radial chamber flow utilizes a porous ring pressurized externally by the supply pressure, P_o. To excite vortex flow, a tangential control port is used which introduces a tangential flow component

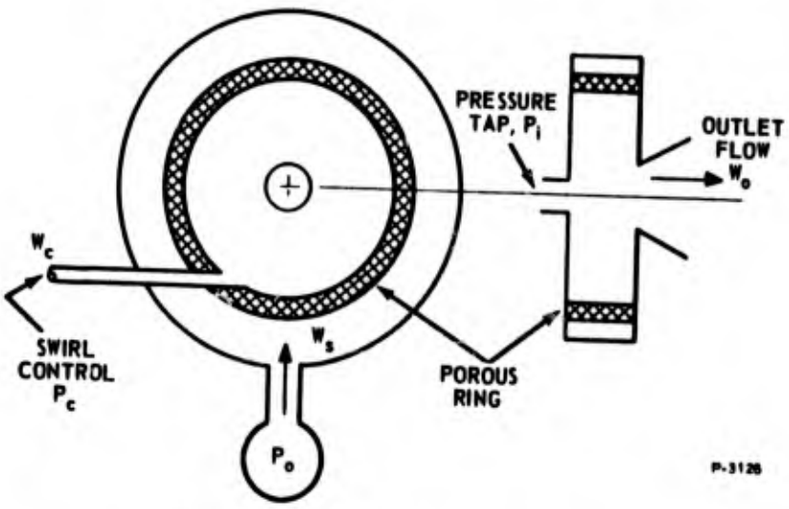

B-1 - Simple Vortex Chamber

just at the inner edge of the porous ring. A number of tangential ports may be used to again achieve a high degree of uniformity in the flow field. The combined flows move towards the exit hole,and in observing this fluid motion,it is readily apparent that the radial velocity of the fluid must increase as the fluid approaches the exit. In addition, if the tangential velocity of a particle of fluid is observed, it will be noted that its tangential velocity increases as it moves towards the exit. This increase in tangential velocity must result if angular momentum of the fluid flow is to be conserved. Here, then, are two velocity amplifying properties of the vortex flow field. The tangential velocity amplification or gain is of particular importance,as it is this gain that is primarily responsible for most of the unique vortex amplifier and sensing devices which are in use today. In particular, the tangential velocity increase leads to a centrifugal pressure buildup across the vortex chamber in a radial direction between the exit hole and the outer wall of the chamber. If such a centrifugal pressure buildup exists, then the chamber should present more resistance to flow as the chamber swirl or control flow component is increased. In order to examine this property of centrifugal pressure drop in its purest form,it is necessary that the porous ring and supply plenum be designed to present a very small resistance to flow in comparison to the exit hole resistance. With the chamber designed in this manner, and operating the chamber with a regulated supply source, P_o, curves of weight flow as a function of control pressure or control flow may be plotted. These characteristic curves have the form shown in Figure B-2.

P-3126

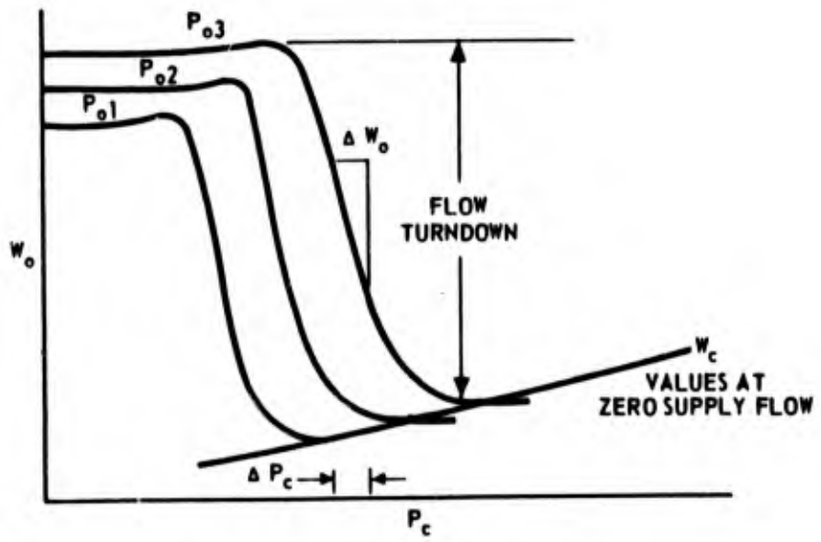

Figure B-2 -Vortex Chamber Characteristic Curves with Regulated Supply

When the supply pressure is regulated, if there is a centrifugal pressure drop across the flow field, less pressure should be available at the exit hole to expel the fluid and the device should throttle flow as demonstrated by the experiment. A number of things are, of course, of immediate interest when one examines the experimental curves. Probably first, is the question of what controls the throttling range or turndown ratio. Looking at the minimum flow point, if the flow at the supply port is measured, it is found that this flow is zero or perhaps slightly reversed. The wall pressure has built-up to the extent that the supply flow is cut off, i.e., there is a value of control flow which causes supply cutoff. The turndown ratio for a given supply pressure is the ratio of maximum flow before throttling starts to the control flow which causes supply cutoff. If centrifugal pressure forces cause this throttling to take place, then tangential velocity of the flow field plays an important role in setting up a wall pressure to cause cutoff. Obviously, if the tangential velocity is high at the outer wall of the chamber and therefore throughout the chamber, the centrifugal pressure buildup should be large. Since the tangential velocity at the outer wall is a function of conserved angular momentum, then higher wall velocities should imply a higher control influx momentum. Writing the expression for outer wall velocity:

$$V_{to} = \frac{W_c V_c}{W_c + W_o}$$

It is noted that V_{to} is larger when the momentum rate, $W_c V_c$, is larger. Now, it is obvious that turndown ratio can be improved if for a given wall velocity, control velocity, V_c, is increased and therefore the control mass flow, W_c, is decreased. The higher control velocity requires a higher control pressure which in some applications may be a disadvantage.

Also, of interest is the flow gain — another amplifying property — of the device, $\Delta W_o / \Delta W_c$. It might be expected that this gain goes hand in hand with the turndown ratio and, therefore, higher flow gains are achieved if high control velocities are used.

The curves may be plotted in another way as shown in Figure B-3. Here the control pressure has been regulated and supply flow is varied to obtain the plots of W_o versus P_o. The upper curve in Figure B-3 defines the maximum flow of the chamber versus supply pressure with no control flow. The upper curve is essentially that of an orifice —

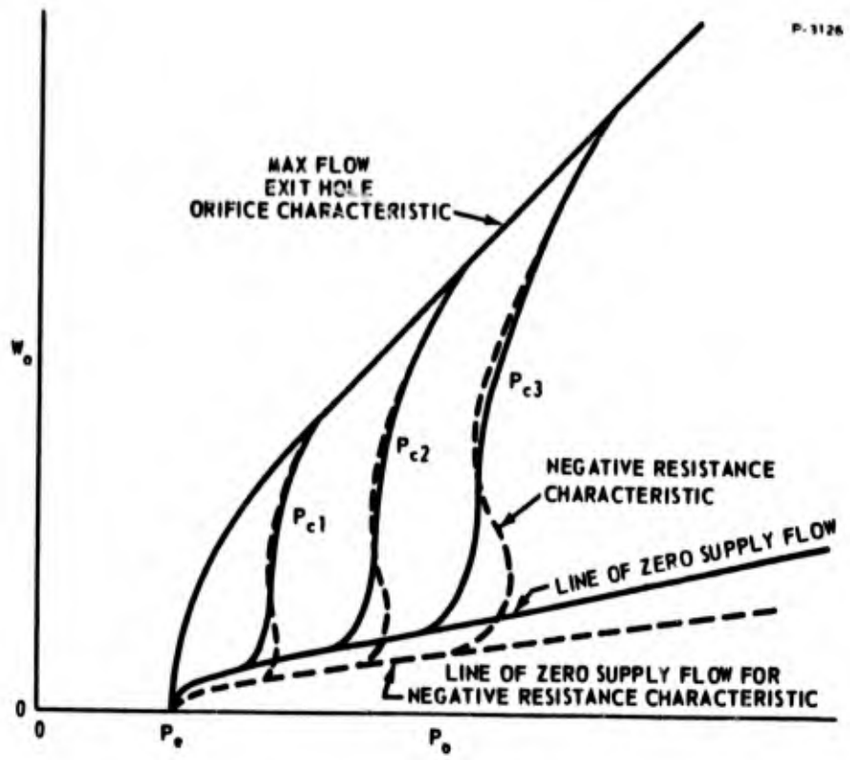

Figure B-3 - Vortex Chamber Characteristic Curves with Regulated Control

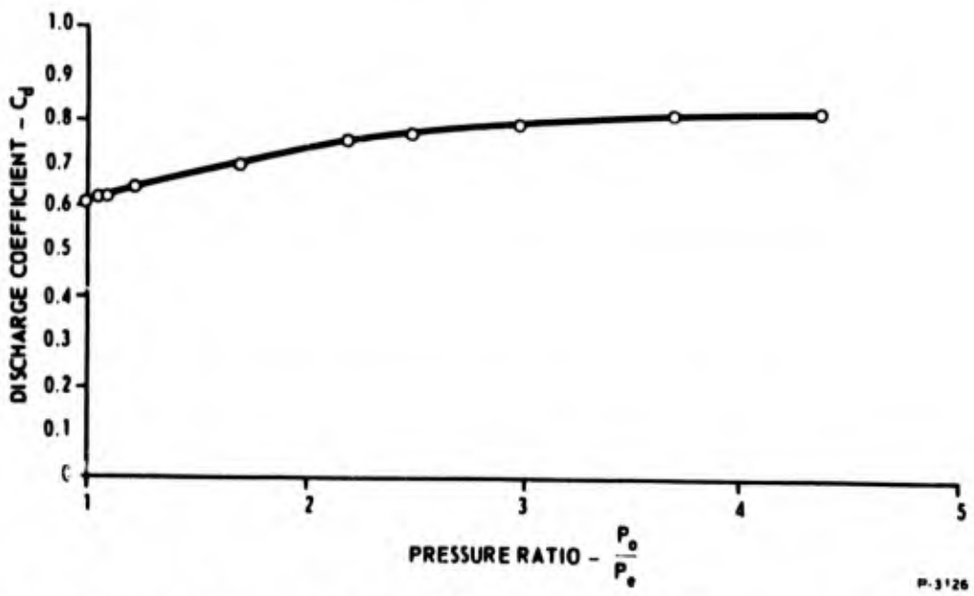

Figure B-4 - Vortex Chamber Maximum Flow Discharge Coefficient

the exit hole — characteristic with a discharge coefficient that varies with supply-to-exit pressure ratio as shown in Figure B-4. This discharge coefficient curve was obtained for a particular chamber and values do change somewhat with geometry of the chamber. The trend in coefficient change is (in general) correct for most pancake-shaped chambers.

Returning to Figure B-3,the locus of points defining the minimum flow through the chamber constitute that characteristic flow curve obtained for control flow alone with supply flow zero. In examining the flow data in Figure B-3, it is interesting to note that the constant control pressure characteristic curves are nearly equally spaced across the map in the direction of increasing control and supply pressure. The equal spacing indicates that a proportional relationship between P_c and P_o exists.

Another interesting observation in testing some chambers is that multivalued flows can exist for a given supply pressure, i.e., the characteristic curves exhibit a region of negative resistance. These negative resistance curves are indicated by the dashed lines in Figure B-3. In general, these negative resistance characteristics show up when the vortex chamber thickness is relatively large and the supply plenum resistance is low in comparison to the exit hole resistance.

Another interesting experiment involves monitoring the pressure, P_i, at the center of the vortex chamber wall as flow changes. (See Figure B-1.) A plot of this pressure, P_i,versus supply pressure for regulated control pressure has a form very similar to the weight flow characteristic curve, (See Figure B-5.) In fact, if the hole for measuring P_i is properly sized,the pressure measured is virtually that average pressure which acts on the exit hole of the vortex device to expel the fluid. Further, as will be discussed later, this pressure is very closely related to the calculated pressure which occurs at the rim of the chamber exit hole.

A close indication of the value of P_i can be found directly from the weight flow characteristic curves if the discharge coefficient for the exit hole is reasonably independent of the degree of chamber swirl or control flow.

This determination of P_i, as demonstrated in Figure B-6, where, for a given set of quiescent operating pressures, and weight flow — the circled point — a dashed line,constructed horizontally across the graph

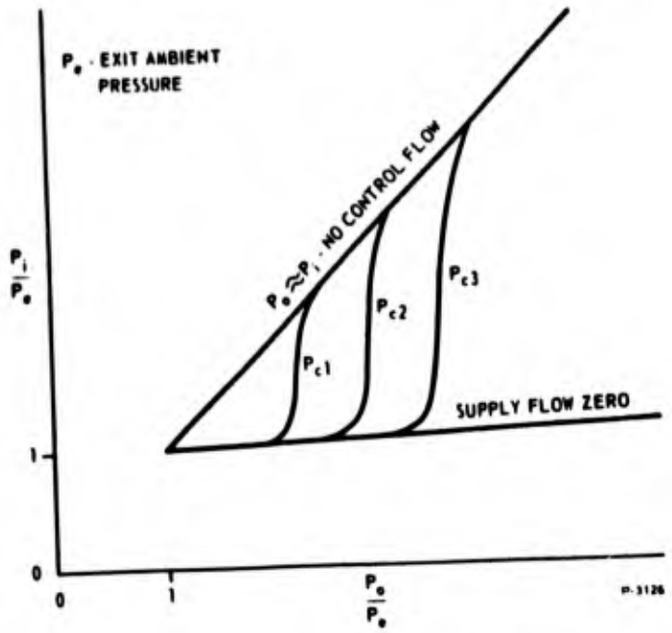

Figure B-5 - Characteristic Curves of Vortex Chamber Center Pressure, P_i

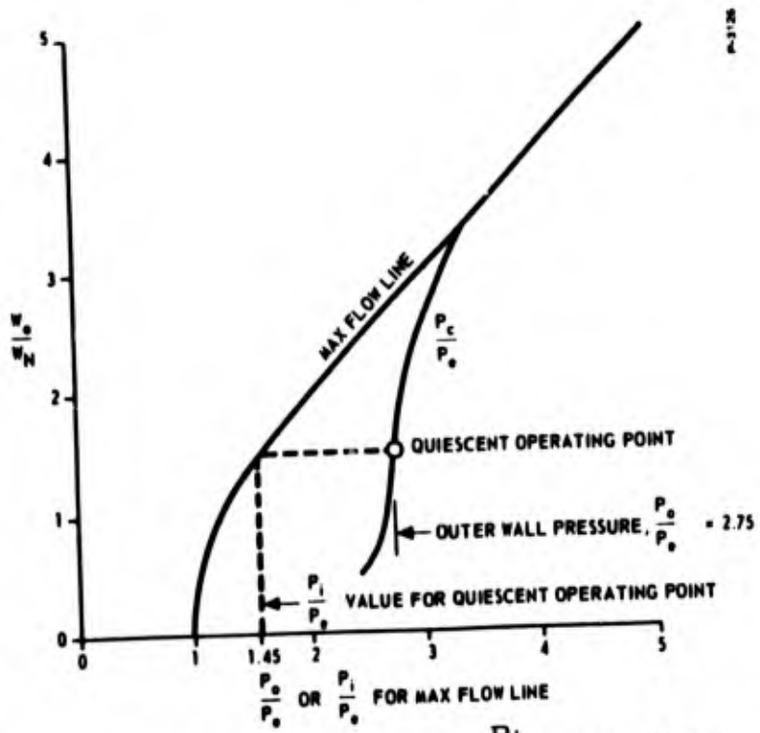

Figure B-6 - Determination of $\frac{P_i}{P_e}$ from Weight Flow Characteristic Curves

to the maximum flow line and then down to the P_o/P_e axis, gives the value of P_i/P_e if the discharge coefficient is independent of swirl. The curves shown in Figure B-6 have been normalized with respect to the ambient or back pressure, P_e, on the exit hole of the valve and a normalizing weight flow, W_N, which is given by:

$$W_N = \frac{C_d C A_e P_e}{\sqrt{T}}$$

This flow parameter, W_N, is then representative of the exit hole size, operating gas media, and gas temperature. This normalization will be used in developing a mathematical model for the vortex chamber.

The pressure ratio across the vortex flow field in the radial direction is given by P_o/P_i or, for the example in Figure B-6, P_o/P_i = 2.75/1.45. It is interesting to note that when the exit hole is flowing sonically, $P_i/P_e > 2$, the pressure ratio across the chamber, P_o/P_e, can be much larger than critical. When the exit hole is flowing sonically, back pressure cannot affect the flow through the chamber for a given supply and control pressure. In the normalized plot, a change in P_e causes a shift in the operating point, but W_N and P_c/P_e change in a manner so that the actual weight flow, W_o, remains constant. An example of how the pressure ratios and weight ratio change for shifting back pressures is shown in Figure B-7, where P_o, P_c, and W_o are all constant. With a starting quiescent point at $P_o/P_e = 8$, with the control port sized so that $P_c/P_e = 10$ and $W_o/W_N = 4$, if the back pressure is doubled, the new operating point will be at $P_c/P_e = 5$ with P_o/P_e at 4 and $W_o/W_N = 2$. Since W_N is doubled if P_e is doubled, W_o is the same value as before. This operation provides some insight into the nature of the vortex valve. It can be looked upon (in general) as an adjustable set of orifices in which the ratio of P_c/P_o defines the apparent size and number of orifices. For the case where the exit hole is known to be sonic, a single orifice can be found to exhibit the same flow relationship versus P_o/P_e.

The normalization selected has some interesting characteristics. The maximum flow line above a P_o/P_e of 2 is a straight line of unity slope, i.e., W_o/W_N equals P_o/P_e above values of 2.

The constant P_c/P_e lines must intersect with the maximum flow line where $P_o/P_e = P_c/P_e$. There is a strong indication that supply flow is always cut off for a given P_c/P_o ratio and, therefore, the line of

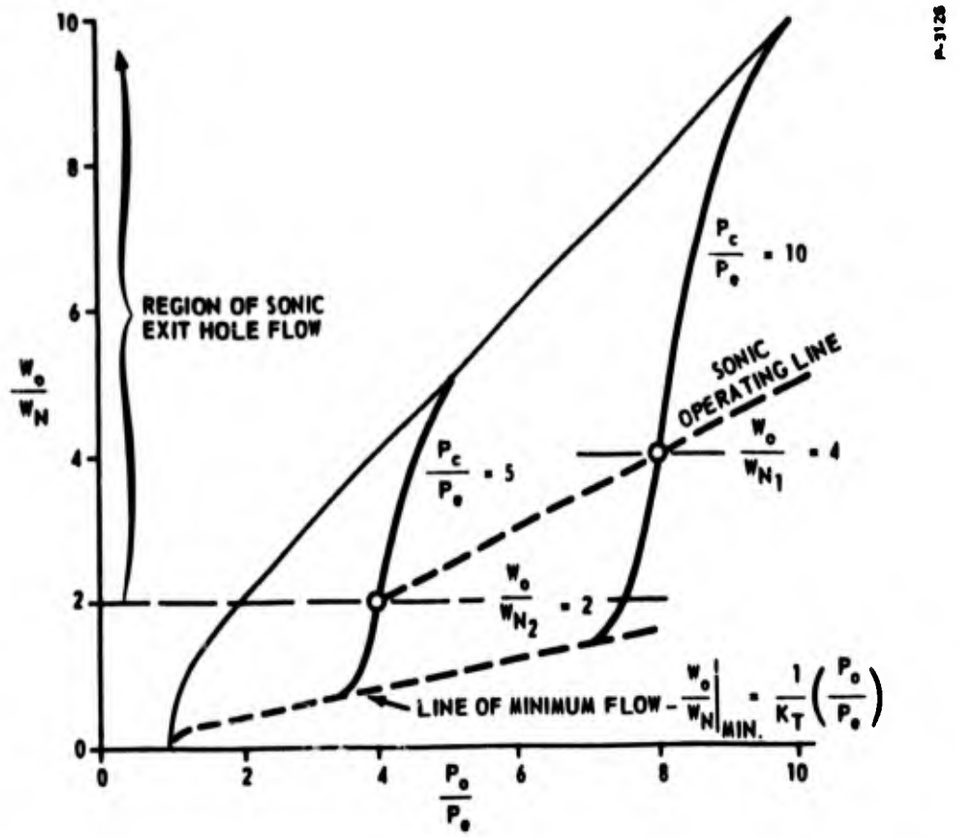

Figure B-7 - Operation of Vortex Valve with Exit Hole Flow Sonic

minimum flow (supply flow zero) is a straight line except at low values of P_o/P_e, and has the equation:

$$\frac{P_o}{P_e} = K_T \left(\frac{W_o}{W_N}\right)$$

where K_T is the turndown ratio $W_{o\,max}/W_c$. There are some experimental discrepancies and theory does not as yet prove this point, but it is a reasonably good approximation as the values (in general) show the same turndown ratio above P_o/P_e pressure ratios of 2.

B.2 THEORETICAL FLOW AND PRESSURE CHARACTERISTICS

In order to determine the behavior of the flow through a vortex chamber, it is first necessary to know the distribution of the tangential velocity as a function of chamber radius. This distribution of tangential velocity depends on chamber geometry, the magnitude of swirl and the

viscosity of the fluid. Where the viscosity is very low, conservation of angular momentum indicates that the tangential velocity must increase with decreasing radius, i.e., the tangential velocity, V_t, at any radius r is given by:

$$V_t = \frac{V_{to} r_o}{r} \qquad \text{(B-1)}$$

where

V_{to} = tangential velocity at the outer wall - in/sec

r_o = maximum chamber radius - in

As viscosity becomes very large, the fluid can rotate as a solid body and then the tangential velocity is given by:

$$V_t = \frac{V_{to} r}{r_o} \qquad \text{(B-2)}$$

In general, the tangential velocity can be expressed as:

$$V_t = V_{to} \left(\frac{r_o}{r}\right)^n \qquad \text{(B-3)}$$

where

n = +1 for a free vortex

n = -1 for solid body rotation.

A plot of these velocity distributions versus chamber radius, r, is shown in Figure B-8 for various values of n. In the case of the free vortex where the viscosity is low, the tangential velocity must eventually peak and then decrease and approach zero velocity at the center of the chamber, since no fluid has completely zero viscosity. Also, for gases, a breakdown in tangential velocity must occur as chamber geometry cannot support supersonic flow. For gases, n can be taken as + 1 until the velocity breaks down, as indicated by the dashed curve in Figure B-8. Since we are interested in the pressure drop developed by the flow field, a suitable "n" value can be found for an experimental unit which gives some indication of the behavior of the tangential flow.

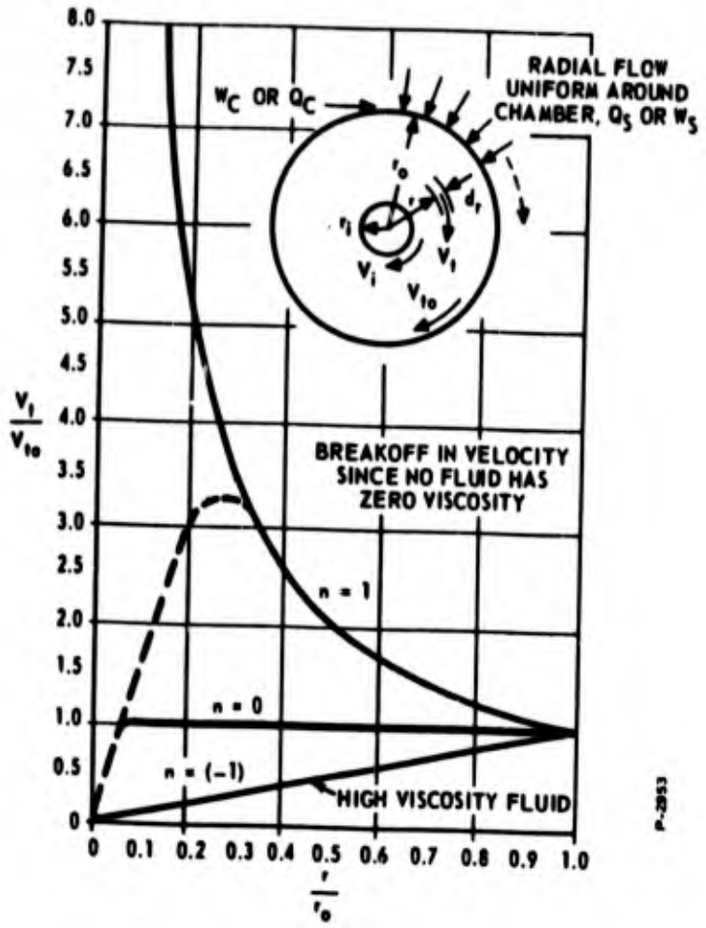

Figure B-8 - Vortex Tangential Velocity Distribution

The differential pressure developed across a differential radius dr is given by:

$$dP = \frac{\rho V_t^2 dr}{r} \qquad \text{(B-4)}$$

where

ρ = fluid mass density - $lb/sec^2/in^4$

V_t = tangential velocity at radius r - in/sec

r = chamber radius - in.

dP = differential pressure across dr - psid

At this point, some assumptions will be made:

(a) Fluid temperature remains nearly constant.

(b) The weight flow leaving the exit hole is very closely a function of P_i at radius r_i.

(c) For gases n = 1, that is free vortex flow exists until a maximum tangential Mach number is reached. (See Figure B-9.)

As noted in Figure B-9, a higher initial outer wall velocity may cause a higher maximum tangential Mach number occurring at radius r_m. This maximum velocity is an unknown and will be found to be a variable, depending on the operating pressure ratio across the chamber. Returning to equation (B-4), the density from the equation of state is $\rho = P/gRT$. Therefore:

$$\frac{dP}{P} = \frac{V_t^2 \, dr}{g R T r} \qquad \text{(B-5)}$$

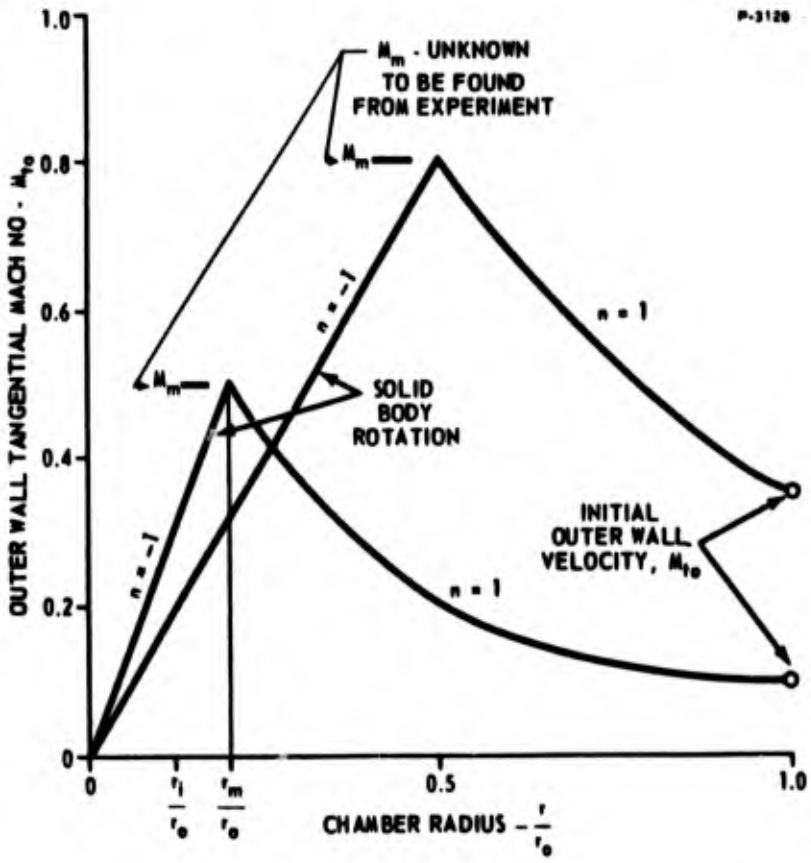

Figure B-9 - Assumed Tangential Velocity Profile for Gases

Sonic velocity for a gas of temperature T is given by:

$$V_s = k g RT \tag{B-6}$$

therefore:

$$\frac{dP}{P} = k M_t^2 \frac{dr}{r} \tag{B-7}$$

where

$$M_t = \frac{V_t}{V_s}$$

Using the velocity profiles of Figure B-9, equation (B-7) may be integrated from radius r_i to r_o for two different conditions. When $r_m < r_i$ or $M_{to}\, r_o / M_m\, r_i < 1$

$$\frac{P_o}{P_i} = \epsilon^{K M_{to}^2} \tag{B-8}$$

where

$$K = \frac{k}{2}\left(\frac{r_o^2}{r_i^2} - 1\right) \tag{B-9}$$

and when $r_m > r_i$ or $\frac{M_{to}\, r_o}{M_m\, r_i} > 1$

$$\frac{P_o}{P_i} = \epsilon^{\frac{k}{2}\left[M_m^2\left(2 - \frac{M_m^2}{M_{to}^2}\frac{r_i^2}{r_o^2}\right) - M_{to}^2\right]} \tag{B-10}$$

It is to be noted that when $M_{to}\, r_o / M_m\, r_i = 1$, equations (B-8) and (B-10) are equal. At low values of M_{to}, the vortex flow behaves as a free vortex for all radii between r_o and r_i.

From conservation of angular momentum, the outer wall velocity is given by:

$$M_{to} = \frac{\eta W_c M_c}{W_c + W_s} = \frac{\eta \frac{W_c}{W_N} M_c}{\frac{W_o}{W_N}} \qquad \text{(B-11)}$$

where

$$W_N = \frac{C_d C A_e P_e}{\sqrt{T}} \qquad \text{(B-12)}$$

$$\frac{W_o}{W_N} = \frac{W_c}{W_N} + \frac{W_s}{W_N} \qquad \text{(B-13)}$$

The expressions for weight flow as a function of pressures must now be developed. It will be recalled that orifice flow is given by:

$$W = \frac{C_d C A P_u}{\sqrt{T}} f_1 \left(\frac{P_d}{P_u}\right) \qquad \text{(B-14)}$$

where

f_1 = ratio of subsonic to sonic flow, (See Figure B-10.)

For sonic flow

$$W = \frac{C_d C A P_u}{\sqrt{T}} \qquad \text{(B-15)}$$

An elliptical approximation to the f_1 function is used in this analysis where:

$$f_1 \left(\frac{P_d}{P_u}\right) = \frac{2 P_d}{P_u} \sqrt{\frac{P_u}{P_d} - 1} \qquad \text{(B-16)}$$

(See Figure B-10.)

The maximum flow error occurs near $P_d/P_u = 0.8$ and is approximately 2.5 percent. Since the discharge coefficient is not known to this accuracy, the approximation of f_1 is considered adequate for purposes of the

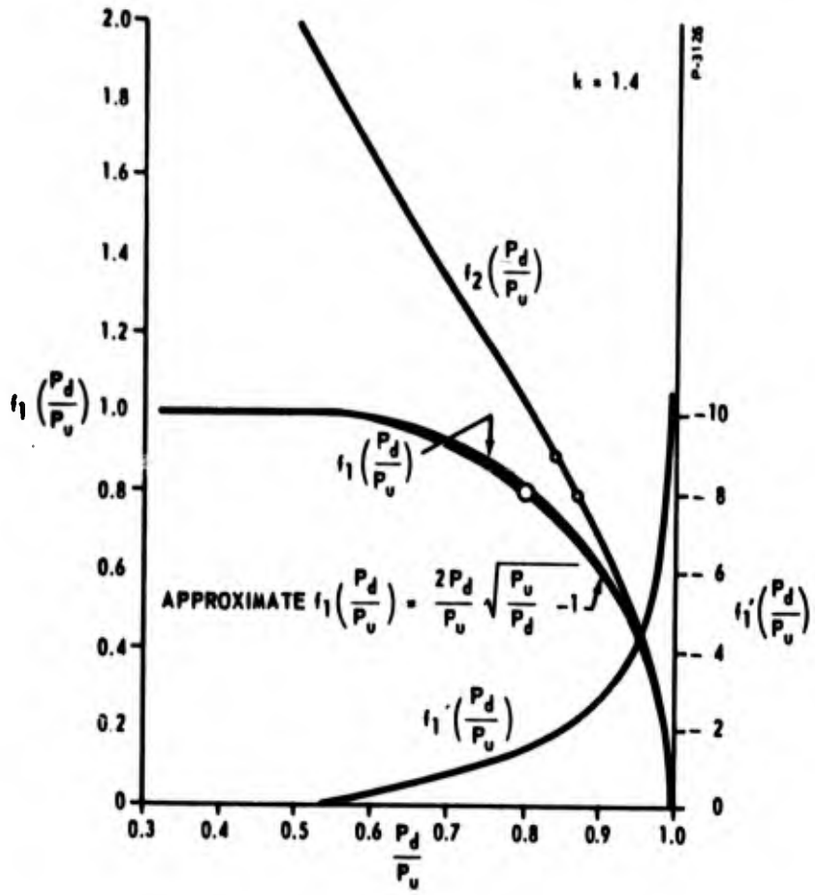

Figure B-10 - Gas Flow Functions

following analysis. Care must be used to remember that when $P_u/P_d \geq 2$, $f_1 (P_d/P_u)$ remains unity.

The momentum expression $W_c M_c/W_N$ can be derived as follows: For sonic flow with k = 1.4

$$\frac{W_c M_c}{W_N} = 0.915 \frac{C_{dc} A_c P_c}{C_d A_e P_e} \qquad \text{(B-17)}$$

where M_c = 0.915, the Mach number at the orifice throat based on the upstream temperature.

For subsonic flow

$$\frac{W_c M_c}{W_N} = 0.915 \left(\frac{C_{dc} A_c P_c}{C_d A_e P_e}\right) f_3 \left(\frac{P_o}{P_c}\right) \qquad \text{(B-18)}$$

where f_3 is plotted in Figure B-11.

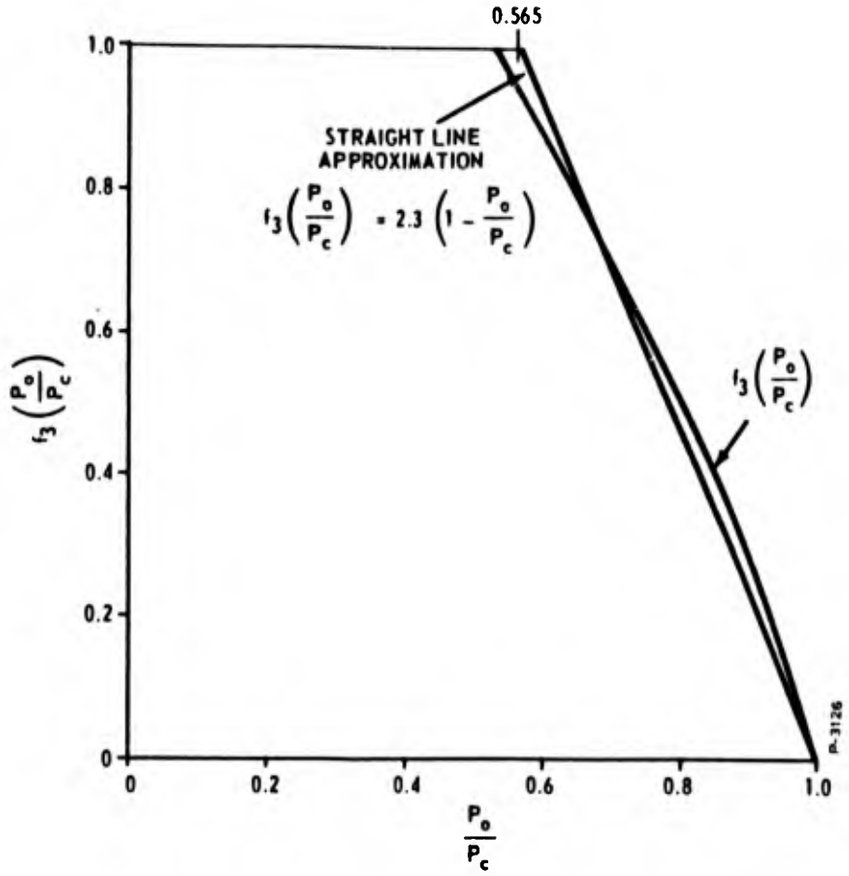

Figure B-11 - Momentum Function - $f_3 \frac{P_o}{P_c}$

A straight line approximation to this function as shown in Figure B-11 describes f_3 as follows:

$$f_3\left(\frac{P_o}{P_c}\right) = 2.3\left(1 - \frac{P_o}{P_c}\right) \qquad \text{(B-19)}$$

and introduces a maximum error of 10 percent in momentum. Even though this error is relatively large, it will be helpful to use the following approximate momentum expression for subsonic flow:

$$\frac{W_c M_c}{W_N} = \frac{2.1\, C_{dc}\, A_c}{C_d\, A_e}\left(\frac{P_c}{P_e} - \frac{P_o}{P_e}\right) \qquad \text{(B-20)}$$

where it is seen that the momentum efflux at the throat of an orifice to a 10 percent maximum error is linearly related to the pressure drop across the orifice for subsonic throat velocities. Again,care must be

used to remember that for $P_c/P_o > 2$, sonic conditions exists and equation (B-17) must be used. Most practical applications of vortex devices involve primarily subsonic flow at the control orifice. P_o is outer wall pressure in the vortex chamber, which acts as a back pressure on the control jet orifice.

The flow leaving the exit hole using equation (B-16) is given by:

$$\frac{W_o}{W_N} = 2 \quad \frac{P_i}{P_e} - 1 \quad \text{for subsonic flow } \frac{P_i}{P_e} < 2 \qquad \text{(B-21)}$$

The exit flow for sonic exit velocity is given by:

$$\frac{W_o}{W_N} = \frac{P_i}{P_e} \quad \text{for sonic flow } \frac{P_i}{P_e} \geq 2 \qquad \text{(B-22)}$$

Recapitulating:

$$\frac{P_o}{P_i} = \epsilon^{f(M_{to})} \qquad \text{(B-23)}$$

where

$$f(M_{to}) = \frac{k}{2}\left[\left(\frac{r_o}{r_i}\right)^2 - 1\right] M_{to}^2 = KM_{to}^2 \text{ for } \frac{M_{to}\, r_o}{M_m\, r_i} < 1$$

or

$$f(M_{to}) = \frac{k}{2}\left[M_m^2\left(2 - \frac{M_m^2\, r_i^2}{M_{to}^2\, r_o^2}\right) - M_{to}^2\right] \text{ for } \frac{M_{to}\, r_o}{M_m\, r_i} > 1.$$

$$M_{to} = \frac{2.1\,\eta\, C_{dc}\, A_c}{C_d\, A_e}\left[\frac{P_c}{P_e} - \frac{P_o}{P_e}\right] \text{ for subsonic control flow, } \frac{P_o}{P_c} > 0.528 \qquad \text{(B-24)}$$

$$M_{to} = \frac{0.915\,\eta\, C_{dc}\, A_c}{C_d\, A_e}\left(\frac{P_c}{P_e}\right) \text{ for subsonic control flow, } \frac{P_o}{P_c} < 0.528 \qquad \text{(B-25)}$$

$$\frac{W_o}{W_N} = 2\sqrt{\frac{P_i}{P_e} - 1} \quad \text{subsonic exit flow, } \frac{P_i}{P_e} < 2 \tag{B-26}$$

$$\frac{W_o}{W_N} = \frac{P_i}{P_e} \quad \text{for sonic exit flow, } \frac{P_i}{P_e} > 2 \tag{B-27}$$

$$\frac{W_o}{W_N} = \frac{W_s}{W_N} + \frac{W_c}{W_N} \tag{B-28}$$

$$W_N = \frac{C_{dc}\, A_e\, P_e}{\sqrt{T}} \tag{B-29}$$

$$M_m = f\left(\frac{P_c}{P_e}\right) \tag{B-30}$$

The maximum tangential Mach number given by equation (B-30) remains to be determined by using the experimental data. As indicated, it is strongly related to the control pressure ratio used. If the assumed velocity profile model is reasonably correct, it can be expected that M_m should never exceed a value of one, as in reality, the vector sum of the tangential and radial velocities cannot exceed one.

Equations (B-23) through (B-30) can now be solved and the theoretical results compared with experimental results.

B-3 THEORETICAL - EXPERIMENTAL CORRELATION

In examining the equations, it will be of interest to assume M_m so large that the vortex flow is considered to be that of a free vortex. The vortex chamber tested had a radius ratio, $r_o/r_i = 8$ and a control parameter, $2.1\,\eta\, C_{dc}\, A_c/C_d\, A_e = 0.2$. The experimental data is plotted in Figure B-12 with the discharge coefficient C_d as given by Figure B-4, used for the maximum flow line; thus, W_o/W_N for maximum flow follows exactly the theoretical form. Since the discharge coefficient for the control characteristic curves is unknown, an assumed value of 0.72 was used to normalize the experimental flow points. The normalizing flow

is given by equation (B-29). It was assumed that the momentum mixing efficiency was at least 90 percent in arriving at the control parameter given as 0.2 above.

Solving the theoretical equations for the values given produced theoretical results which plotted well to the left of the experimental points for all three control pressure ratios shown in Figure B-12. Two choices were now open to adjust parameters to effect a correlation. One choice was the reduction in η, the mixing efficiency, which would move the theoretical data points to the right (in the direction of increasing P_o/P_e). The other choice involved a reduction in radius ratio, below that of the theoretical value of 8. It will be noted that as long as M_m is large, the equations always use the parameter η^2 multiplied by $k/2\ (r_o^2/r_i^2 - 1)$ and the choice in adjustment is arbitrary. However, for the lower flow portion of the characteristic curves,this arbitrary product does not occur as $f(M_{to})$ involves the use of M_m. In order to get a satisfactory correlation at low flows, r_o/r_i had to be reduced to a value of 5.08 compared with the theoretical value of 8. It can be reasoned that a real fluid with viscosity could cause losses at the chamber walls, which in effect reduce the apparent radius ratio.

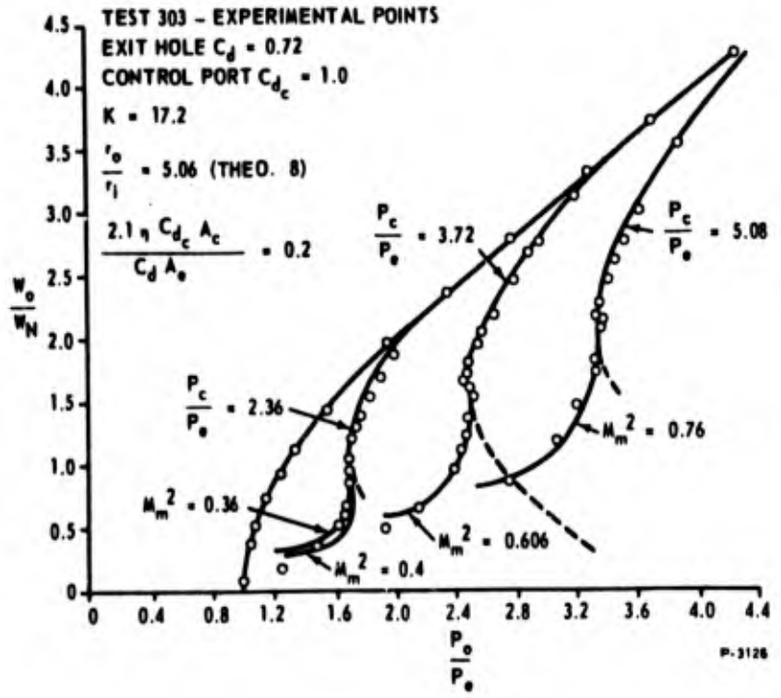

Figure B-12 - Theoretical-Experimental Correlation P_o/P_e

As a specific example, where M_m is assumed very large, the theoretical characteristic curve for $P_c/P_e = 3.72$ is shown in Figure B-12. The dashed portion indicates the solution if no maximum tangential velocity is reached. Here then, is theoretical behavior indicating the existence of a negative resistance characteristic. The pressure ratio P_o/P_i is strongly exponentially increasing with M_{to}^2, and if no limit is reached on tangential velocity in the chamber, the centrifugal pressure buildup can increase so rapidly that P_o/P_e must be increased at lower flows to maintain the flow. Since only the slightest negative resistance is indicated by the particular experiment used, M_m must be nearly equal to $(r_o/r_i)\, M_{to}$ taken at the point of curve verticality, $P_o/P_e \approx 2.47$. The value of M_m^2 determined in this manner was approximately 0.6. Since a slight negative resistance is involved, a value of $M_m^2 = 0.606$ gave the best correlation. Using the same reduced, r_o/r_i, $(r_o/r_i = 5.06)$, the other theoretical curves for $P_c/P_e = 2.36$ and 5.08 were constructed. Surprisingly, the fit was good, indicating that whatever the loss mechanism is that effectively reduces r_o/r_i, it seems to hold for the range of pressure ratios, P_o/P_e, studied. Again, to get correlation at the low flows, it was necessary to find the proper values of M_m. The interesting aspect of the theoretical model selected is that M_m seems to remain virtually constant for a given P_c/P_e but must be increased with increasing P_c/P_e, as shown in Figure B-13. At this time,

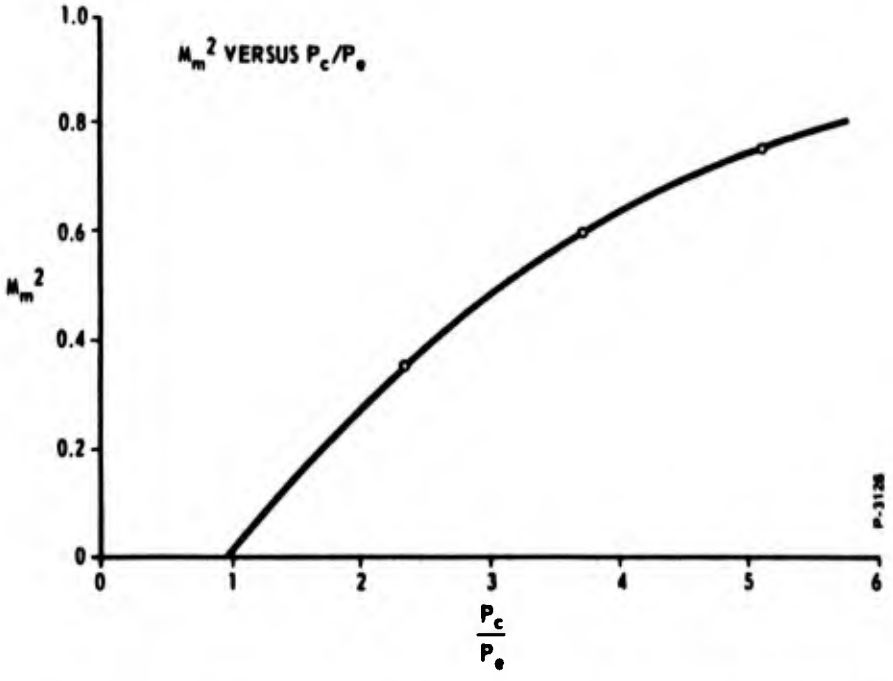

Figure B-13 - Maximum Tangential Mach Number Versus P_c/P_e

it must be concluded that the velocity profile selected (See Figure B-9). has caused this empirical relationship between M_m and P_c/P_e, and that some profile other than solid body rotation from the radius at which a maximum Mach number occurs could change this empirical relationship. However, the theoretical model may become more complex and less amenable to hand analysis should other profiles be used.

It is interesting to note the effect of increasing the maximum tangential Mach number. For the case of P_c/P_e - 2.36, M_m^2 was increased from 0.36 to 0.4 and the results are plotted in Figure B-12. As can be seen, a higher M_m causes more negative resistance and produces a better turndown ratio. The higher M_m, implies a chamber with less loss, and, therefore, better gain, turndown ratio, and negative resistance should result. If the losses are less, then the effective r_o/r_i should increase slightly, which will swing the upper portion of the weight flow curve (that portion above the point of verticality) to the left, thus further augmenting the negative resistance.

For the portion of the flow curves above the upper point of verticality, equations (B-8), (B-24), and (B-26) are again linearized to yield the following gain expressions:

$$\frac{\partial P_i}{\partial P_o} = \frac{\dfrac{P_{io}}{P_{oo}} + 2K M_{to}^2 \left[\dfrac{P_{io}}{P_e}\right]}{1 - \dfrac{K M_{too}^2 \left[\dfrac{P_{io}}{P_e}\right]}{\dfrac{P_{io}}{P_e} - 1}} \qquad \text{(B-31)}$$

$$\frac{\partial P_i}{\partial P_c} = \frac{-2K M_{too}^2 \left[\dfrac{P_{io}}{P_e}\right] \Big/ \left[\dfrac{P_{co}}{P_e} - \dfrac{P_{oo}}{P_e}\right]}{1 - \dfrac{K M_{too}^2 \left[\dfrac{P_{io}}{P_e}\right]}{\dfrac{P_{io}}{P_e} - 1}} \qquad \text{(B-32)}$$

$$\frac{\partial\left[\frac{W_o}{W_{oo}}\right]}{\partial\left[\frac{P_c}{P_e}\right]} = \frac{-1}{\left[\frac{P_{co}}{P_e} - \frac{P_{oo}}{P_e}\right]} \left[\frac{K M_{too}^2 \left[\frac{P_{io}}{P_{io} - P_e}\right]}{1 - \frac{K M_{too}^2 P_{io}}{P_{io} - P_e}}\right] \quad \text{(B-33)}$$

To find the flow gain $\partial W_o / \partial W_c$,

$$\frac{W_c}{W_N} = \frac{2 C_{dc} A_e P_o}{C_d A_e P_e} \sqrt{\frac{P_c}{P_o} - 1}$$

$$\frac{\partial\left[\frac{W_c}{W_{co}}\right]}{\partial\left[\frac{P_c}{P_e}\right]} = \frac{1}{2\left[\frac{P_c}{P_e} - \frac{P_{oo}}{P_e}\right]} \quad \text{(B-34)}$$

$$\frac{\partial\left[\frac{W_o}{W_{oo}}\right]}{\partial\left[\frac{W_c}{W_{co}}\right]} = \frac{-2 K M_{too}^2 \left[\frac{P_{io}}{P_{io} - P_e}\right]}{1 - \frac{K M_{too}^2 P_{io}}{P_{io} - P_e}} \quad \text{(B-35)}$$

It is, of course, interesting to note the denominator in each gain expression. When $K M_{too}^2 P_{io}/(P_{io}-P_e)$ equals unity, all gains are infinite, which indicates, of course, that the quiescent operating point is at the point of verticality on the characteristic curve. The denominator can be thought of as a regenerative effect which becomes more dominant as M_{to} or bias control is increased.

B-4 NOMENCLATURE FOR APPENDIX B

A_c = control jet area - in^2

A_e = exit hole area - in^2

C = gas constant - $°R^{1/2}/sec$

C_d = exit hole discharge coefficient

C_{dc} = control jet discharge coefficient

K = vortex sensitivity constant

K_T = vortex chamber turndown ratio

M_c = control jet Mach number

M_m = maximum tangential velocity Mach number

M_t = tangential Mach number of flow field

M_{to} = outer wall Mach number

P_c = control jet pressure - psia

P_d = pressure downstream of an orifice - psia

P_e = back pressure on vortex chamber - psia

P_i = vortex static pressure at radius r_i - psia

P_o = vortex chamber - outer wall pressure - psia

P_s = supply pressure - psia

P_u = pressure upstream of an orifice - psia

R = gas constant - in.-lbf/lbm - °R

T = gas temperature - °R

V_c = control jet velocity entering chamber - in/sec

V_s = sonic velocity of gas at temperature, T - in/sec

V_t = tangential velocity of vortex flow field at radius r - in/sec

V_{to} = outer wall tangential velocity of vortex flow field - in/sec

W_c = control flow to vortex chamber · lbm/sec

W_N = normalizing weight flow

W_o = total flow leaving vortex chamber - lbm/sec

W_s = supply flow to vortex chamber - lbm/sec

$f_1\left(\frac{P_d}{P_u}\right)$ = see Figure B-10

$f_3\left(\frac{P_o}{P_c}\right)$ = see Figure B-11

g = local acceleration of gravity - in/sec^2

k = ratio of gas specific heats

ℓ = chamber thickness or length - in

n = vortex tangential velocity characteristic exponent

r = vortex chamber radius - in

r_o = vortex chamber outer radius - in.

r_m = radius at which M_m occurs - in.

η = momentum mixing efficiency

ρ = fluid density - lbm/in^3

Note: Additional subscript zeros indicate quiescent value of variables.

BLANK PAGE

APPENDIX C

HYBRID REGULATOR DYNAMIC ANALYSIS

This Appendix describes the dynamic analysis used on the hybrid regulator in order to determine the design parameters. The parameters were selected to provide a dynamically-stable regulator under all operating pressures. A mechanical model of the regulator is shown in Figure C-1, along with the flow schematic. The following list of nomenclatures defines the various quantities used in the analysis and in Figure C-1.

Pressures (psia)

P_B = storage bottle pressure

P_s = gas pressure downstream of variable orifice A_m and confined-jet amplifier supply pressure

P_c = confined-jet amplifier output pressure

P_o = vortex chamber pressure

P_i = vortex chamber exit hole pressure

P_R = regulated pressure, also confined-jet amplifier vent pressure

P_e = ambient pressure

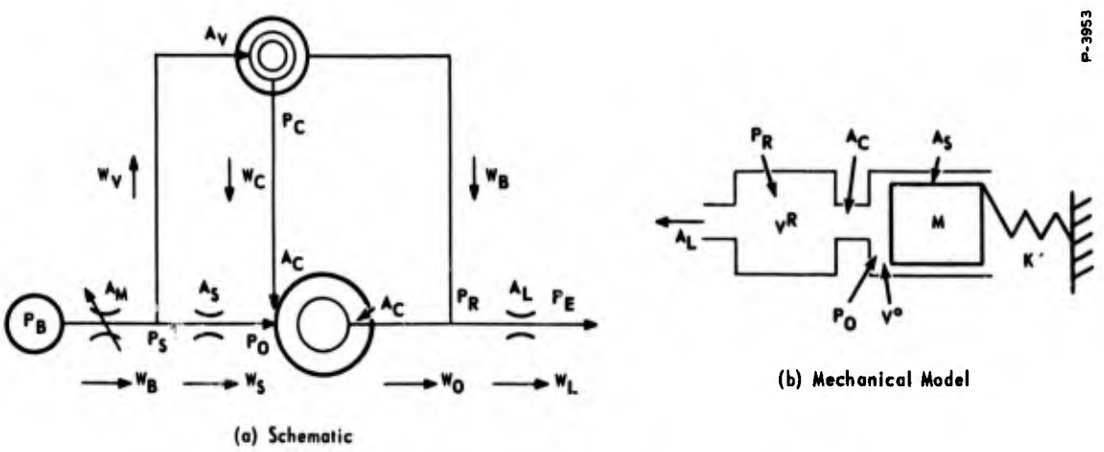

Figure C-1 - Flow Schematic and Mechanical Model

Flows (lb/sec)

W_B = storage bottle delivery flow

W_s = vortex chamber supply flow

W_v = confined-jet amplifier supply flow

W_c = vortex chamber control flow

W_o = vortex chamber exit flow

W_b = confined-jet amplifier vent flow

W_L = load flow

W_{po} = vortex volume pressurization flow

W_{pR} = regulated pressure volume pressurization flow

W_D = vortex volume displacement flow

Areas (in^2)

A_m = variable mechanical area

A_s = fixed orifice in vortex chamber supply

A_v = confined-jet amplifier supply area

A_c = vortex control port area

A_e = vortex chamber exit area

A_L = load area

Miscellaneous

K = vortex chamber gain

K' = spring rate lb/in

M_{to} = control port Mach number

$\mathscr{S}$ = swirl factor

A = spool area - in^2

M = spool mass - lbm

y = spool position - in

S = Laplace operator

Flow equations were established for all flow paths and linearized about quiescent operating points. Dynamic pressures and flows are indicated by single subscripts (i.e., P_s, P_o, etc.) whereas quiescent pressures and flows are indicated by the single subscripts followed by "o". (i.e., P_{so}, P_{oo}, etc.) The linearized equations are:

Flows

$$\frac{W_B}{W_{Bo}} = -\delta y \qquad A_m \text{ sonic} \qquad (1)$$

$$\delta = \frac{1}{y_o} \qquad (2)$$

$$\frac{W_s}{W_{so}} = \frac{P_s}{P_{so}} \qquad A_s \text{ sonic} \qquad (3)$$

$$\frac{W_L}{W_{Lo}} = \frac{P_R}{P_{Ro}} \qquad A_L \text{ sonic} \qquad (4)$$

$$\frac{W_v}{W_{vo}} = \frac{P_s}{P_{so}} \qquad A_v \text{ sonic} \qquad (5)$$

$$\frac{W_c}{W_{co}} = \left(1 + K_c \frac{P_{oo}}{P_{co}}\right) \frac{P_c}{P_{co}} - K_c \frac{P_o}{P_{co}} \qquad (6)$$

$$K_c = \frac{f_1' \left(\frac{P_{oo}}{P_{co}}\right)}{f_1 \left(\frac{P_{oo}}{P_{co}}\right)} \qquad (7)$$

$$\frac{W_o}{W_{oo}} = \frac{P_i}{P_{io}} \qquad A_e \text{ sonic} \qquad (8)$$

$$W_D = \frac{A P_{oo}}{R T} S y \tag{9}$$

$$W_{po} = \frac{V^o}{k RT} S P_o \tag{10}$$

$$W_{pR} = \frac{V^R}{k RT} S P_R \tag{11}$$

Pressures

$$\frac{P_o}{P_{oo}} = \frac{P_i}{P_{io}} + 2 K M_{too} (M_{to}) \tag{12}$$

Vortex Relationships

$$\frac{M_{to}}{M_{too}} = \frac{\rho}{\rho_o} - \frac{W_s + W_c}{W_{oo}} \tag{13}$$

$$\frac{\rho}{\rho_o} = \left(1 + K_m \frac{P_{oo}}{P_{co}}\right) - K_m \frac{P_o}{P_{co}}$$

$$K_m = \frac{f_3'}{f_3} \left(\frac{P_{oo}}{P_{co}}\right) \tag{14}$$

Force Balance

$$P_o A = M S^2 y + K' y \tag{15}$$

By substituting the various equations into each other, the relationships result in a fourth order characteristic equation given below:

$$C_4 S^4 + C_3 S^3 + C_2 S^2 + C_1 S + C_o \tag{16}$$

where the coefficients are given by

$$C_o = W_{Bo}\,\delta + \frac{W_{Lo}\,K'\,B}{P_{Ro}\,A\,a\,K} \tag{17}$$

$$C_1 = \frac{V^o K^1}{kRTA} + \frac{AP_{oo}}{RT} + \frac{V^R \beta K^1}{kRTAaK} + \frac{V^o K^1 W_{Lo}}{kRTW_{oo} P_{Ro} AaK} + \frac{W_{Lo} A P_{oo}}{RTW_{oo} P_{Ro} aK} \tag{18}$$

$$C_2 = \frac{A P_{oo} V^R}{k(RT)^2 W_{oo}\, a\, K} + \frac{V^o V^R K^1}{k(RT)^2 W_{oo}\, A\, a\, K} + \frac{W_{Lo}\,\beta M}{P_{Ro}\, a\, AK} \tag{19}$$

$$C_3 = \frac{V^o M}{kRTA} + \frac{V^o W_{Lo} M}{kRTW_{oo}\, A\, a\, K\, P_{Ro}} + \frac{V^R \beta M}{kRT\, a\, KA} \tag{20}$$

$$C_4 = \frac{V^o V^R M}{(kRT)^2\, A\, a\, K\, W_{oo}} \tag{21}$$

where

$$a = \frac{1}{P_{co}} + \frac{K_m P_{oo}}{(P_{co})^2} \tag{22}$$

$$\beta = \frac{1}{P_{oo}} + \frac{K_m}{P_{co}} \tag{23}$$

The physical constants of the regulator are:

regulated flow	0.014 lb/sec
regulated pressure	30 psia
Poppets mass (calculated)	0.0001 lb-sec^2/in

V^o	0.01 in^3
A	0.2 in^2
V^R	0.1 in^3 (minimum)
$W_{oo} = 0.2\ W_{Lo}$	(assumed)
P_{so}	115 psia
P_{co}	90 psia
P_{oo}	60 psia
P_{Ro}	30 psia
K_m	2.5
K^1	500 lb/in

Substituting these quantities into the characteristic equation yields:

$$5.35 \times 10^{-15} S^4 + 5.39 \times 10^{-11} S^3 + 14.11 \times 10^{-8} S^2 + 6.13 \times 10^{-4} S + 0.0697 + 0.014\ \delta = 0 \qquad (24)$$

To find the maximum allowable gain, Routh's stability criterion is applied. Routh's array for a fourth order equation is given by

$$\begin{array}{lll} C_4 & C_2 & C_o \\ C_3 & C_1 & \\ b_1 & C_o & \\ c_1 & & \\ C_o & & \end{array}$$

where

$$b_1 = \frac{C_3 C_2 - C_4 C_1}{C_3}$$

$$c_1 = \frac{b_1 C_1 - C_3 C_1}{b_1}$$

Substitution of equation (24) yields for absolute stability

$$\delta < 90$$

and applying a 6 db gain margin yields an allowable poppet gain of

$$\delta = 45 .$$

This gain can be obtained by a conventional spherical seat design, which will be used.

The spring rate of the suspension washers is calculated, using a formula from "Formulas for Stress and Strain", R. J. Roark, which gives

$$K^1 = \frac{F}{y} = \frac{P_o A}{y} = \frac{E t^3}{0.092 a^2}$$

where

E = modulus of elasticity

t = thickness of plate

a = outer radius of plate .

Using a 0.4 inch radius and a thickness of 0.006 inch yields

$$K^1 = \frac{30 \times 10^6 (0.006)^3}{(0.092)(0.4)^2} = 440 \text{ lb/in} .$$

BLANK PAGE

APPENDIX D

FLOW CHARACTERISTICS OF n ORIFICES IN SERIES

D.1 ANALYTICAL BASIS

Consider n orifices in series as indicated in Figure D-1. Here the orifices are counted from the upstream side so that the nth orifice is at the outlet. The inlet pressure may be denoted P_o, the outlet pressure of the first orifice, P_1, and so on, to the outlet pressure of the downstream orifice, which is denoted P_n. The "P's" are all measured in absolute units, so that the pressure ratio across the overall array of orifices is P_n/P_o.

For the unchoked condition, the flow of an ideal gas through a single orifice is given by:

$$\dot{w} = C_d A g \sqrt{\frac{2k}{R(k-1)}} \frac{P_u}{\sqrt{T}} \left(\frac{P_d}{P_u}\right)^{1/k} \sqrt{1 - \left(\frac{P_d}{P_u}\right)^{(k-1)/k}} \qquad \text{(D-1)}$$

Given a series of orifices, the weight flow of gas through any orifice must be equal to the weight flow through any other orifice. For a given orifice, we can write from equation (D-1) where $2 \leq j \leq n$.

$$\dot{w}_{j-1} = C_d A_{j-1} g \sqrt{\frac{2k}{R(k-1)}} \frac{P_{j-2}}{\sqrt{T}} \left(\frac{P_{j-1}}{P_{j-2}}\right)^{1/k} \sqrt{1 - \left(\frac{P_{j-1}}{P_{j-2}}\right)^{(k-1)/k}} \qquad \text{(D-2)}$$

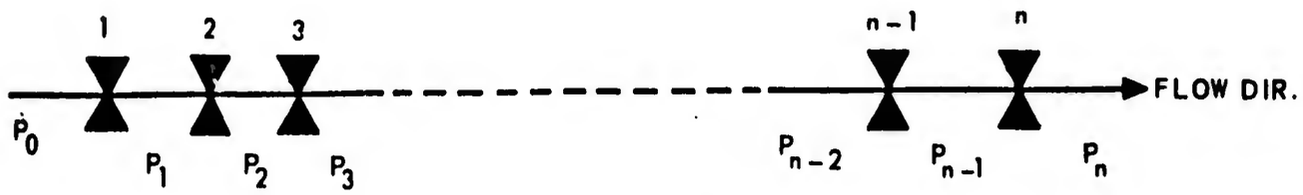

Figure D-1-Orifice and Pressure Notation

For the next orifice:

$$\dot{w}_j = C_d A_j g \sqrt{\frac{2k}{R(k-1)}} \frac{P_{j-1}}{\sqrt{T}} \left(\frac{P_j}{P_{j-1}}\right)^{1/k} \sqrt{1 - \left(\frac{P_j}{P_{j-1}}\right)^{(k-1)/k}} \qquad \text{(D-3)}$$

Since $\dot{w}_{j-1} = \dot{w}_j$, we can combine equations (D-2) and (D-3) to obtain:

$$\left(\frac{A_{j-1}}{A_j}\right)\left(\frac{P_{j-2}}{P_{j-1}}\right)\left(\frac{P_{j-1}}{P_{j-2}}\right)^{1/k} \sqrt{1 - \left(\frac{P_{j-1}}{P_{j-2}}\right)^{(k-1)/k}} =$$

$$\left(\frac{P_j}{P_{j-1}}\right)^{1/k} \sqrt{1 - \left(\frac{P_j}{P_{j-1}}\right)^{(k-1)/k}} \qquad \text{(D-4)}$$

Equation (D-4) shows that for fixed areas, defining the pressure ratio across either orifice defines the pressure ratio across the other. This may be generalized to the statement that defining the pressure ratio across any orifice defines the pressure ratio across any adjacent orifice. The corollary conclusion is that setting the pressure across any single orifice in the series defines the pressure ratio across every other orifice in the series and since:

$$\frac{P_n}{P_o} = \left(\frac{P_n}{P_{n-1}}\right)\left(\frac{P_{n-1}}{P_{n-2}}\right) \cdots \left(\frac{P_3}{P_2}\right)\left(\frac{P_2}{P_1}\right)\left(\frac{P_1}{P_o}\right) \qquad \text{(D-5)}$$

the overall pressure ratio is also defined.

The effective area of a series of n orifices may be defined as:

$$A_m = \frac{\dot{w}}{C_d g \sqrt{\frac{2k}{R(k-1)}} \frac{P_o}{\sqrt{T}} \left(\frac{P_n}{P_o}\right)^{1/k} \sqrt{1 - \left(\frac{P_n}{P_o}\right)^{(k-1)/k}}} \qquad \text{(D-6)}$$

with the restriction that

$$\left(\frac{P_n}{P_o}\right)^{1/k}\sqrt{1-\left(\frac{P_n}{P_o}\right)^{(k-1)/k}} = 0.2588 \text{ for } \frac{P_n}{P_o} < 0.528 \text{ and } k = 1.4$$

The area of the first orifice is given by:

$$A_1 = \frac{\dot{w}}{C_d g\sqrt{\frac{2k}{R(k-1)}}\ \frac{P_o}{\sqrt{T}}\left(\frac{P_1}{P_o}\right)^{1/k}\sqrt{1-\left(\frac{P_1}{P_o}\right)^{(k-1)/k}}} \qquad \text{(D-7)}$$

We can divide equation (D-6) by (D-7) to obtain:

$$\frac{A_m}{A_1} = \frac{\left(\frac{P_1}{P_o}\right)^{1/k}\sqrt{1-\left(\frac{P_1}{P_o}\right)^{(k-1)/k}}}{\left(\frac{P_n}{P_o}\right)^{1/k}\sqrt{1-\left(\frac{P_n}{P_o}\right)^{(k-1)/k}}} \qquad \text{(D-8)}$$

D.2 RESULTS

Equations (D-4), (D-5), and (D-8) have been used to calculate the significant pressure flow characteristics of n orifices in series. Since the equations are not suited for hand computation, the calculations were performed using a digital computer.

In many of the applications involving the use of a series of orifices, the primary interest is in obtaining the maximum change in effective area as pressure ratio changes. Therefore, the first set of computations was used to determine the distribution of individual orifice areas in a series string which gives the greatest change in ratio A_m/A_1 as P_n/P_o changes. For this set of computations, n = 5 and A_5/A_1 ranged from 0.1 to 10 with areas A_2, A_3, and A_4, varying in both arithmetic and geometric progressions.

The results of the first set of calculations shows that the greatest change in the ratio A_m/A_1 for a given change in P_n/P_o occurs when all orifices in the series have the same area. All other calculations were performed in this case.

Examination of equation (D-4) shows that for the case in which adjacent orifice areas are equal, the downstream orifice will have the pressure ratio closest to the critical value. Thus, as the overall pressure ratio P_n/P_o is decreased, the first orifice to choke will be the downstream orifice. Once the downstream orifice has choked, its effective pressure ratio will remain fixed at the critical value as the ratio P_n/P_o decreases further. Since fixing one pressure ratio fixes all others in the series string, the pressure ratios across all orifices in the string are invariant, once the downstream orifice has choked and the weight flow of gas is a function of the upstream conditions only.

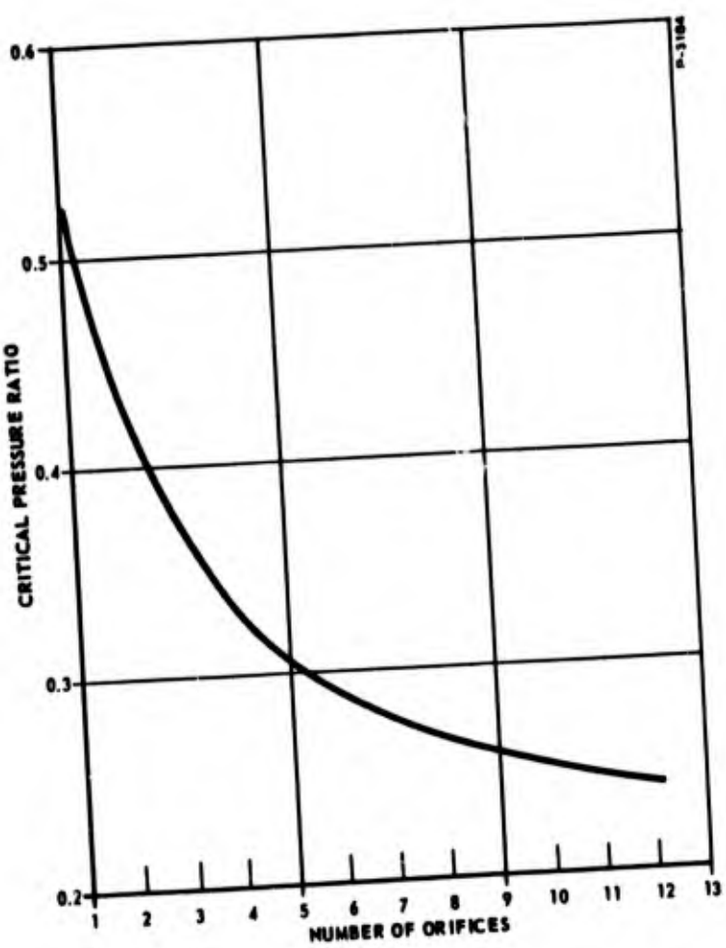

Figure D-2 - Critical Pressure Ratio for Equal Orifices in Series as a Function of the Number of Orifices k = 1.4

Since the overall pressure ratio across a string of orifices is always smaller than the pressure ratio across any individual orifice, the critical pressure ratio of a series of orifices is less than that of a single orifice. This is a highly useful property. Figure D-2 shows the critical pressure ratio as a function of the number of orifices for a diatomic gas (k = 1.4). This has been plotted from a curve given in the Reference.

The flow through a series of equal orifices may be computed by means of an effective area which is a function of the pressure ratio. Table D-1 gives the values of the effective areas for values of n = 2, 5, and 10 at pressure ratios with increments of 0.05. The table has been computed from the simultaneous solution of the system of equations (D-4), (D-5) and (D-8).

The nondimensional effective areas given in the table may be used to compute the flow of a diatomic gas through a series string of equal area orifices by means of the following equation:

$$\dot{w} = C_d A_1 \left(\frac{A_m}{A_1}\right) g \sqrt{\frac{2k}{R(k-1)}} \left(\frac{P_o}{\sqrt{T}}\right) \left(\frac{P_n}{P_o}\right)^{1/k} \sqrt{1 - \left(\frac{P_n}{P_o}\right)^{(k-1)/k}} \qquad \text{(D-9)}$$

Table D-1 - Nondimensional Effective Areas of Equal Orifices in Series for Various Pressure Ratios

Press Ratio	Number of Orifices		
	2	5	10
0.95	0.7124	0.4526	0.3205
0.90	0.7183	0.4585	0.3252
0.85	0.7249	0.4651	0.3304
0.80	0.7322	0.4724	0.3363
0.75	0.7404	0.4807	0.3428
0.70	0.7497	0.4900	0.3502
0.65	0.7601	0.5006	0.3586
0.60	0.7720	0.5128	0.3682
0.55	0.7854	0.5269	0.3794
0.50	0.7991	0.5425	0.3918
0.45	0.8064	0.5553	0.4026
0.40	---	0.5651	0.4119
0.35	---	0.5715	0.4189
0.30	---	---	0.4243

3164

where values of A_m/A_1 for a given pressure ratio are obtained from Table D-1 and using

$$\left(\frac{P_n}{P_o}\right)^{1/k} \sqrt{1 - \left(\frac{P_n}{P_o}\right)^{(k-1)/k}} = 0.2588 \text{ for } \frac{P_n}{P_o} < 0.528$$

REFERENCE

Robinson, C.S. L., "Flow of a Compressible Fluid through a Series of Identical Orifices," Journal of Applied Mechanics Vol. 15, n 4 December 1948 pp. 308-10.

SUPPLEMENTARY

INFORMATION

AD-489 923 Bendix Corp., Southfield, Mich. Research Labs. Div. Technical documentary rept. Feb 65-Jun 66. Rept. no. RLD-3509 15 Jun 66 Contract DA-01-021- AMC-11805(Z)	No Foreign without approval of Army Missile Command, Attn: Army Inertial Guidance and Control Lab., Redstone Arsenal, Ala.	No limitation	OASD, DoD, 29 May 69